Systematic mining and reanalysis of volcano seismo-acoustic waveform datasets

Robin S. Matoza

Department of Earth Science; University of California, Santa Barbara

image: Tyson Fisher

D. Fee

A. Austin

N. Key

A. Austin

Large volcano-seismic waveform datasets

- Seismicity plays a central role in understanding how volcanoes work
- Growing seismic data volumes: develop techniques for systematic analyses
- Event detection and cataloging, high-precision earthquake relocation, acoustic localization, waveform and spectral event classification, and source mechanism inversions

Mount St. Helens, WA November 2004; 48-hr seismogram ~2 km from summit

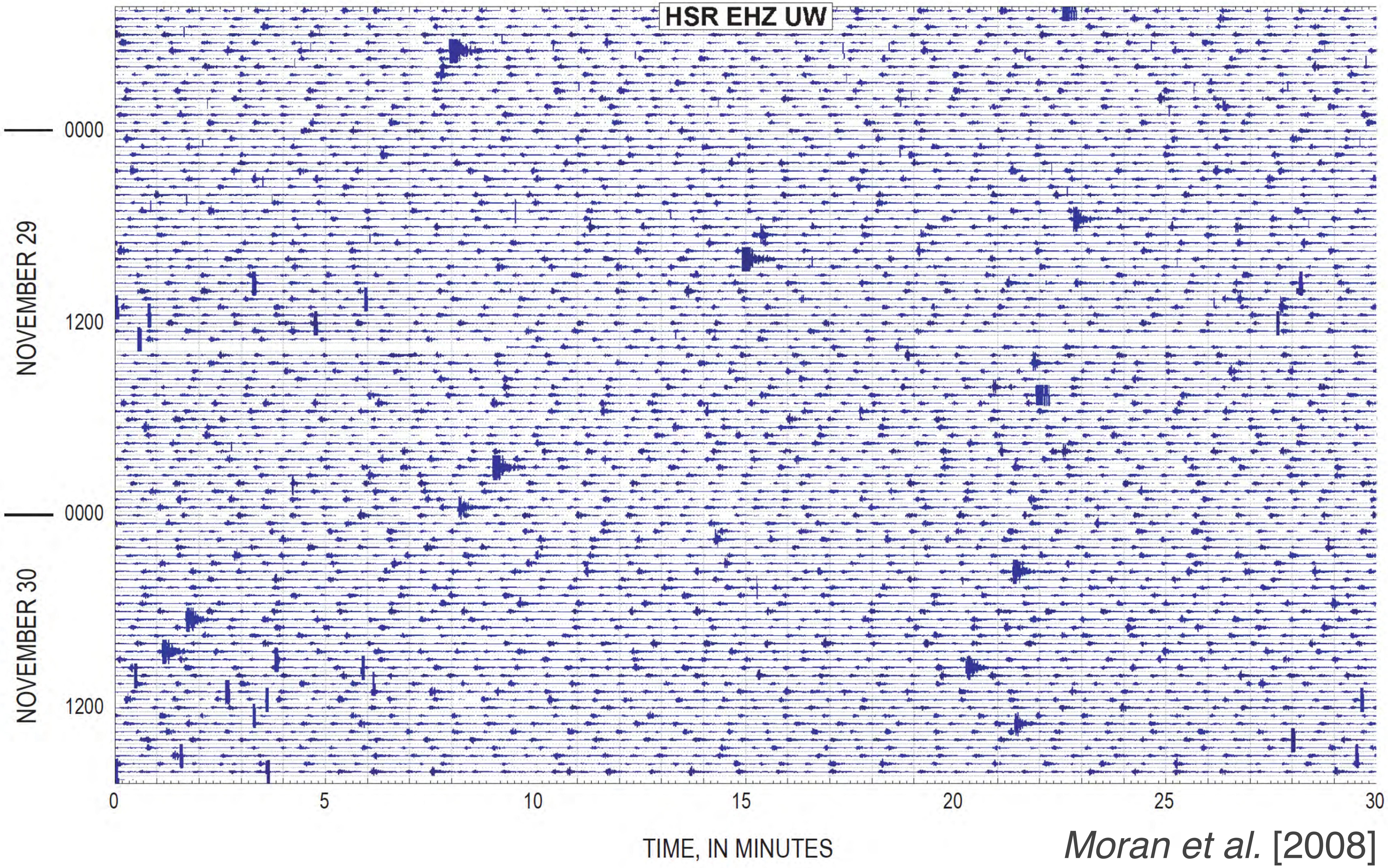

Moran et al. [2008]

Volcano seismology and acoustics

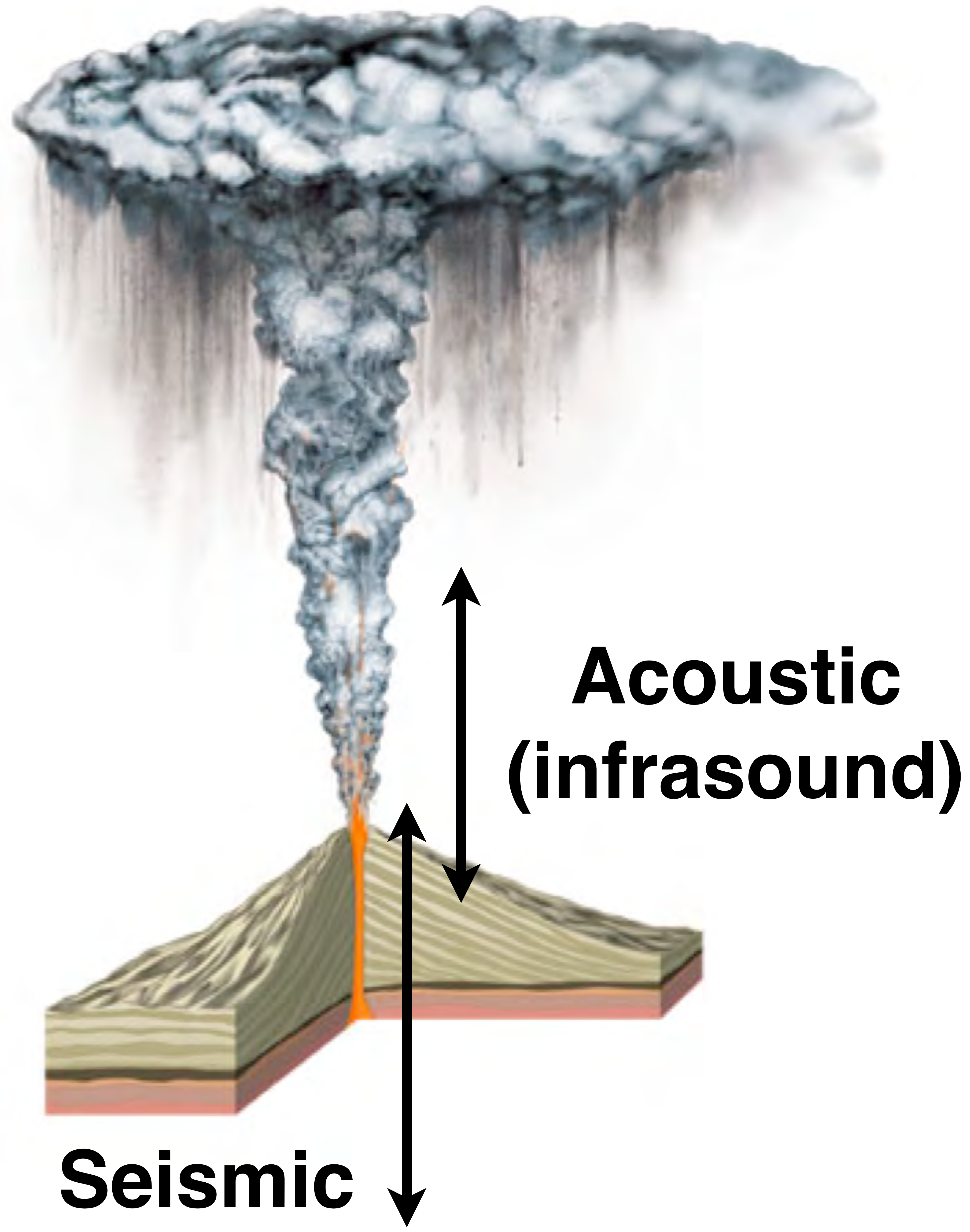

Acoustic

- Atmospheric acoustics (infrasound): ~0.01-20 Hz
- Variety of shallow and subaerial sources
- Explosive volcanism: powerful signals

Seismic

- Migration of fluid from mantle depths to surface
- Faulting & fluid transport in the solid earth
- Limited propagation < few hundred km

Phreatic eruption, Mount St. Helens, 8 March 2005

Seismic

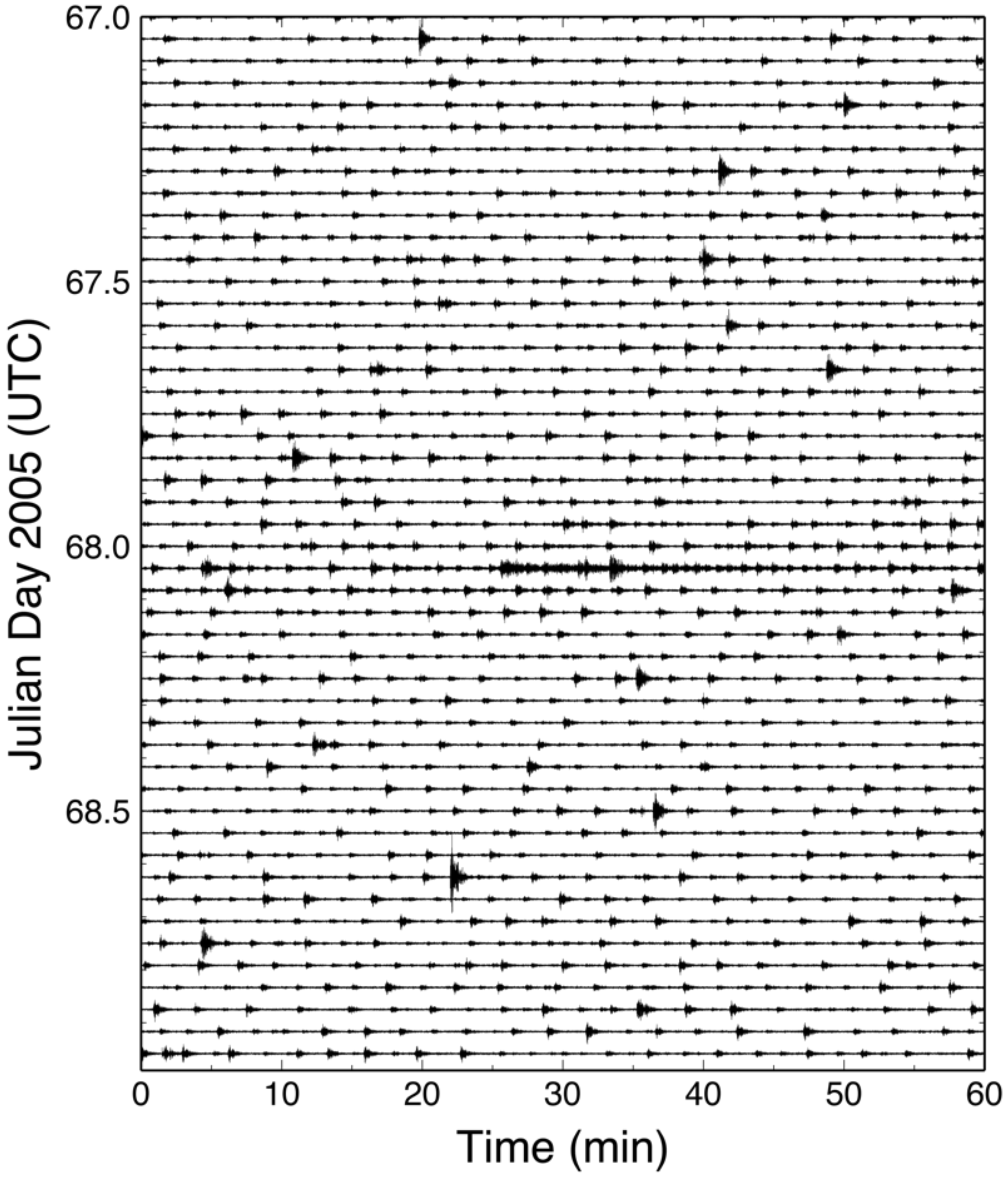

Acoustic

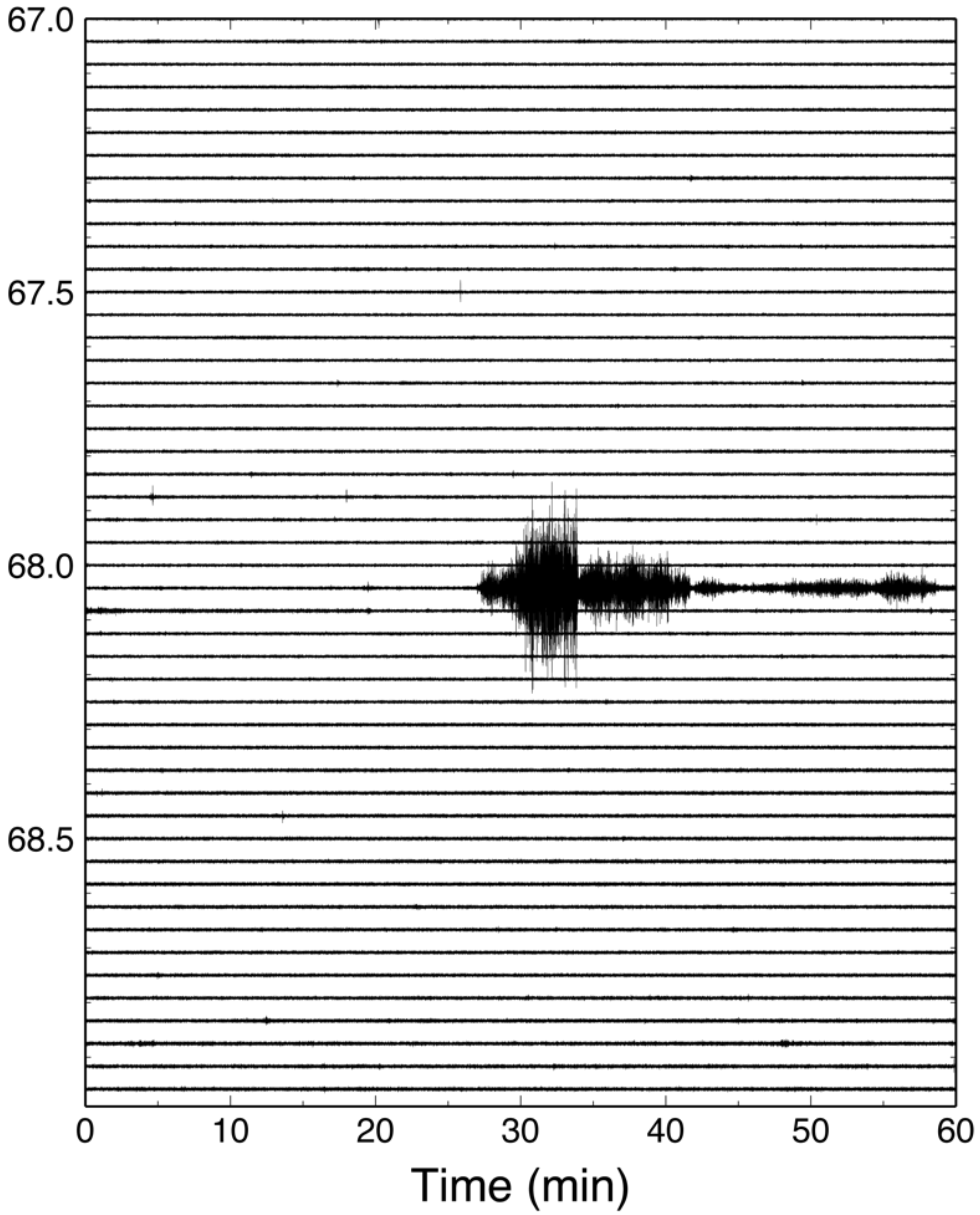

Matoza et al. [2007]

Volcano seismology

Two broad classes of volcano-seismic signals worldwide

1) **Volcano-tectonic (VT)**

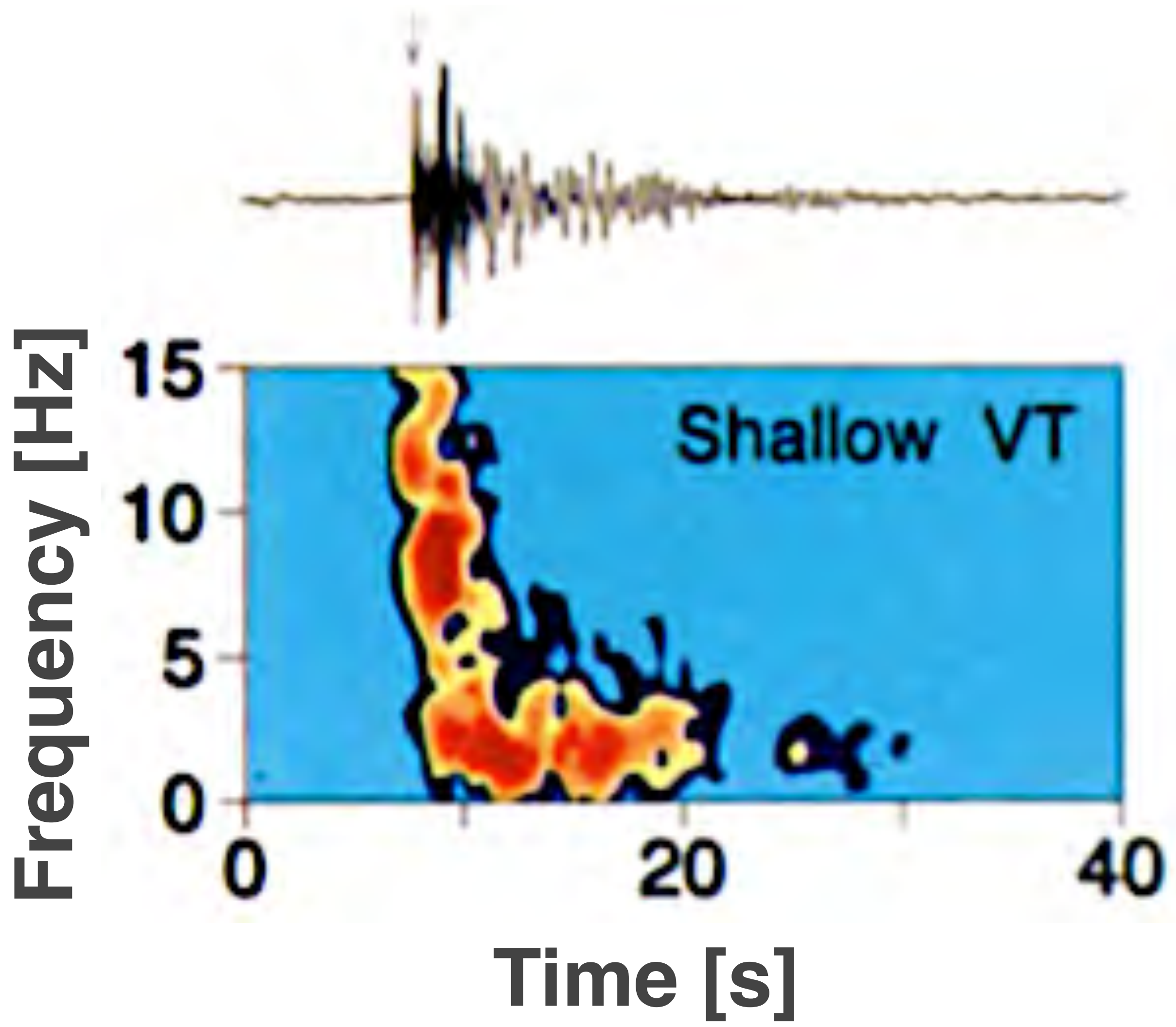

2) **Long-period (LP)** [0.5-5 Hz]

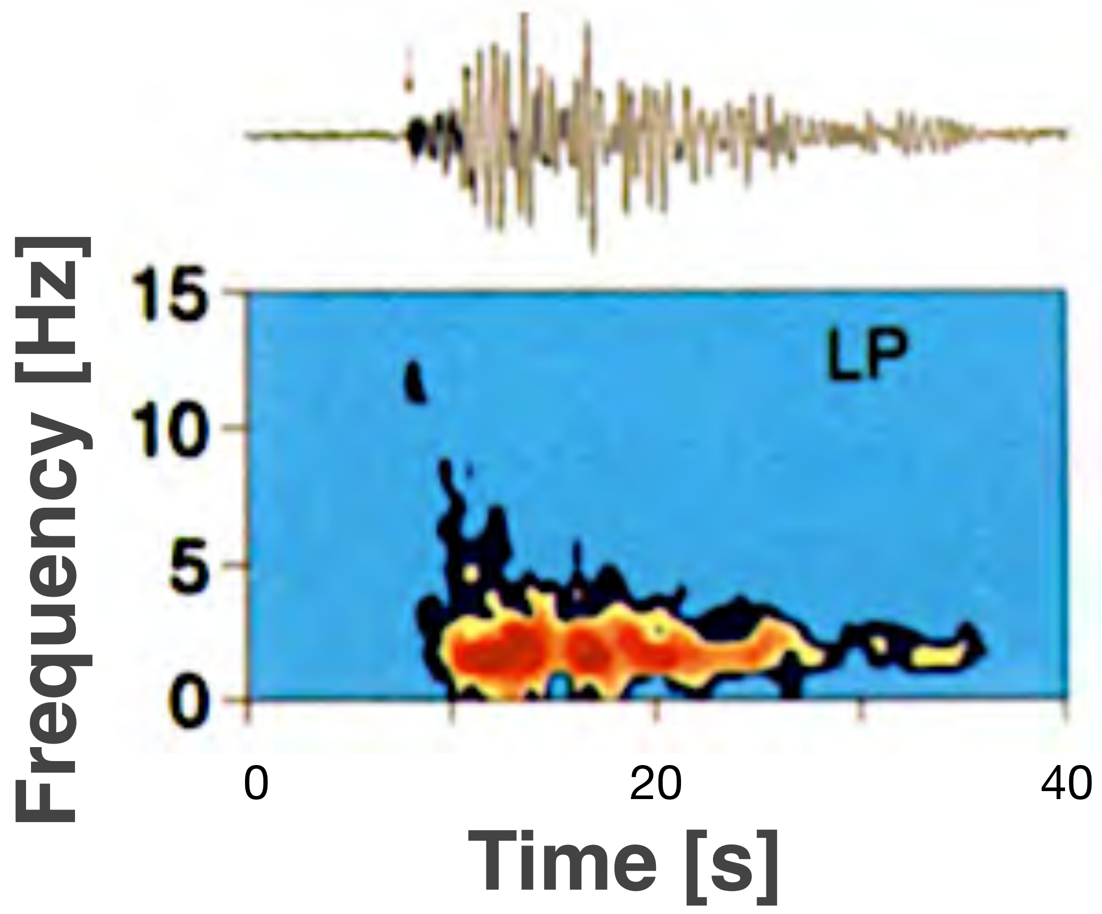

Chouet [1996]

Two broad classes of volcano-seismic signals worldwide

1) **Volcano-tectonic (VT)**
- Shear/tensile failure in brittle solid
- e.g., intrusions, loading and deformation

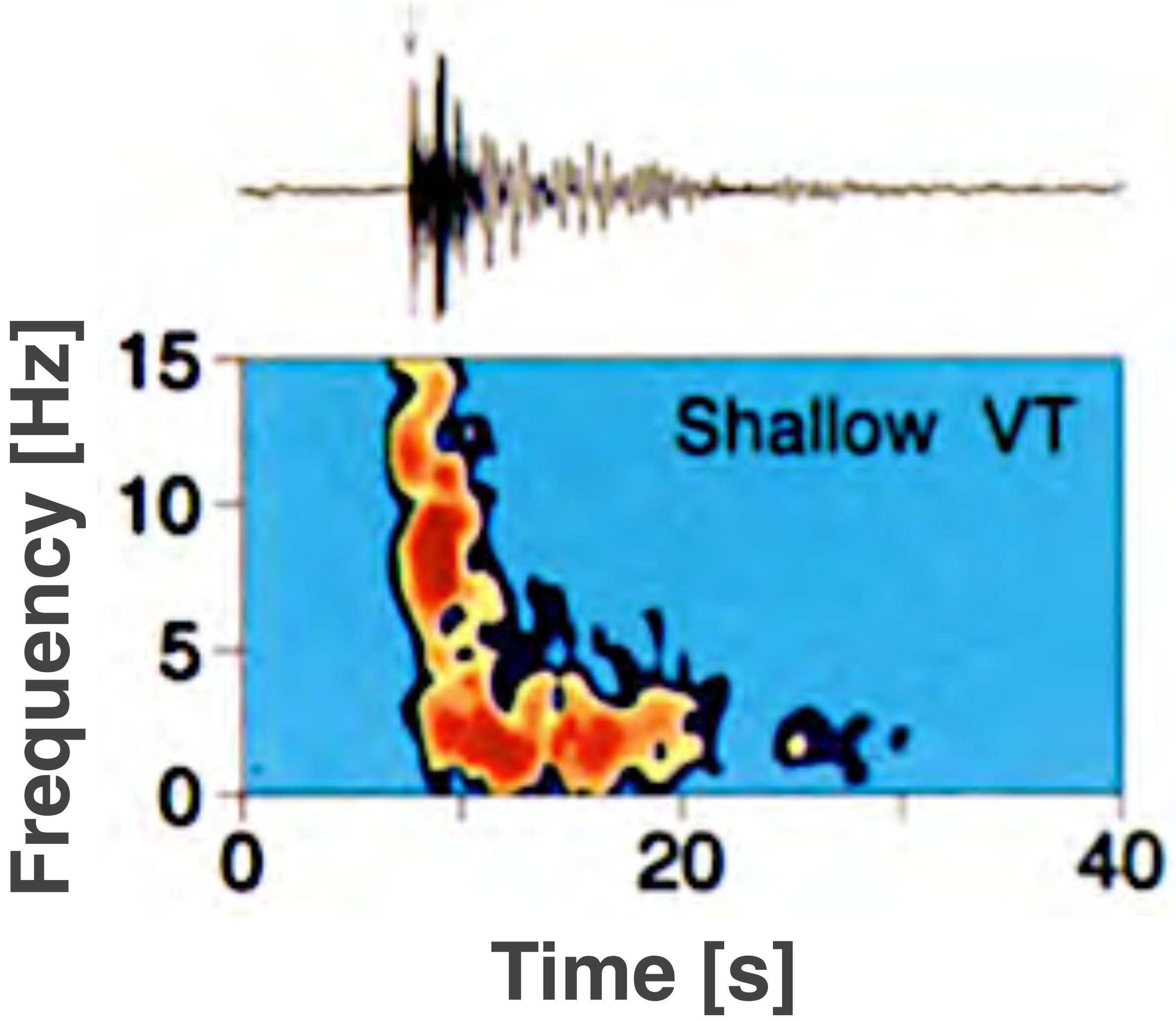

2) **Long-period (LP)** [0.5-5 Hz]
- Actively involve a fluid

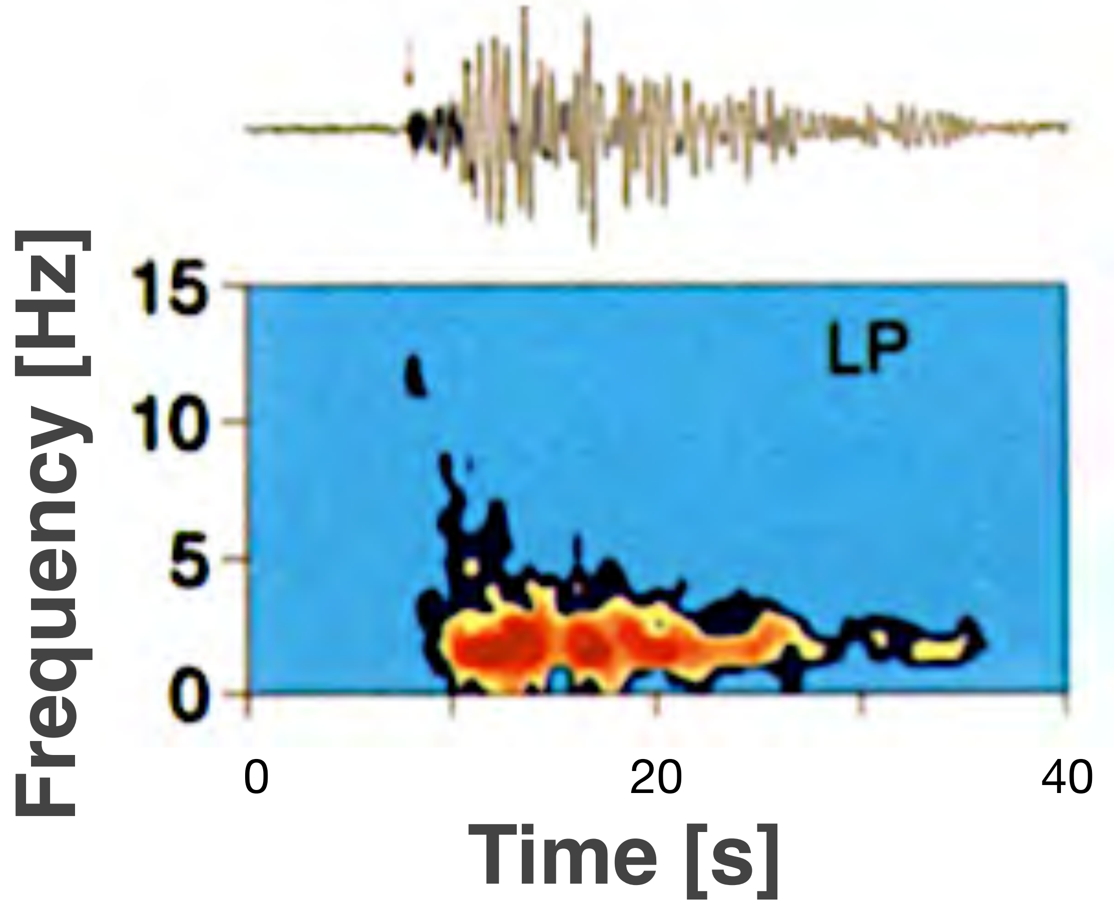

Chouet [1996]

Volcano seismology

Two broad classes of volcano-seismic signals worldwide

1) **Volcano-tectonic (VT)**
   - Shear/tensile failure in brittle solid
   - e.g., intrusions, loading and deformation

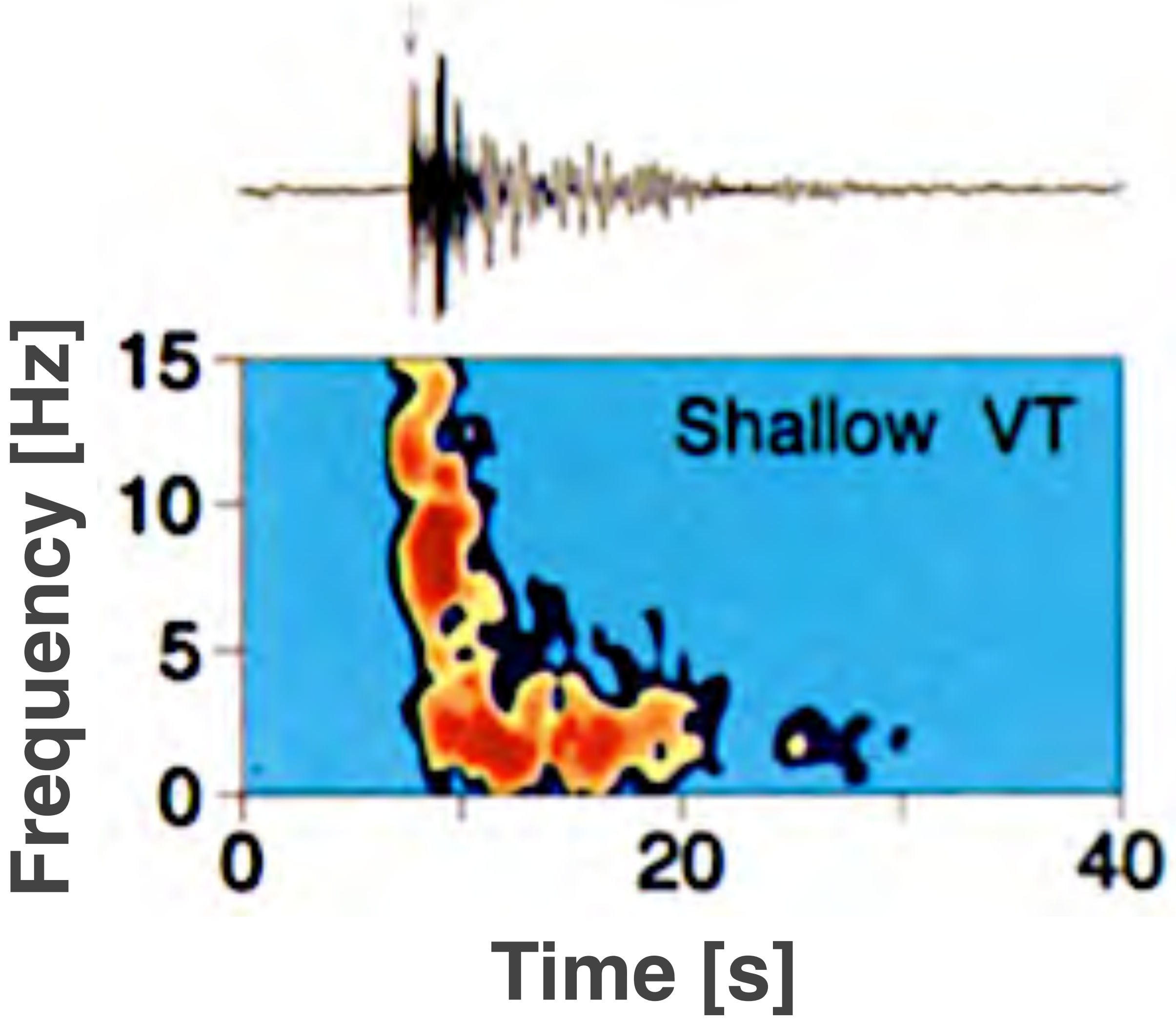

2) **Long-period (LP)** [0.5-5 Hz]
   - Actively involve a fluid
   - Includes **LP events** and **tremor**

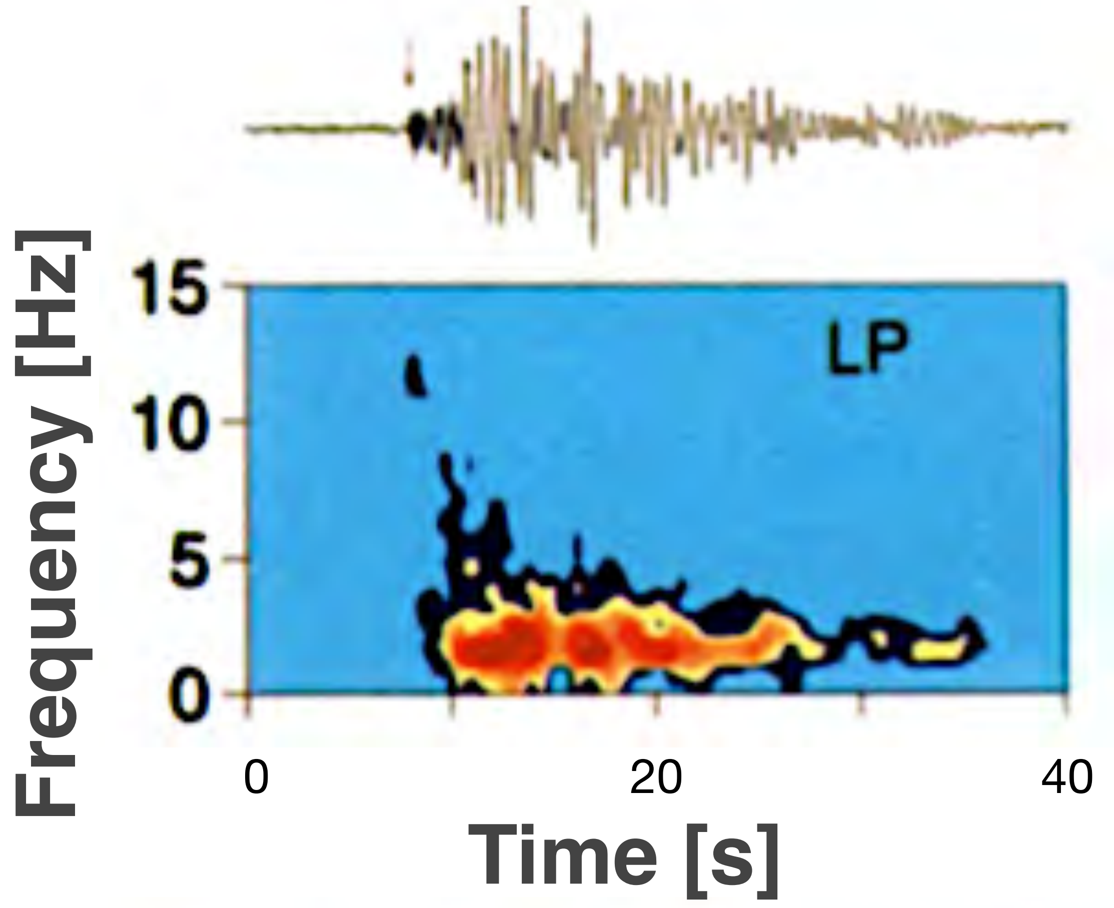

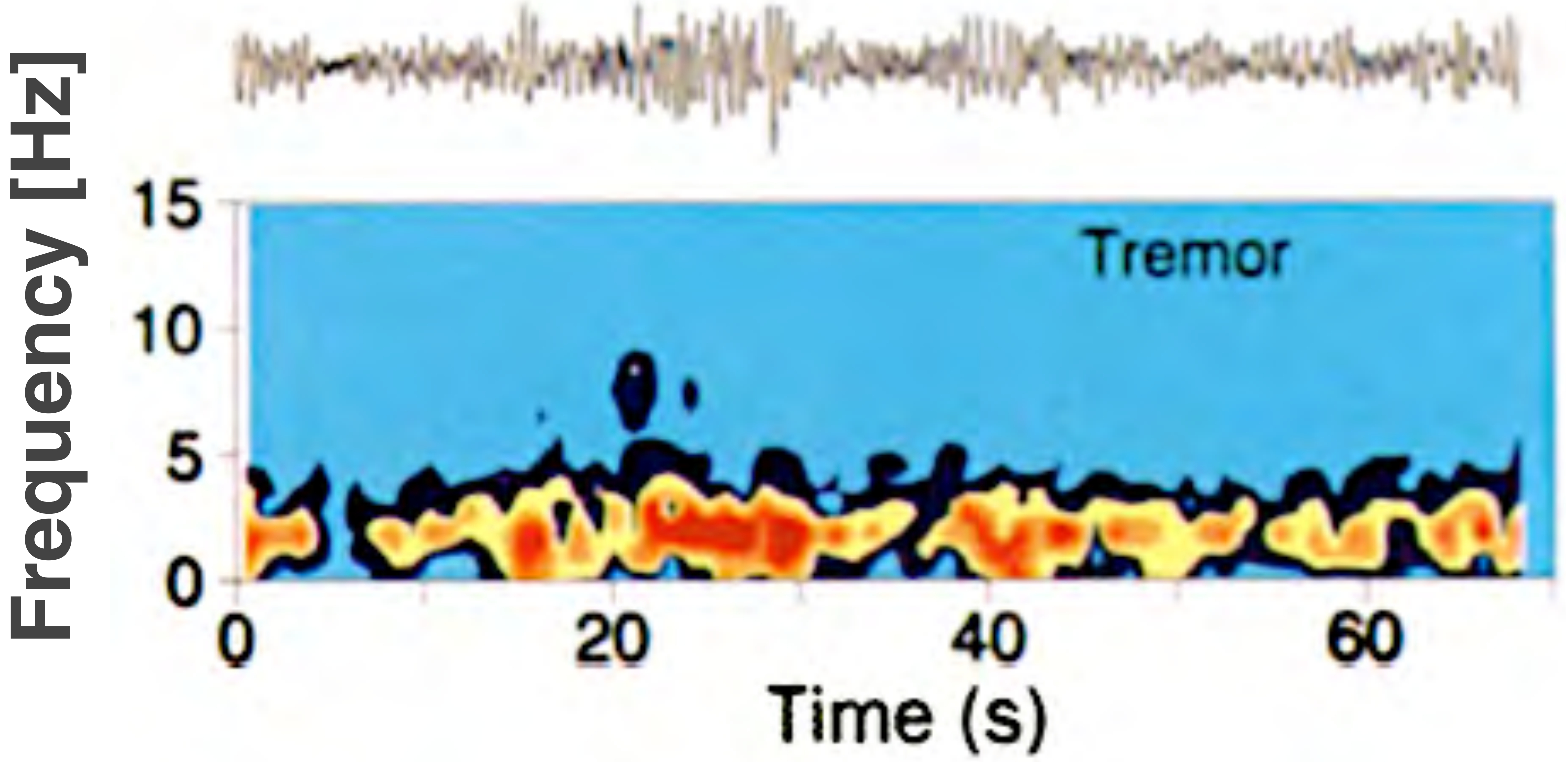

Chouet [1996]

Mount St. Helens 2004–2008 eruption

Spine extrusion and long-period (LP, 0.5–5 Hz) seismicity: some "drumbeats"

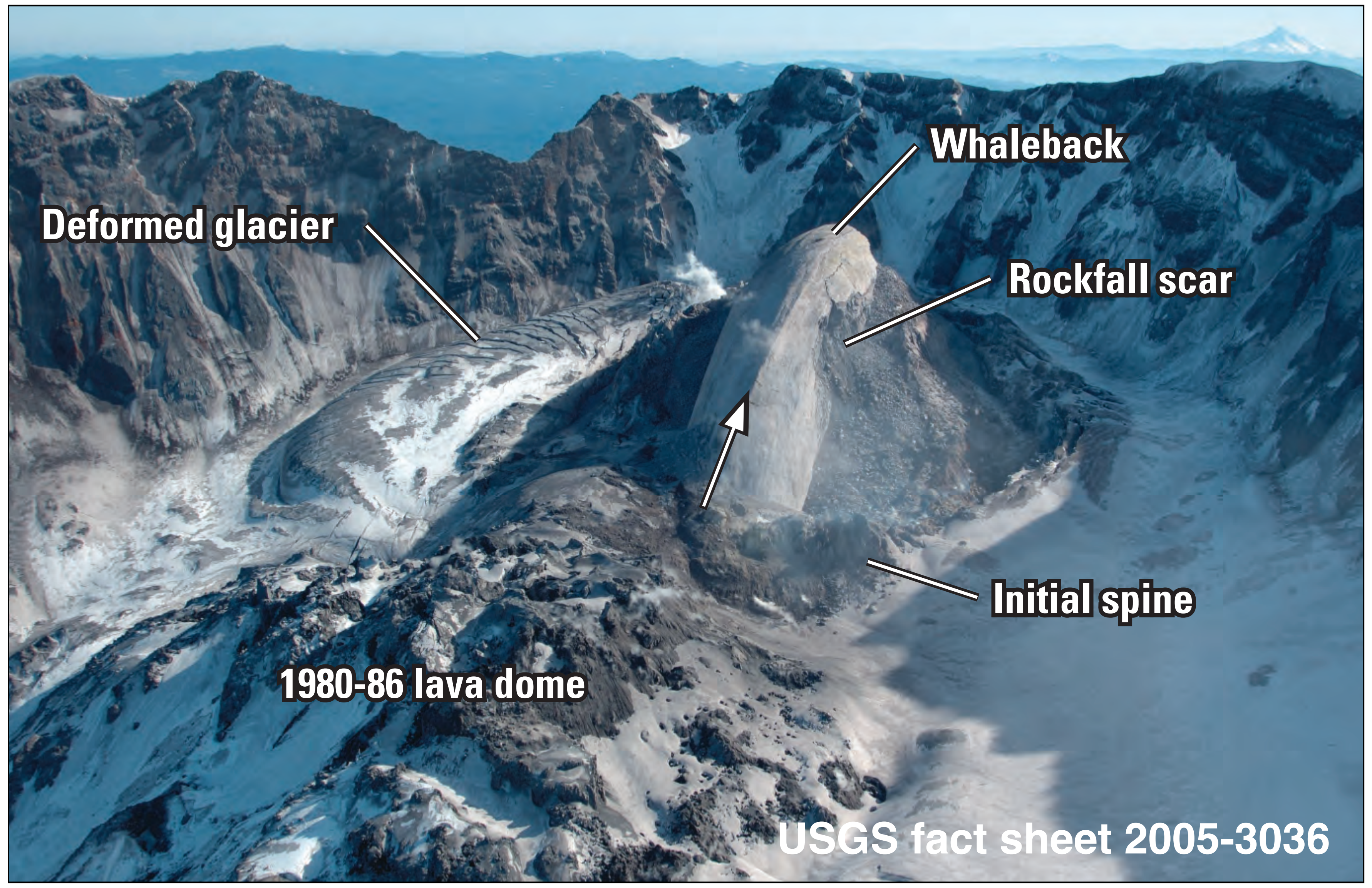

48-hr seismogram ~2 km from summit, November 2004

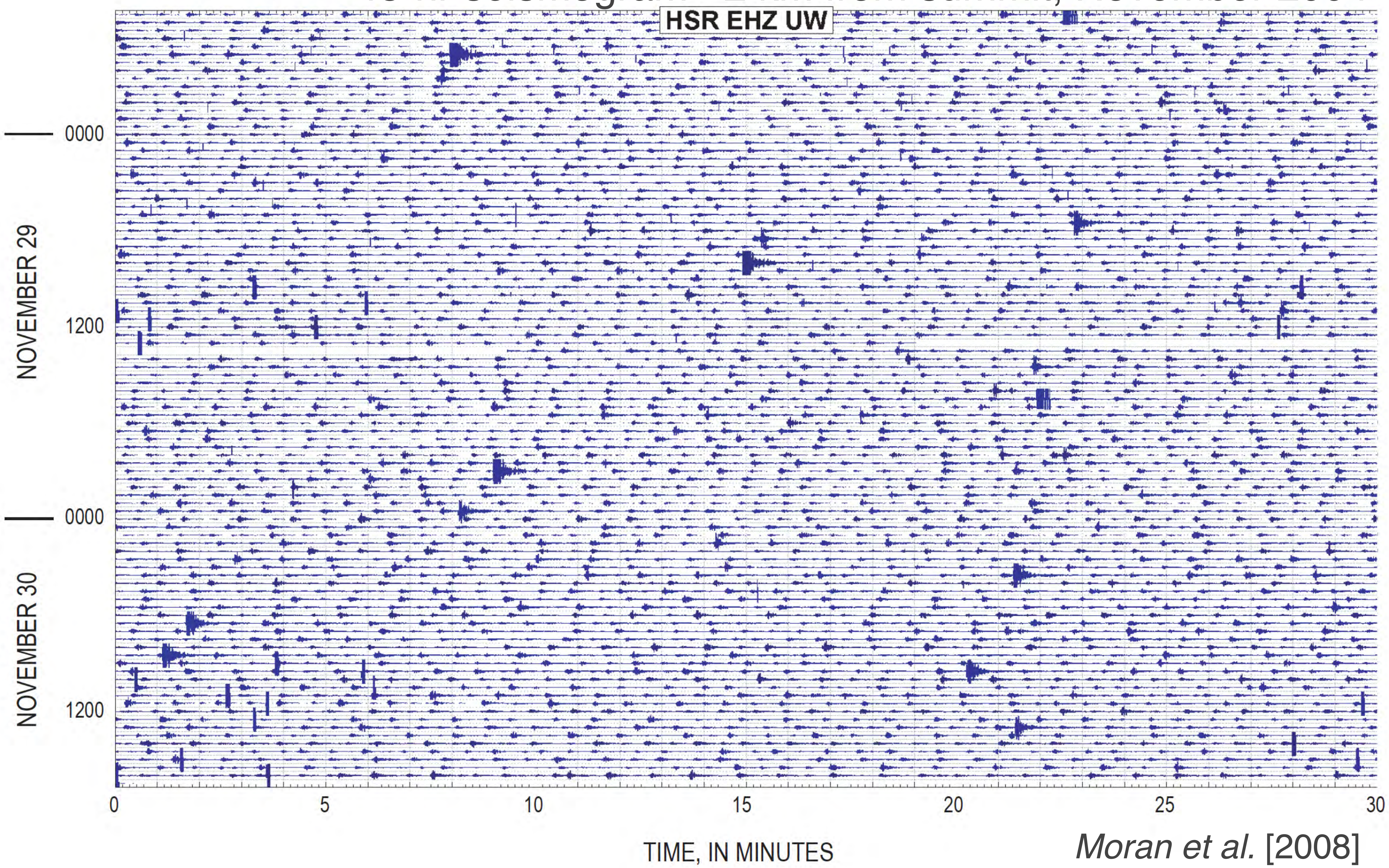

Moran et al. [2008]

Mount St. Helens 2004–2008 eruption

Solid extrusion, plug stick-slip

Iverson et al. [2006]

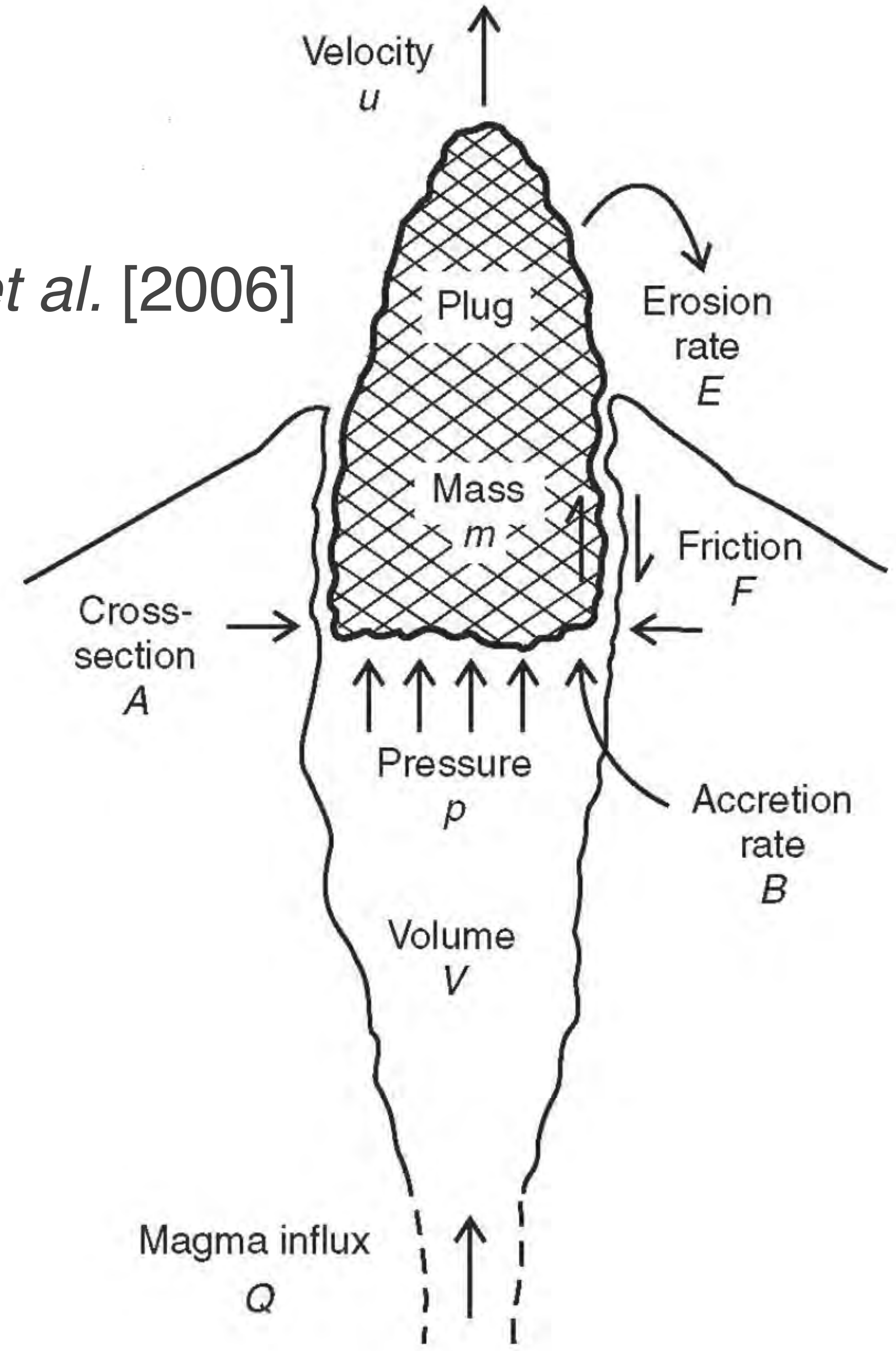

e.g., *Iverson et al.* [2006]; *Harrington and Brodsky* [2007]; *Iverson* [2008]; *Kendrick et al.* [2014]

Cyclic recharge-collapse of a hydrothermal crack

Schematic of Kusatsu-Shirane, Japan

Nakano et al. [2003]

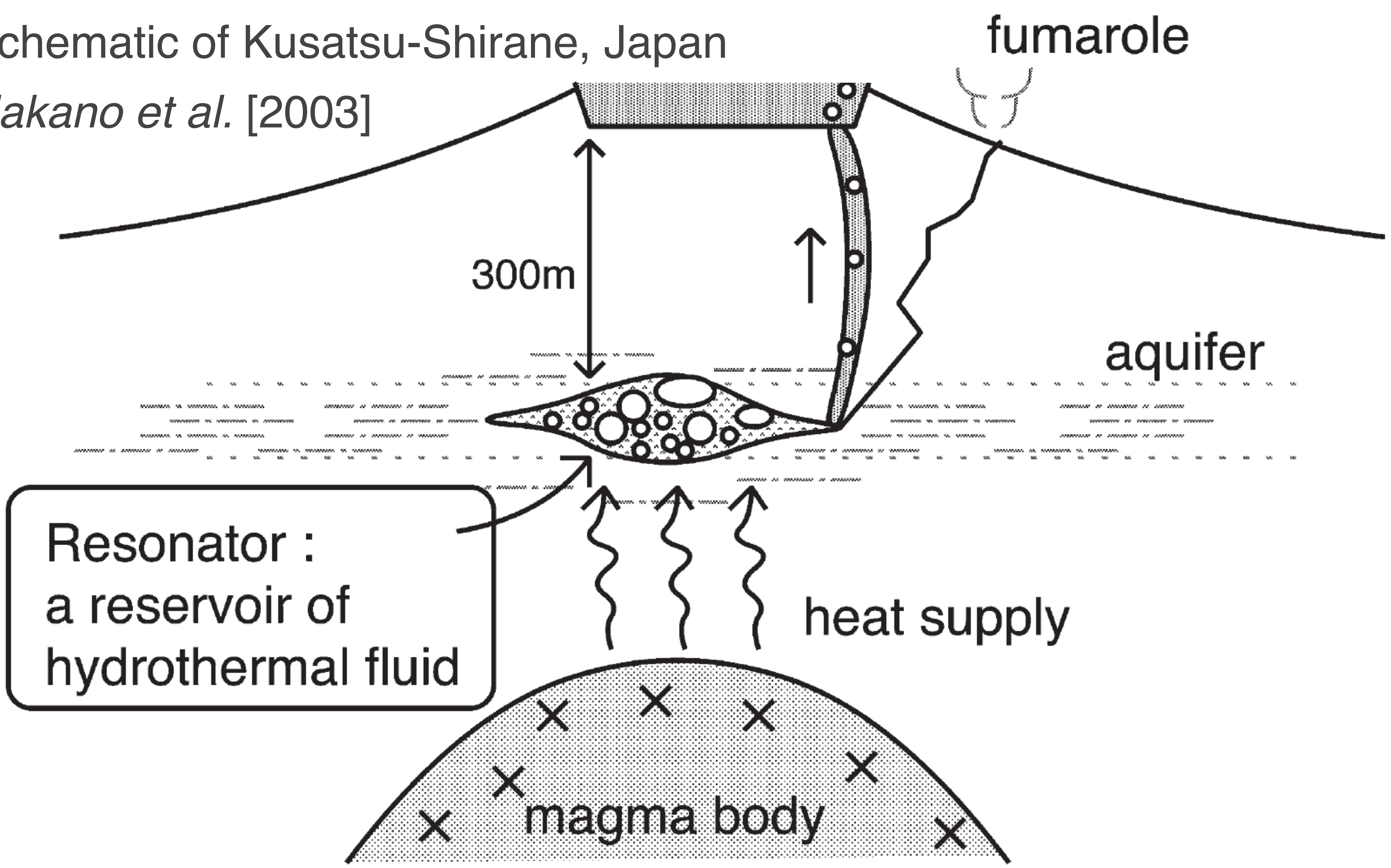

e.g., *Waite et al.* [2008]; *Matoza et al.* [2009]; *Matoza and Chouet* [2010]

LP "subevents" or small LPs

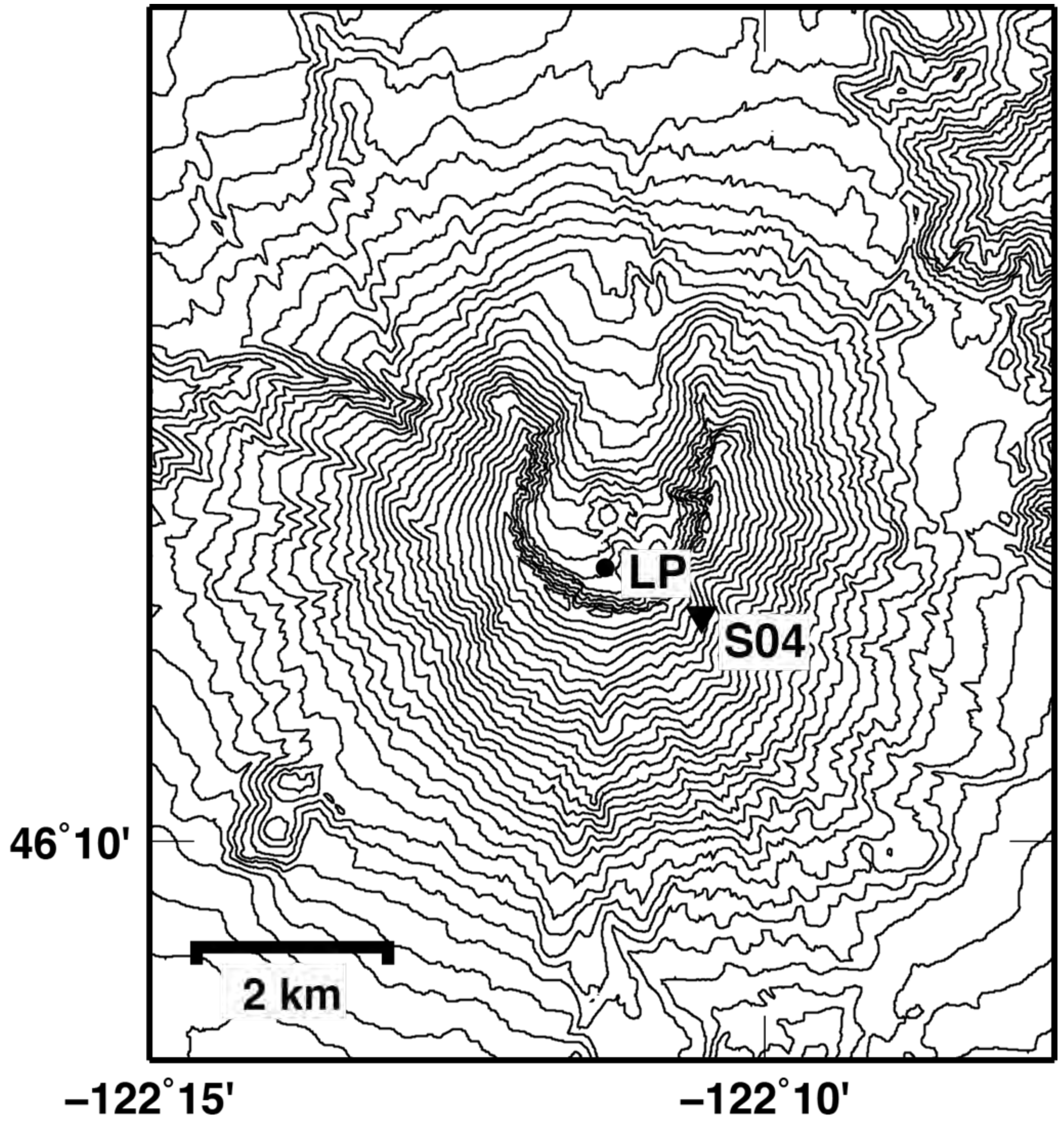

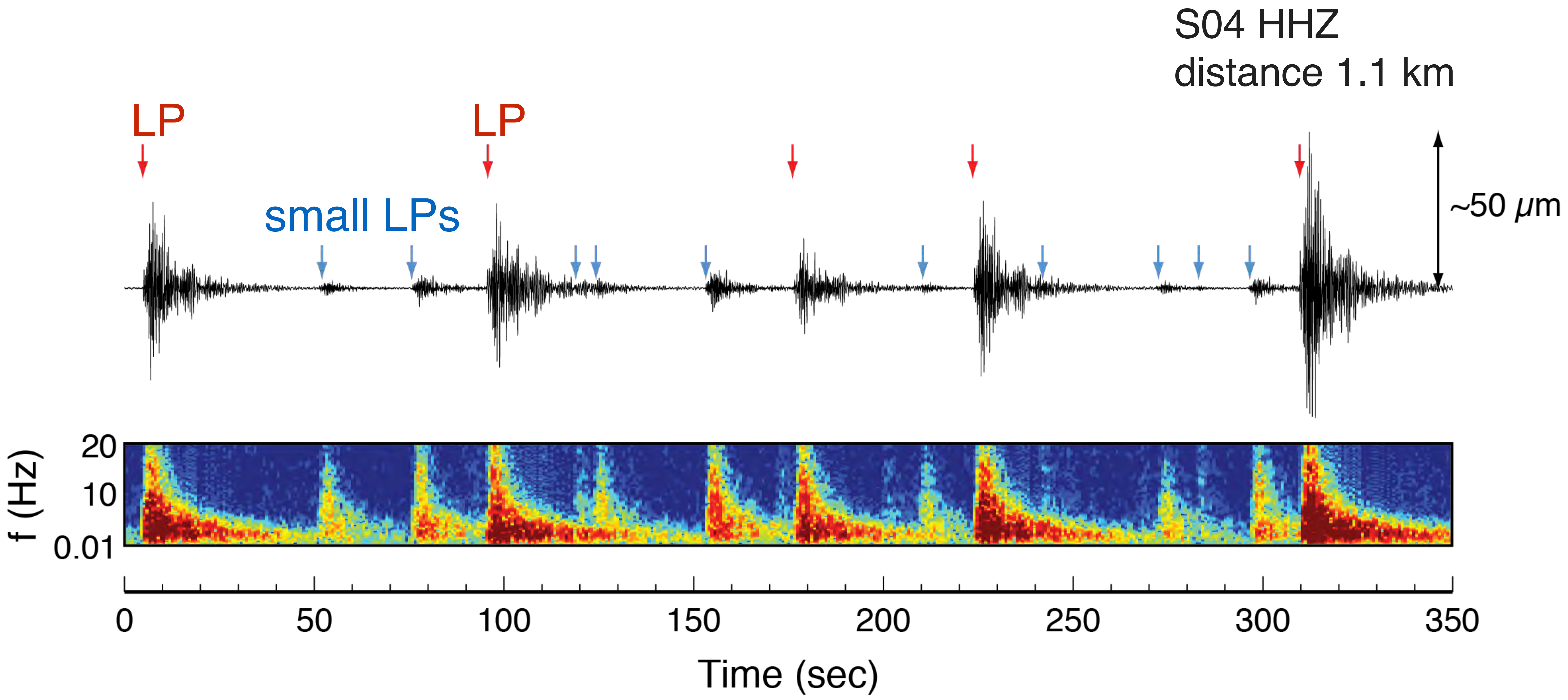

Matoza and Chouet [2010]

LP “subevents” or small LPs

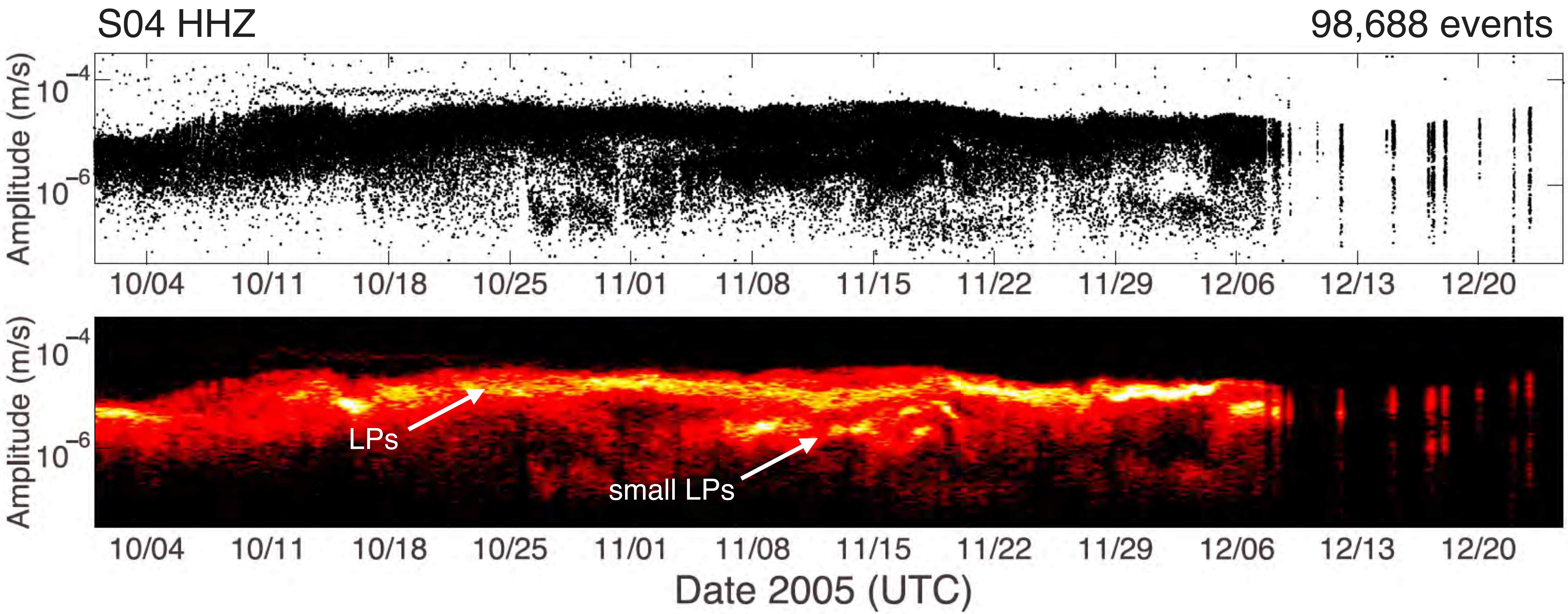

Matoza and Chouet [2010]

Single-station cross-correlation to separate event types

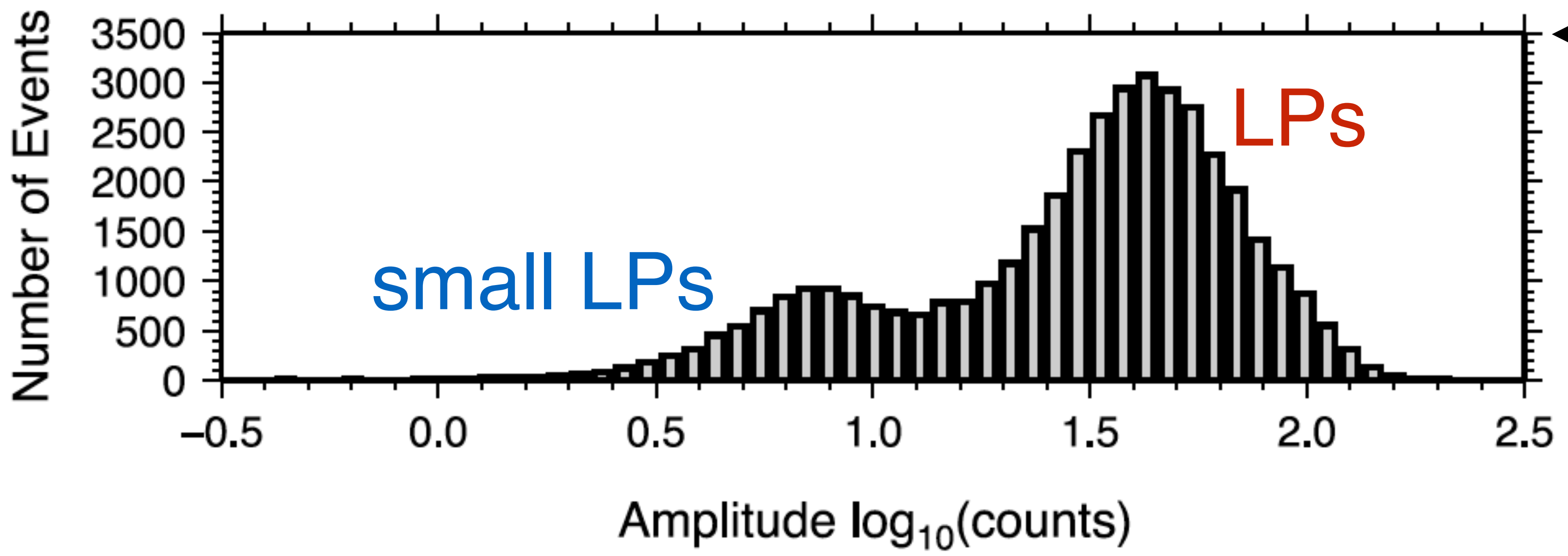

Station BLIS 4–16 November 2004

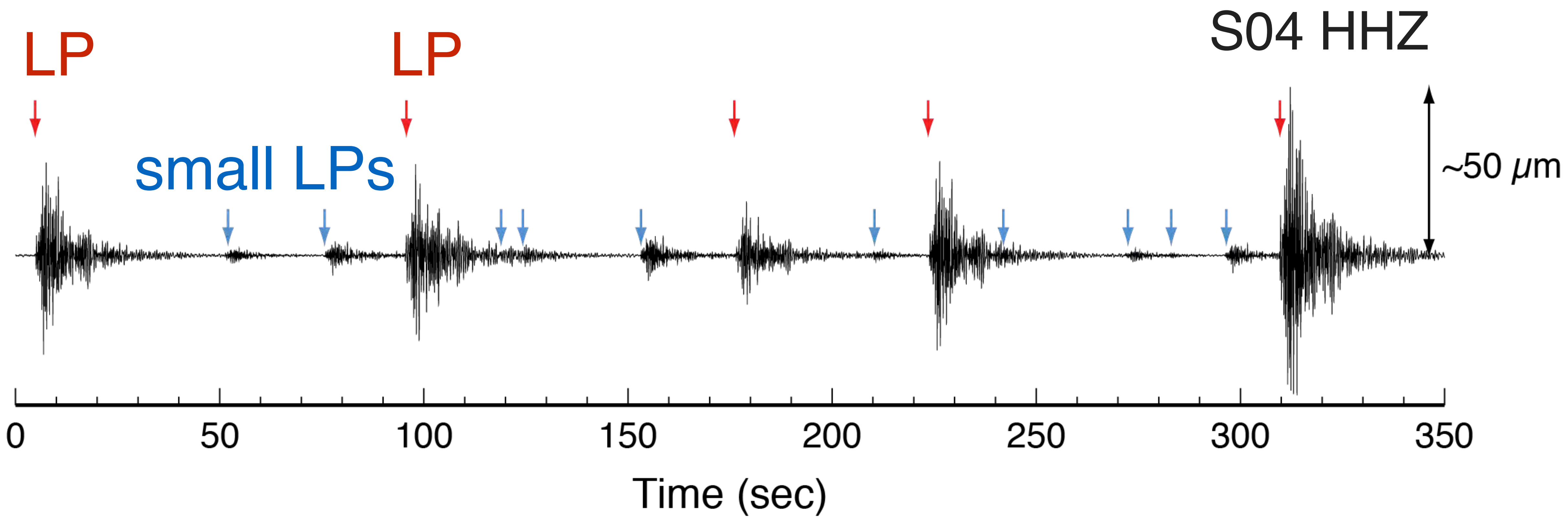

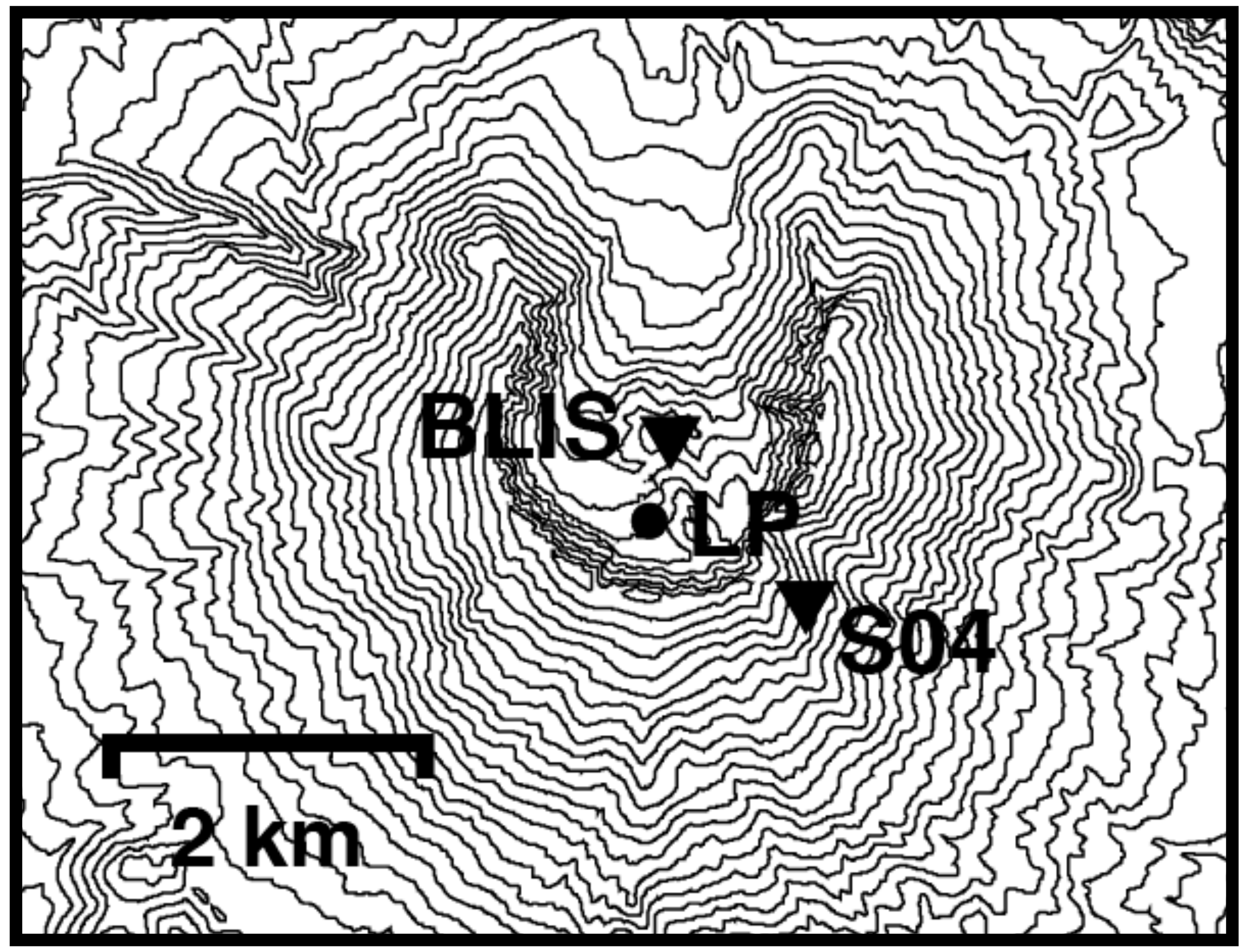

Matoza and Chouet [2010]

Single-station cross-correlation to separate event types

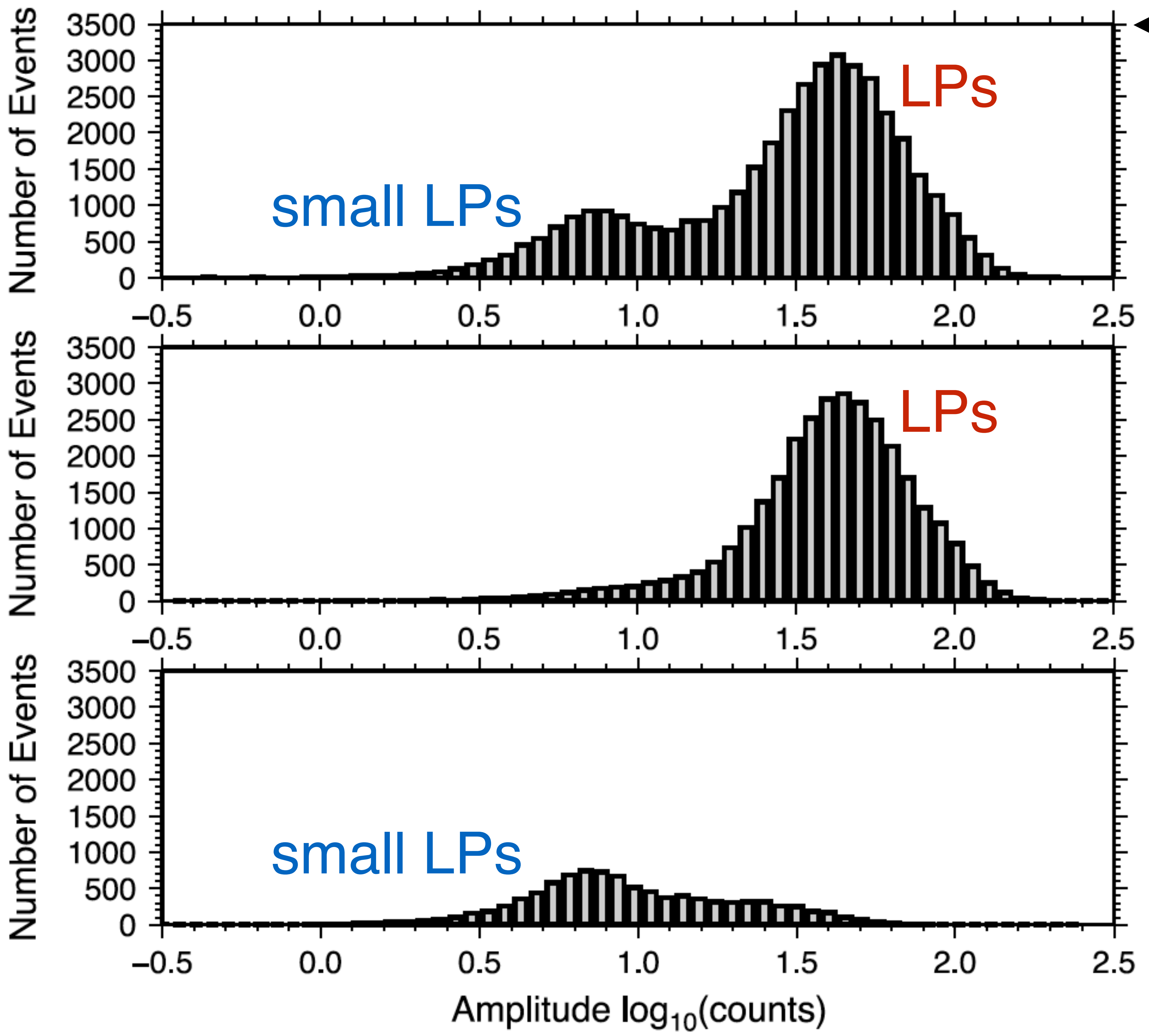

Station BLIS 4–16 November 2004

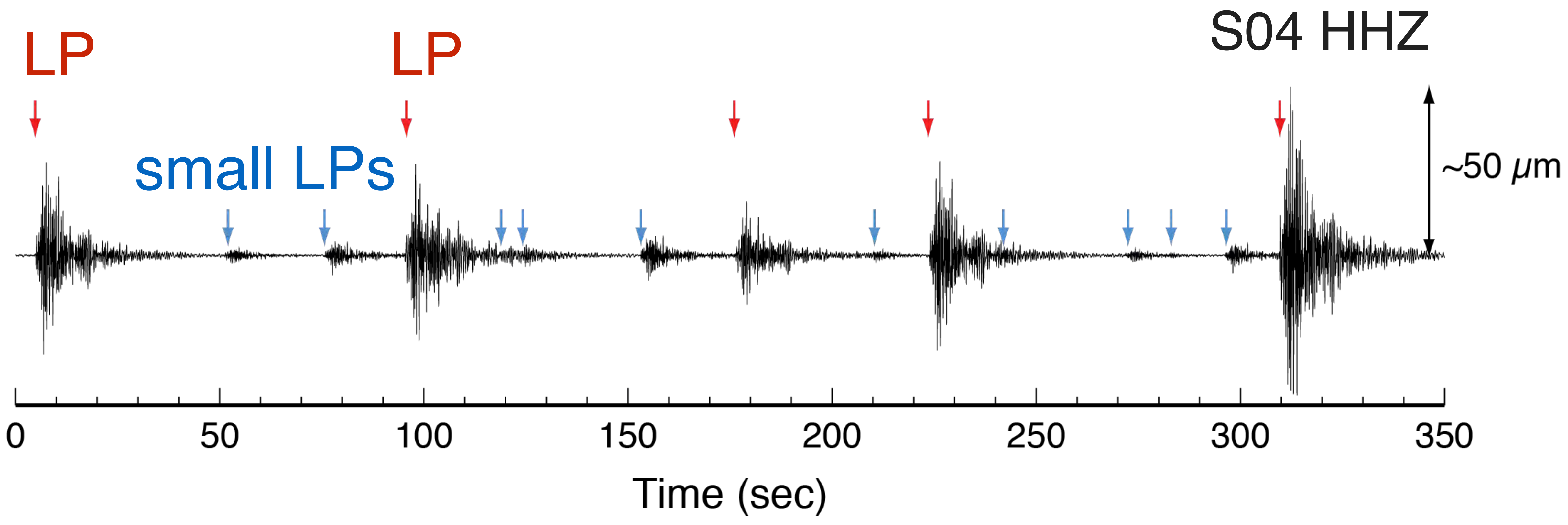

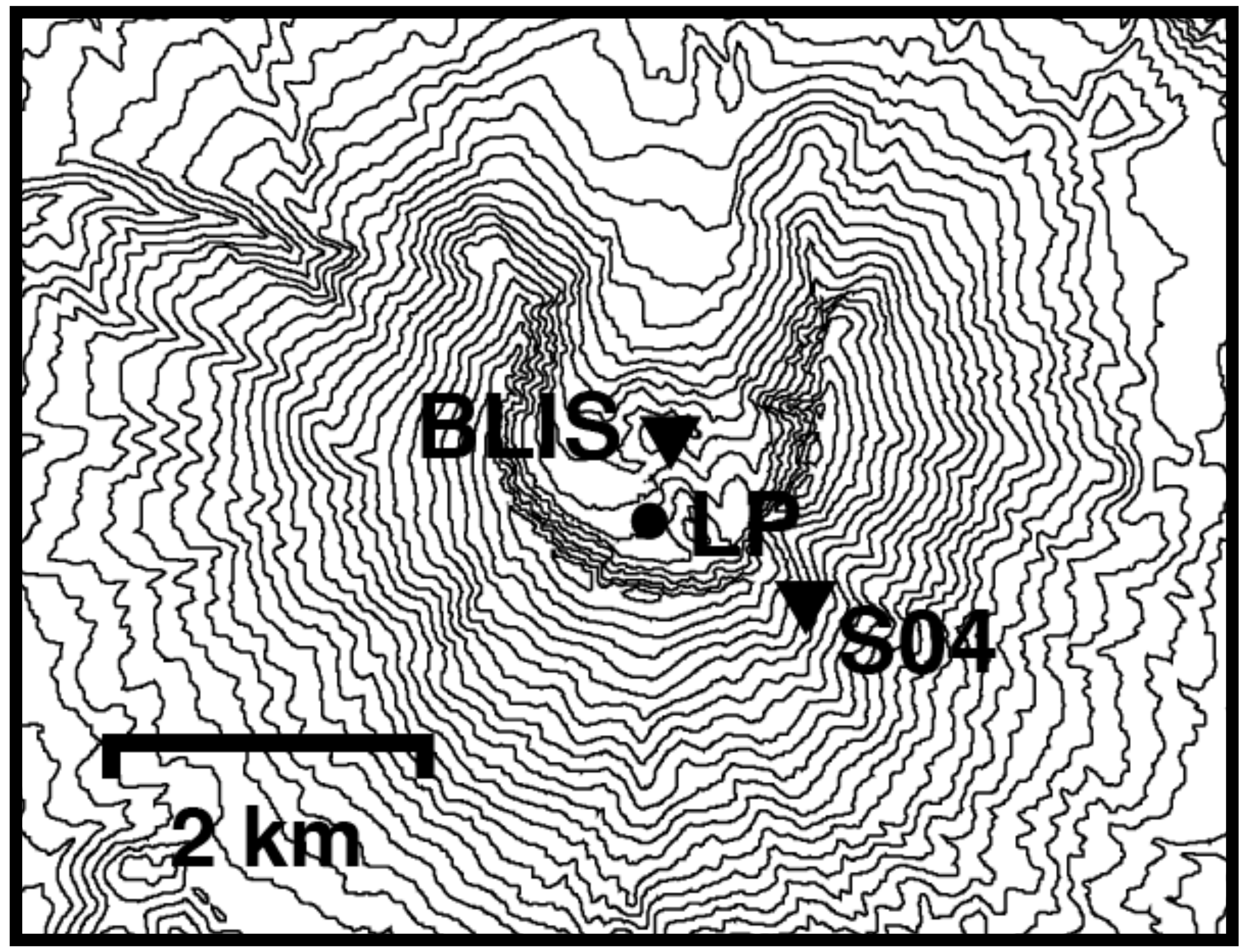

Matoza and Chouet [2010]

Single-station cross-correlation to separate event types

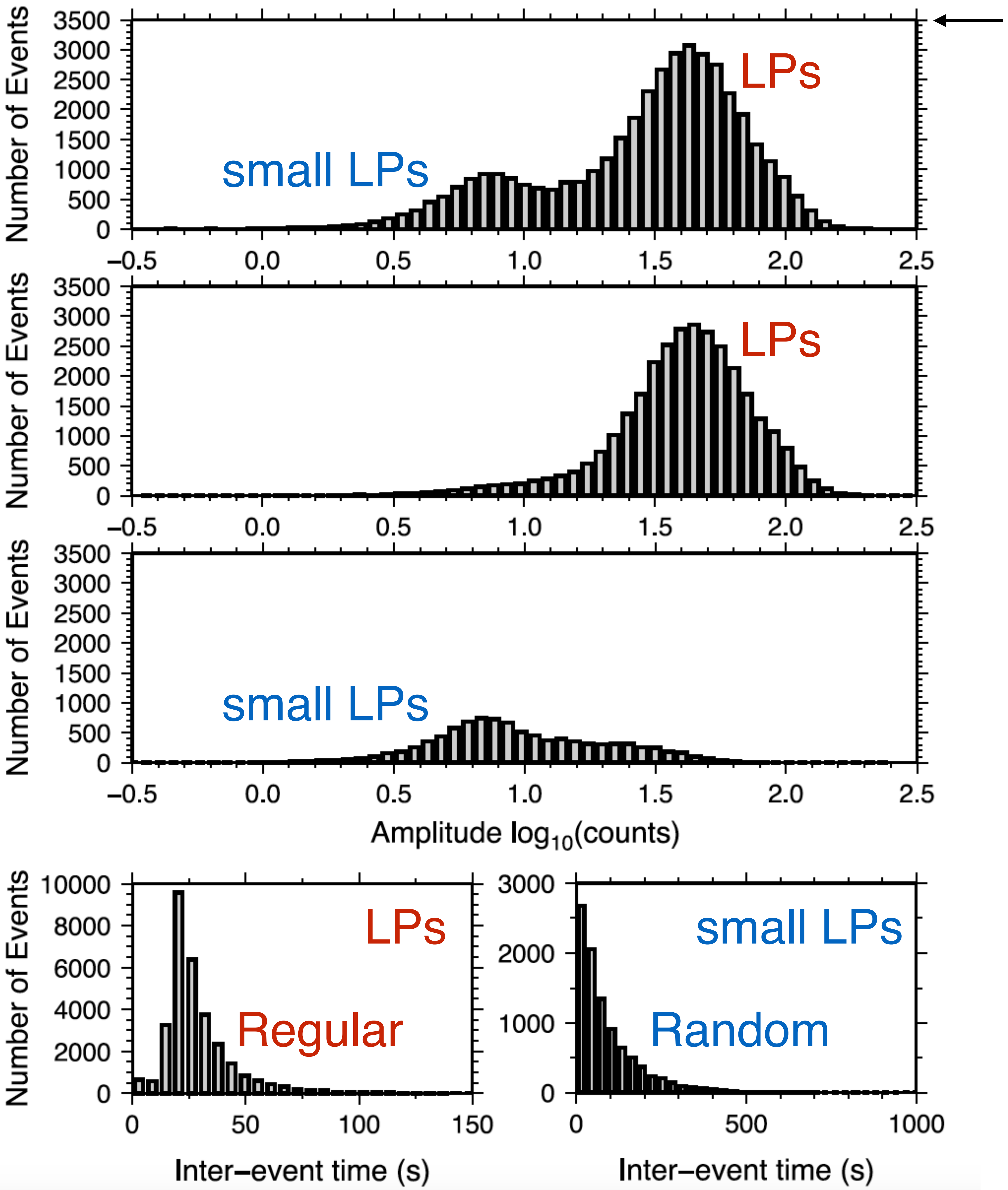

Station BLIS 4–16 November 2004

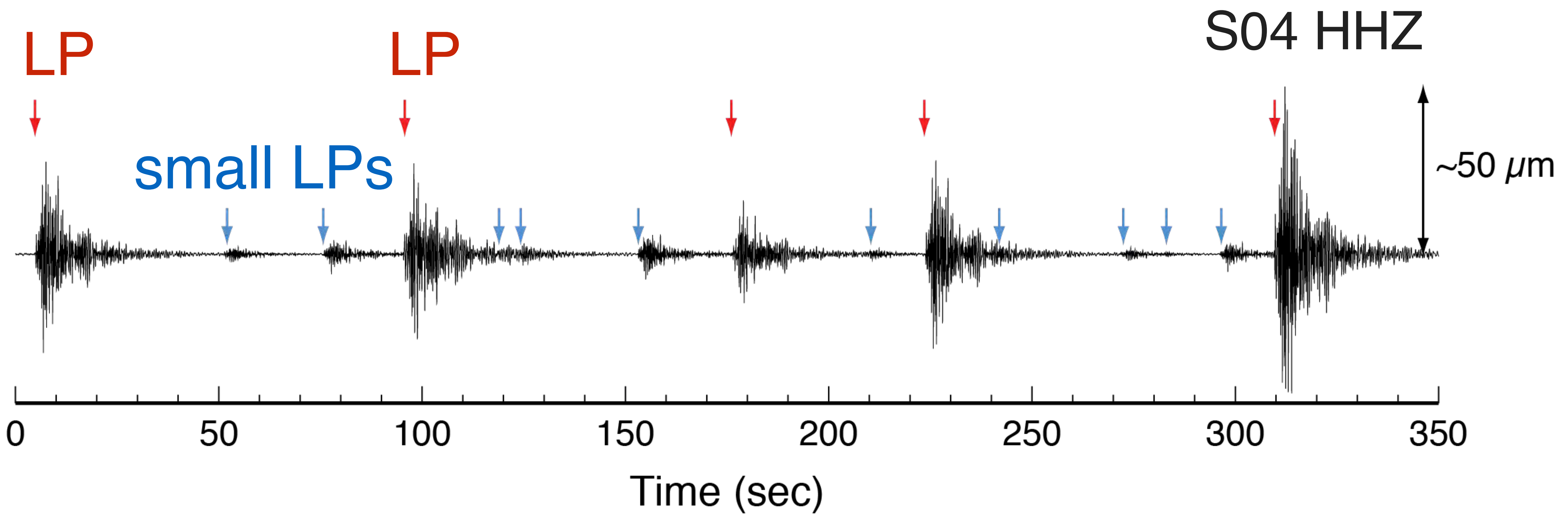

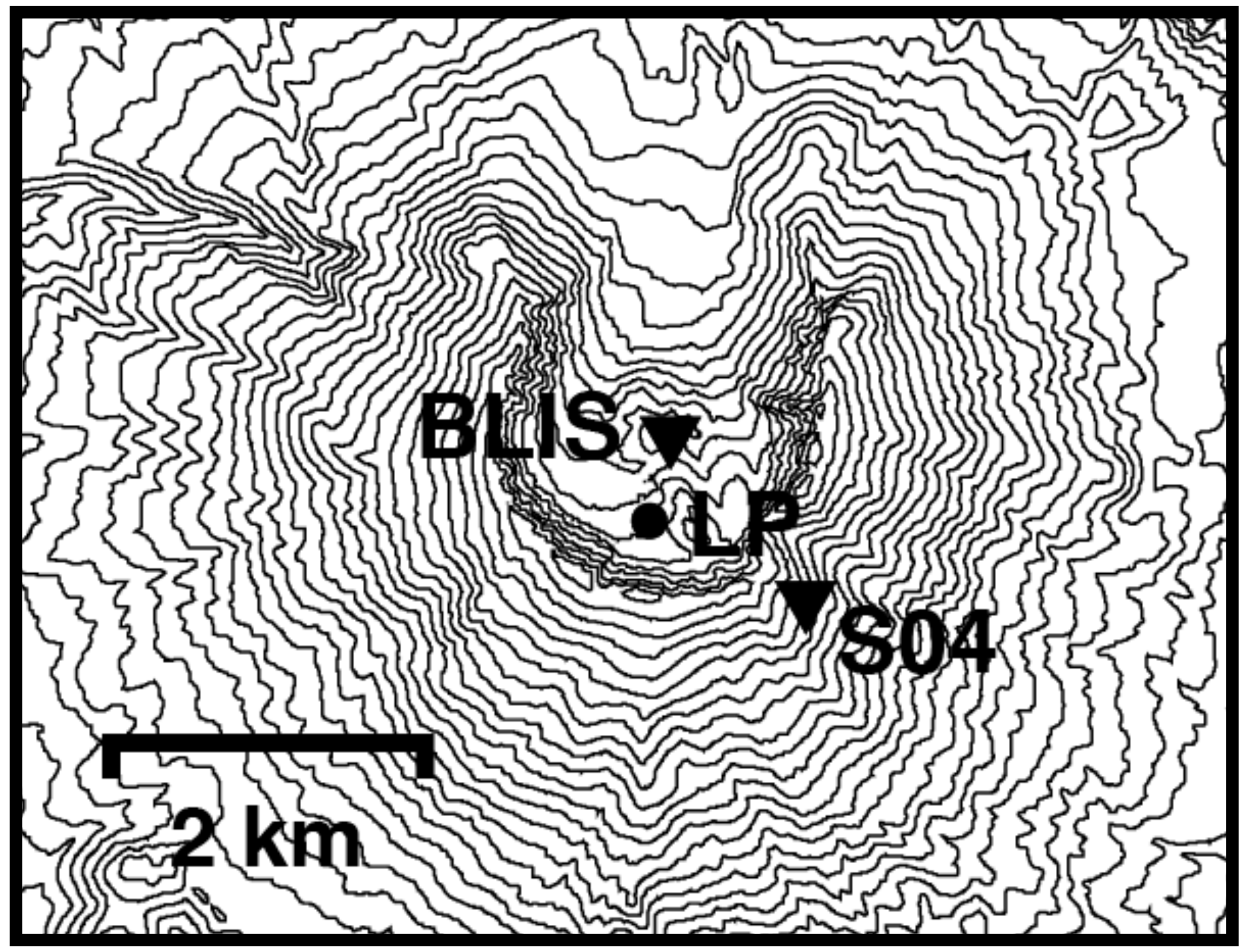

Matoza and Chouet [2010]

Network-based detection and stacking

- Employ network-based template matching and stacking to boost SNR for waveform inversion
  - e.g., *Gibbons and Ringal* [2006], *Shelly et al.* [2007], *Shelly and Hill* [2011]

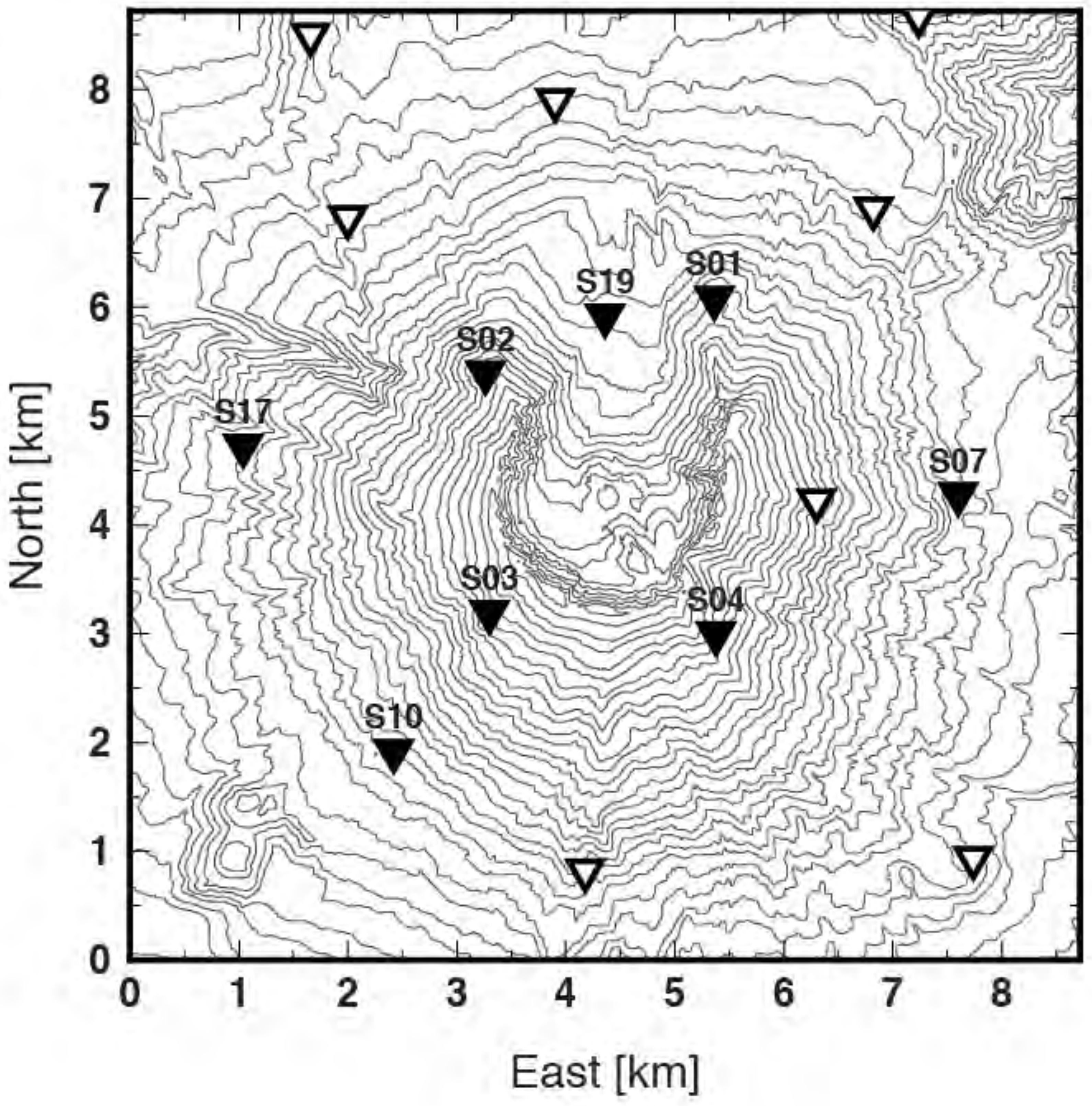

Broadband Array at Mount St. Helens [*Waite et al.,* 2008]

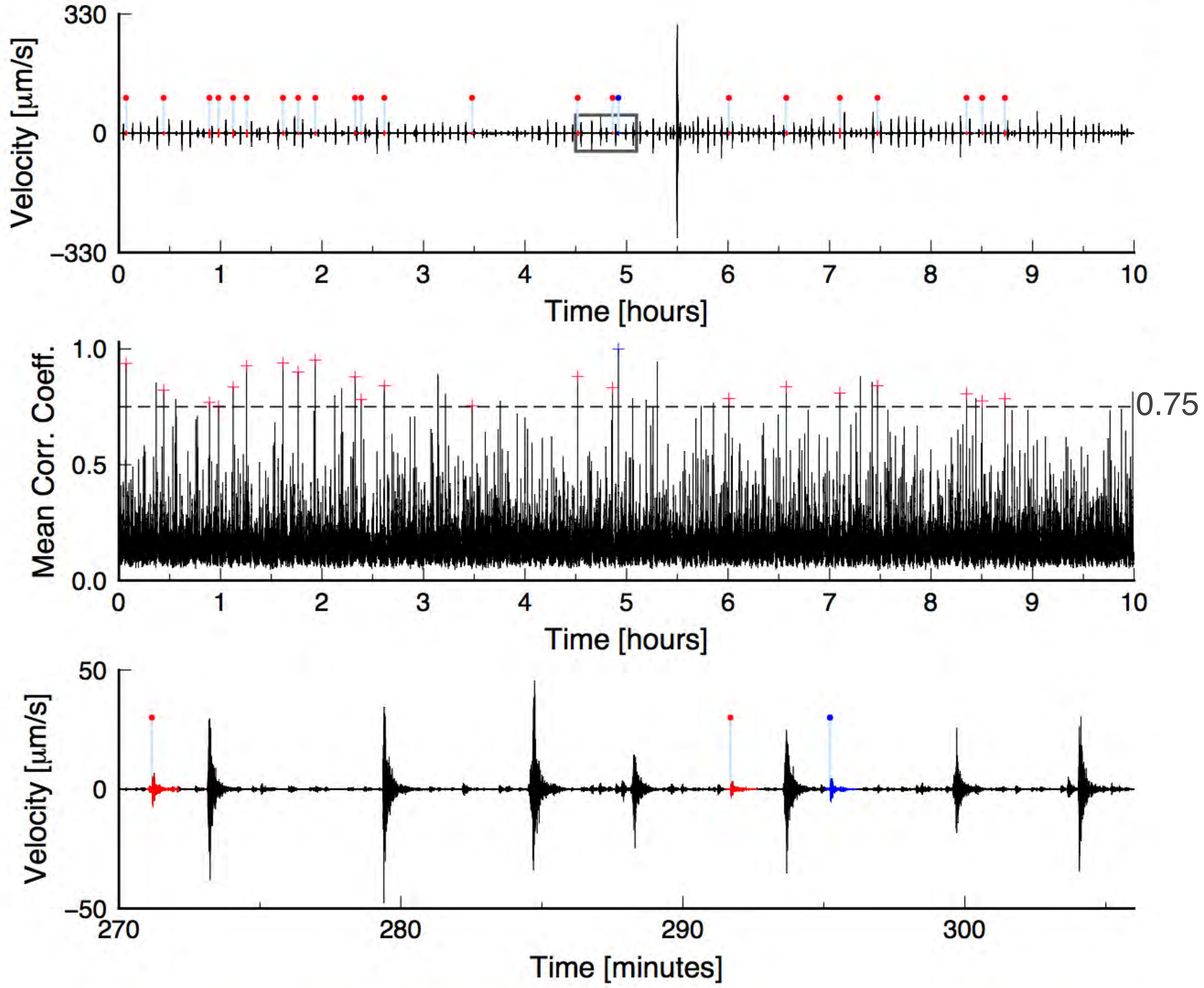

Matoza et al. [2015]

Network-based detection and stacking

- Slide initial “seed” event through 10-hr waveform; all stations and components
- Compute network-mean correlation coefficient
- Form master event; repeat using 8-days of data 29 June to 7 July 2005

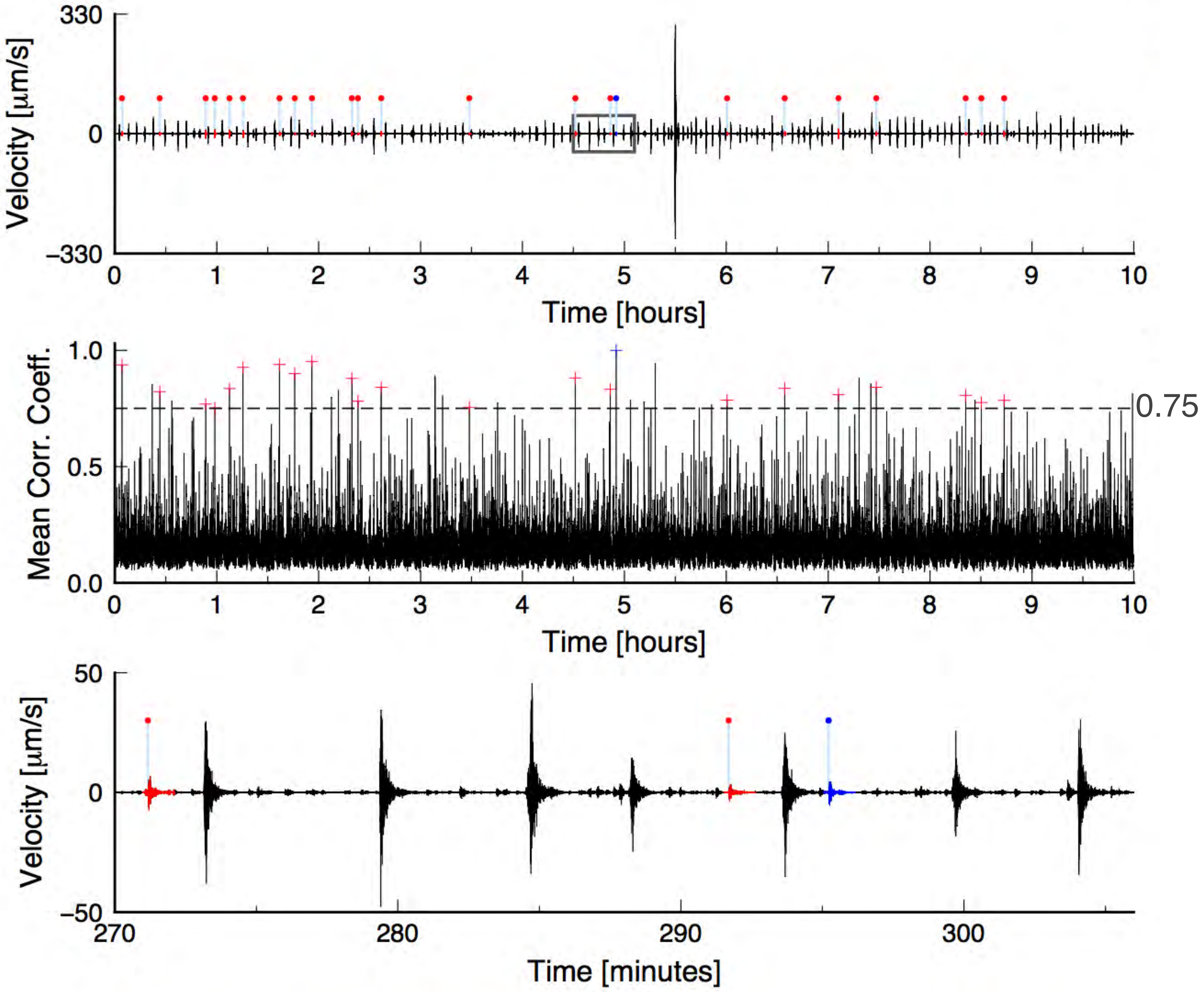

Matoza et al. [2015]

Network-based detection and stacking

- 29 June to 7 July 2005
- 8 days: 892 network triggers
- Stack 359 high-quality triggers
- Linear (mean) stack in 2-hr periods
- Phase-weight stack the 2-hr stacks
  [*Schimmel et al.*, 2011; *Thurber et al.*, 2014]
- tf-PWS: Coherence of instantaneous phase
- Repeat for all stations and components

Example at station S04

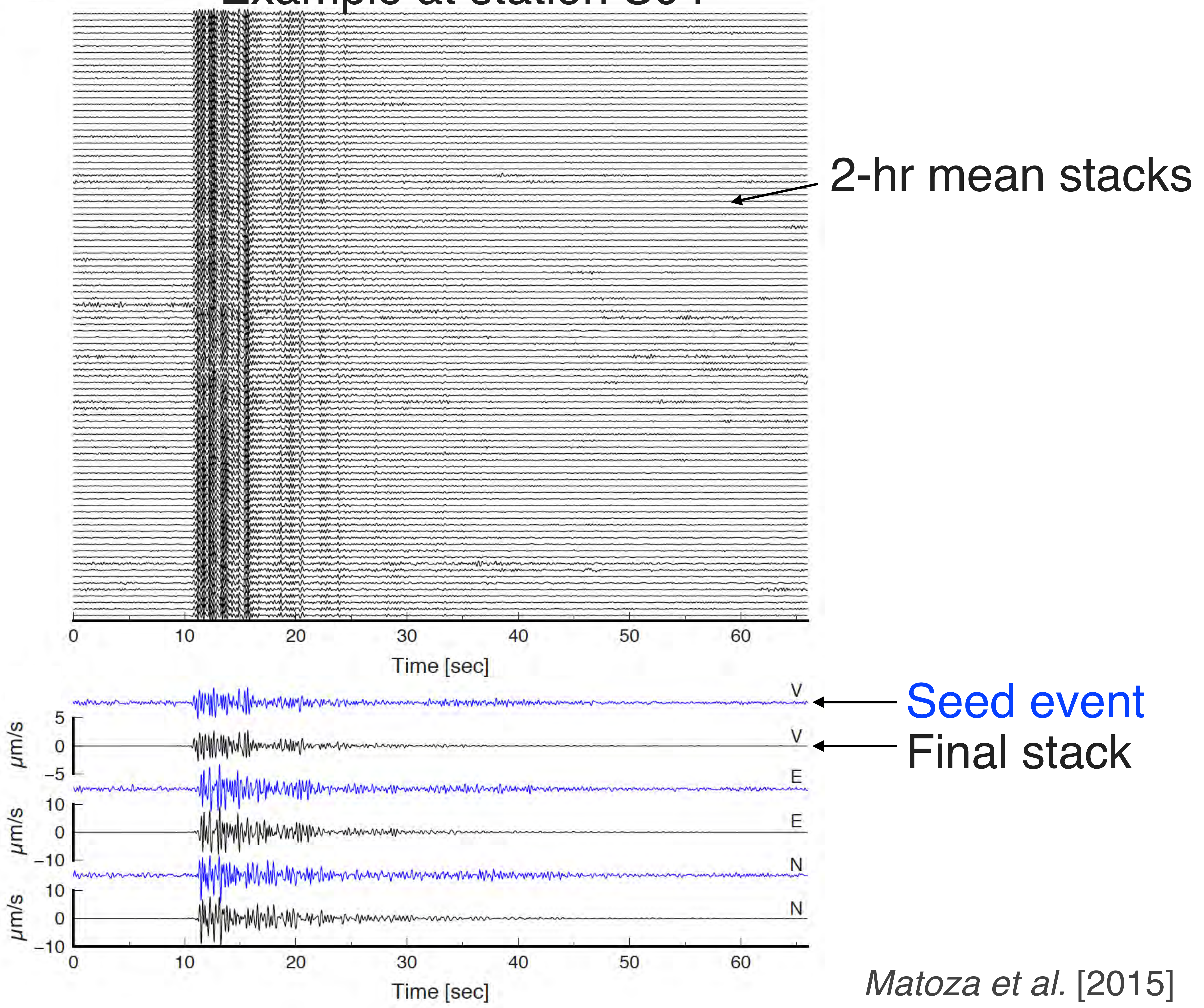

Matoza et al. [2015]

Full-waveform inversion

- Full seismic waveform inversion for a point-source moment-tensor and single force vector representation of the source [e.g., *Ohminato et al.* 1998; *Chouet et al.* 2003; *Dawson et al.* 2011; *Matoza et al.,* 2015]
- A free inversion without constraining the source geometry.

Moment-tensor

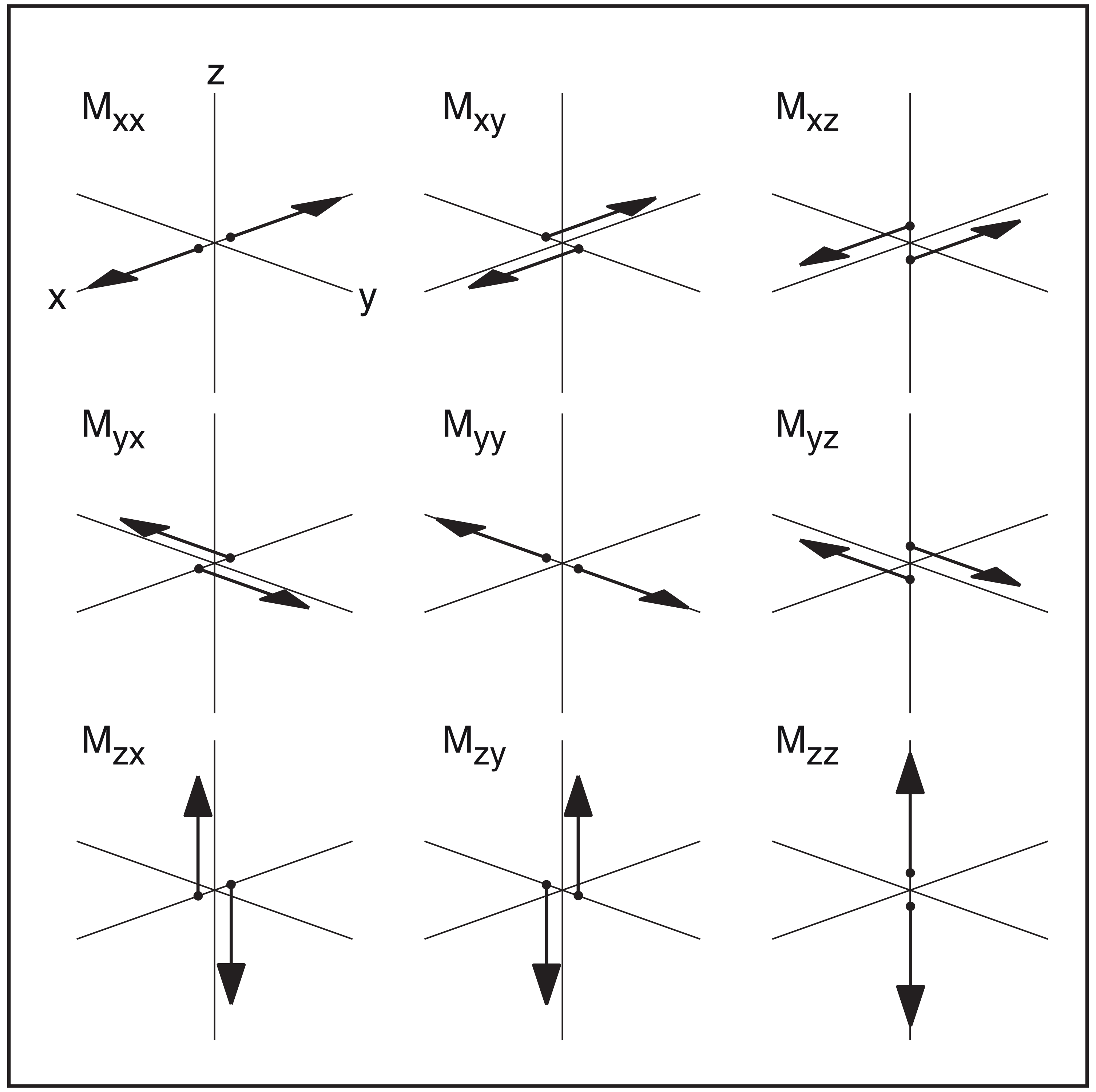

$$\mathbf{M} = \begin{bmatrix} M_{xx} & M_{xy} & M_{xz} \\ M_{yx} & M_{yy} & M_{yz} \\ M_{zx} & M_{zy} & M_{zz} \end{bmatrix}$$

$$\mathbf{F} = \begin{bmatrix} F_x \\ F_y \\ F_z \end{bmatrix}$$

Full waveform inversion:
fit the whole waveform

Observed
Synthetic

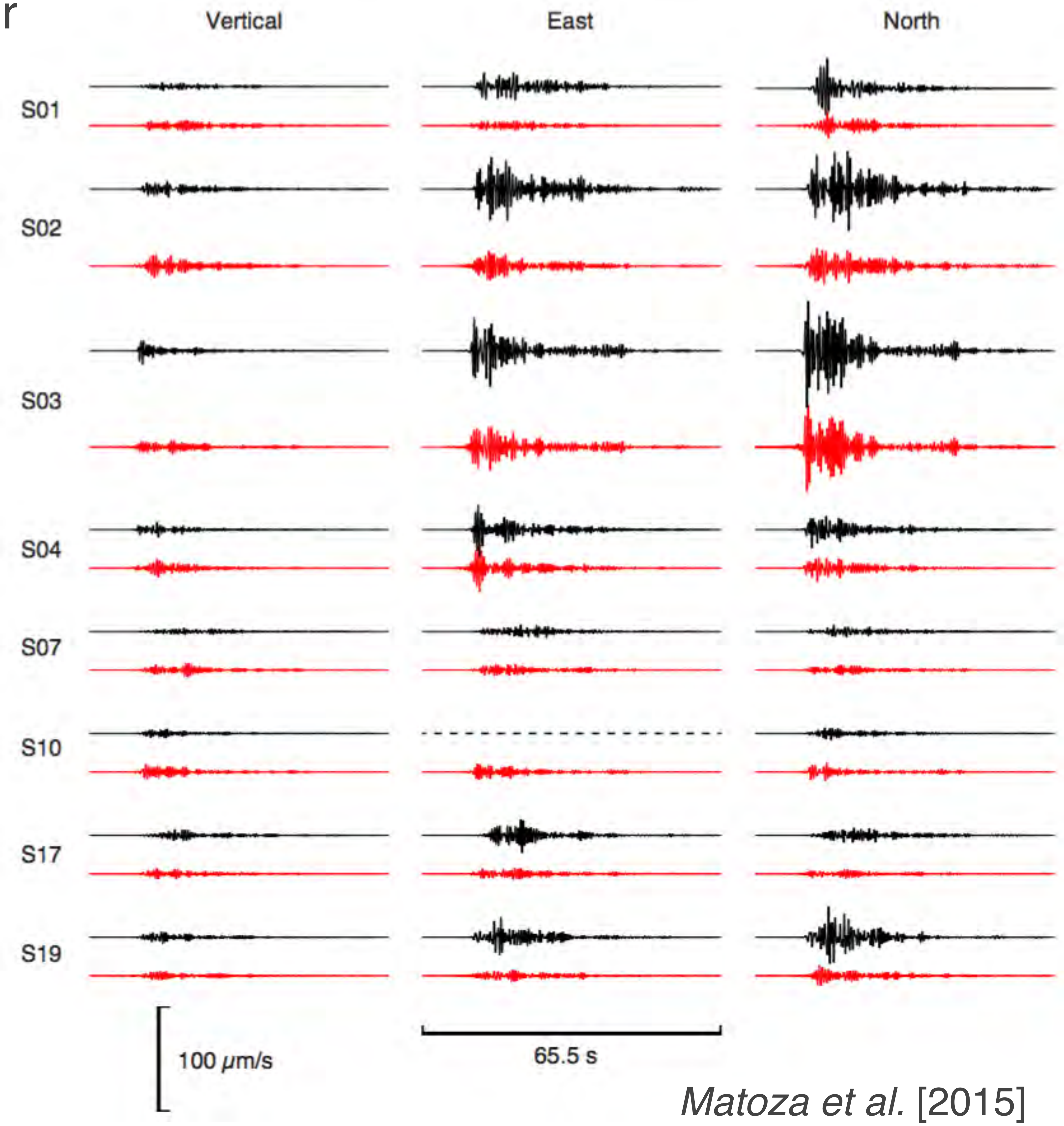

Matoza et al. [2015]

Full-waveform inversion

- Green's functions estimated using 3D finite-differences [*Ohminato et al.*, 1998] with 20-m discretized topography
- 3D velocity model of *Waite and Moran* [2009]

$$u_n(\underline{x}, t) = M_{pq}(t) * G_{np,q}(\underline{x}, t) + F_p(t) * G_{np}(\underline{x}, t),$$

ground displacement | moment-tensor | Green's fn., spatial deriv. | Force vector | Green's fn.

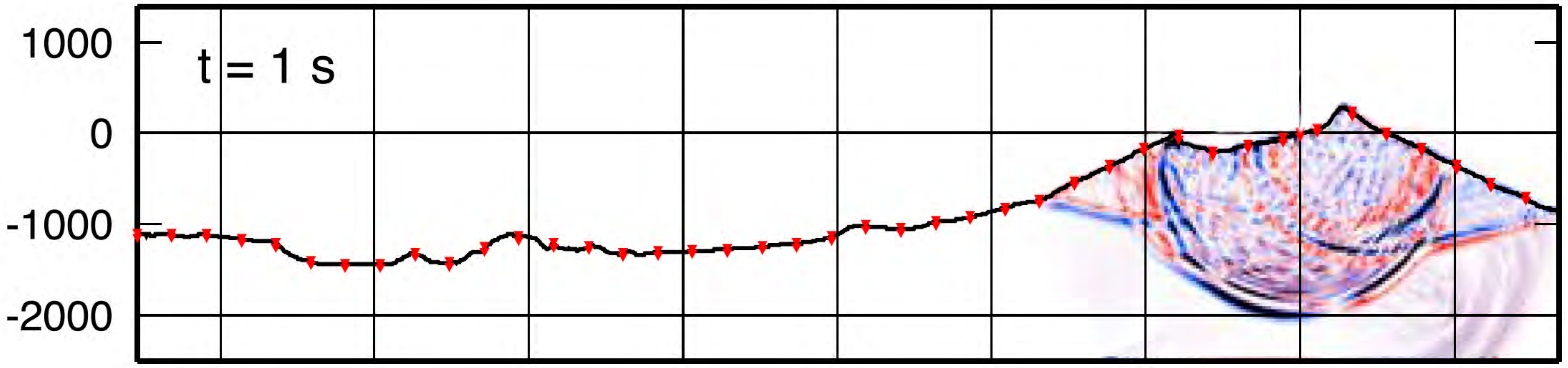

Compute using 3D finite differences [Ohminato and Chouet,1997]

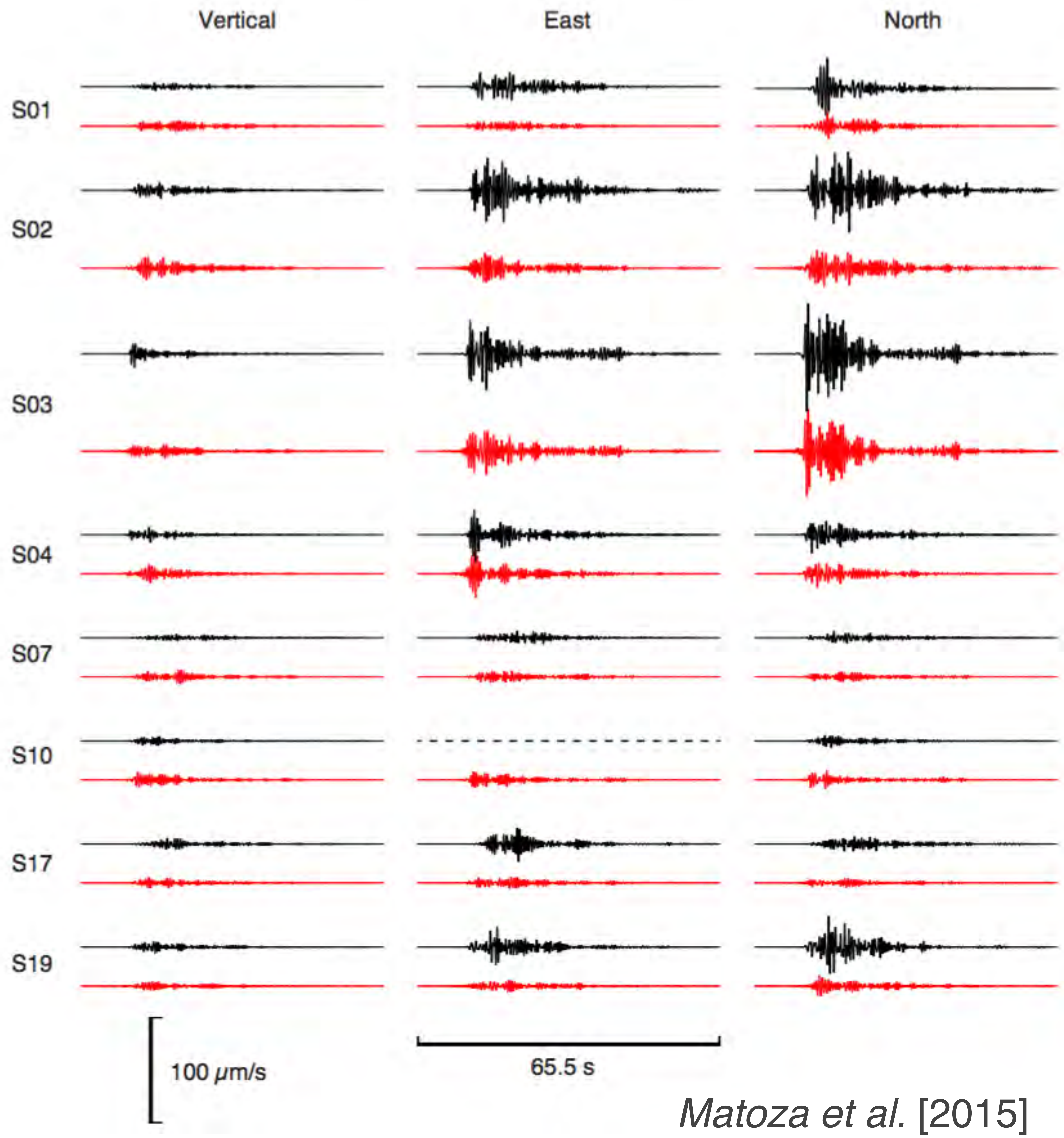

Observed
Synthetic

Matoza et al. [2015]

Full-waveform inversion of a single subevent multiplet

- Perform a grid search over trial source nodes with increasing spatial density
- Define solution with the minimum E_1 residual error and a metric for waveform stability

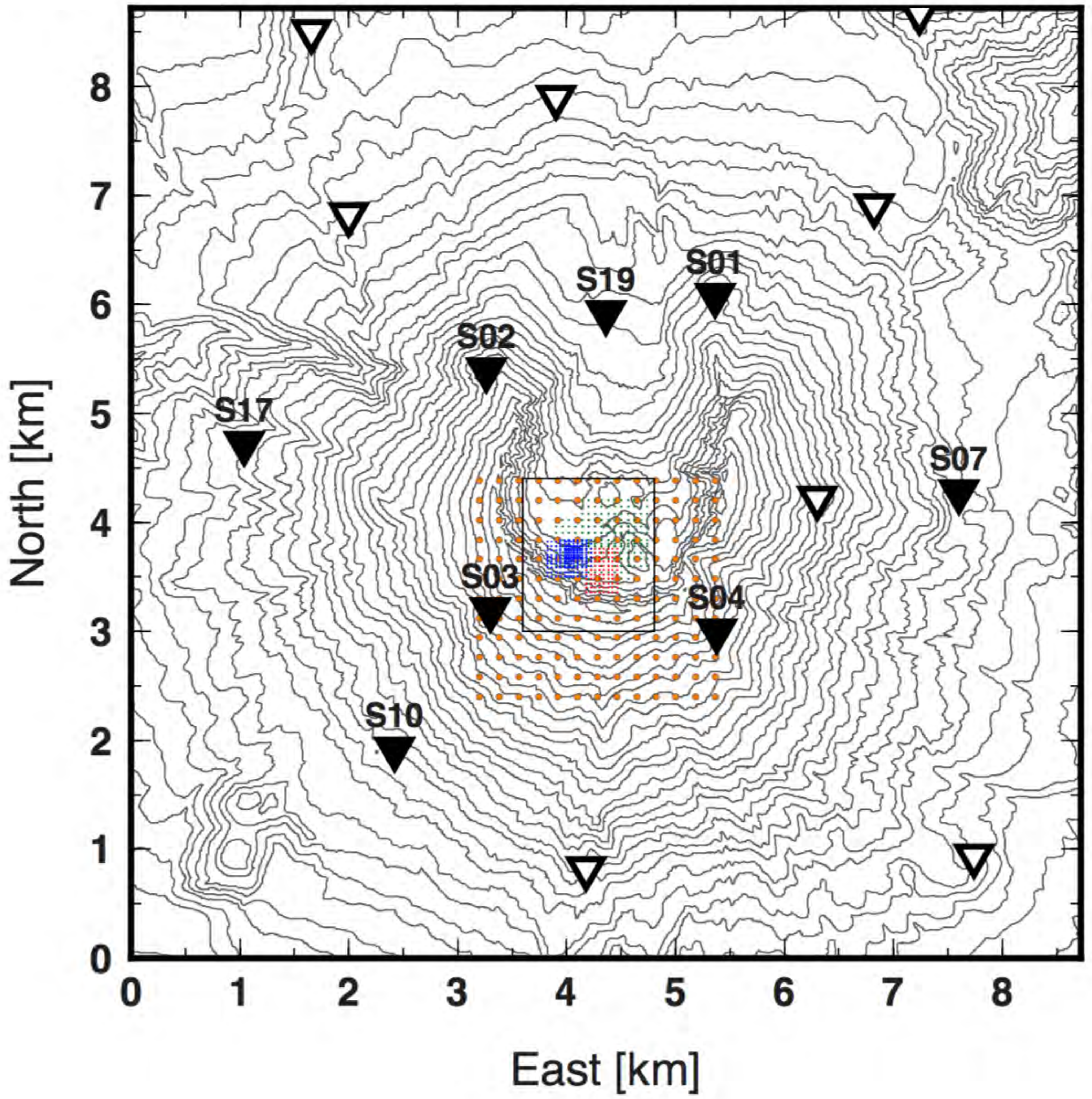

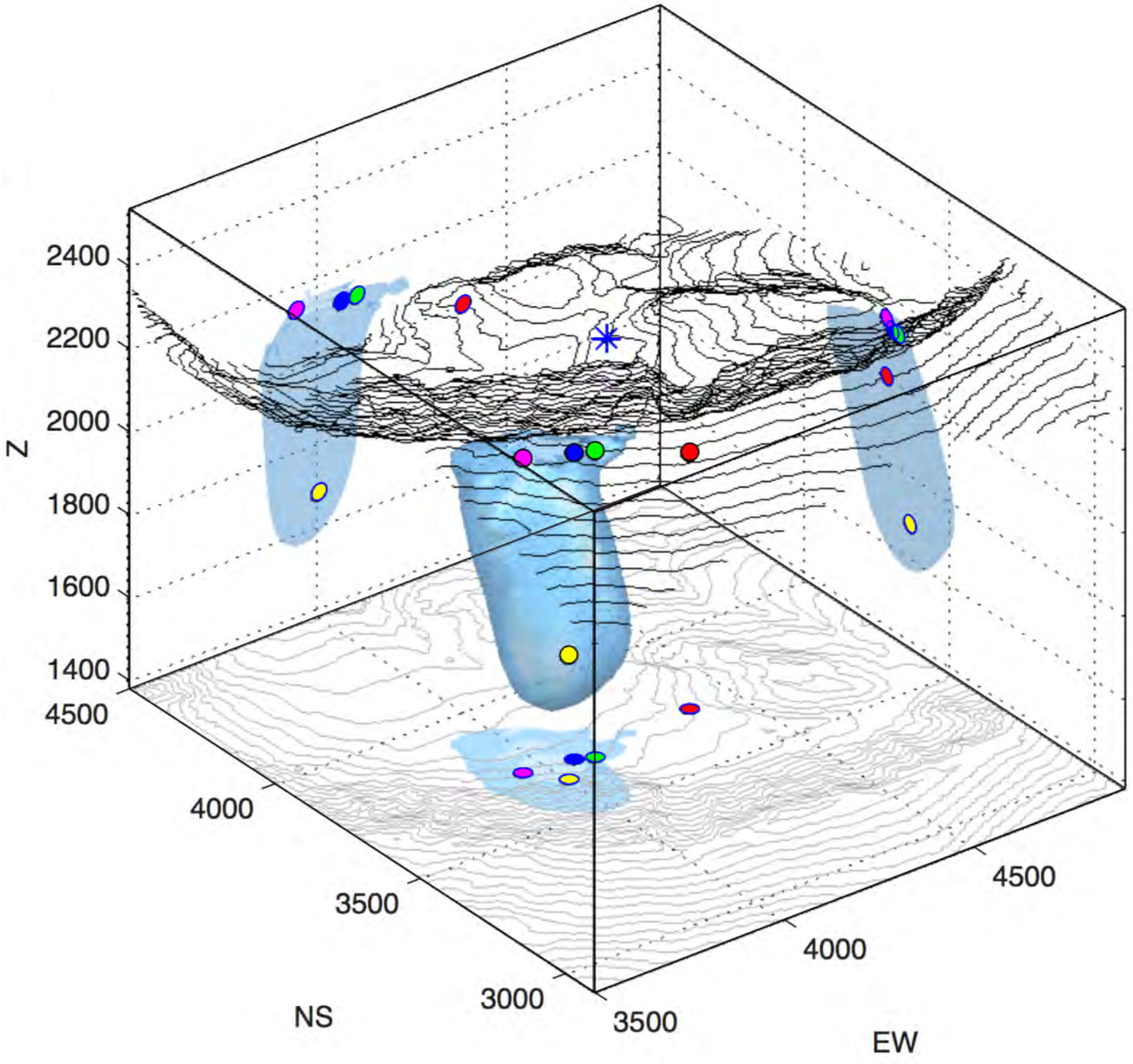

5% E1 residual isosurface

$$E_1 = \frac{\sum_{n=1}^{N_\tau} \sum_{p=1}^{N_s} (u_n^o(p\Delta t) - u_n^s(p\Delta t))^2}{\sum_{n=1}^{N_\tau} \sum_{p=1}^{N_s} (u_n^o(p\Delta t))^2}$$

$$\gamma = [\sigma^2(3\frac{\alpha_1}{\alpha_3}) + \sigma^2(3\frac{\alpha_2}{\alpha_3})]^{\frac{1}{2}}$$

Standard deviation of the moment-tensor eigenvalues

Matoza et al. [2015]

Full-waveform inversion of a single subevent multiplet

- Volumetric ~10 m^3 source mechanism consistent with subhorizontal crack (assume Poisson solid, μ = 12 GPa)
- Shallow depth ~30 m in southern part of crater

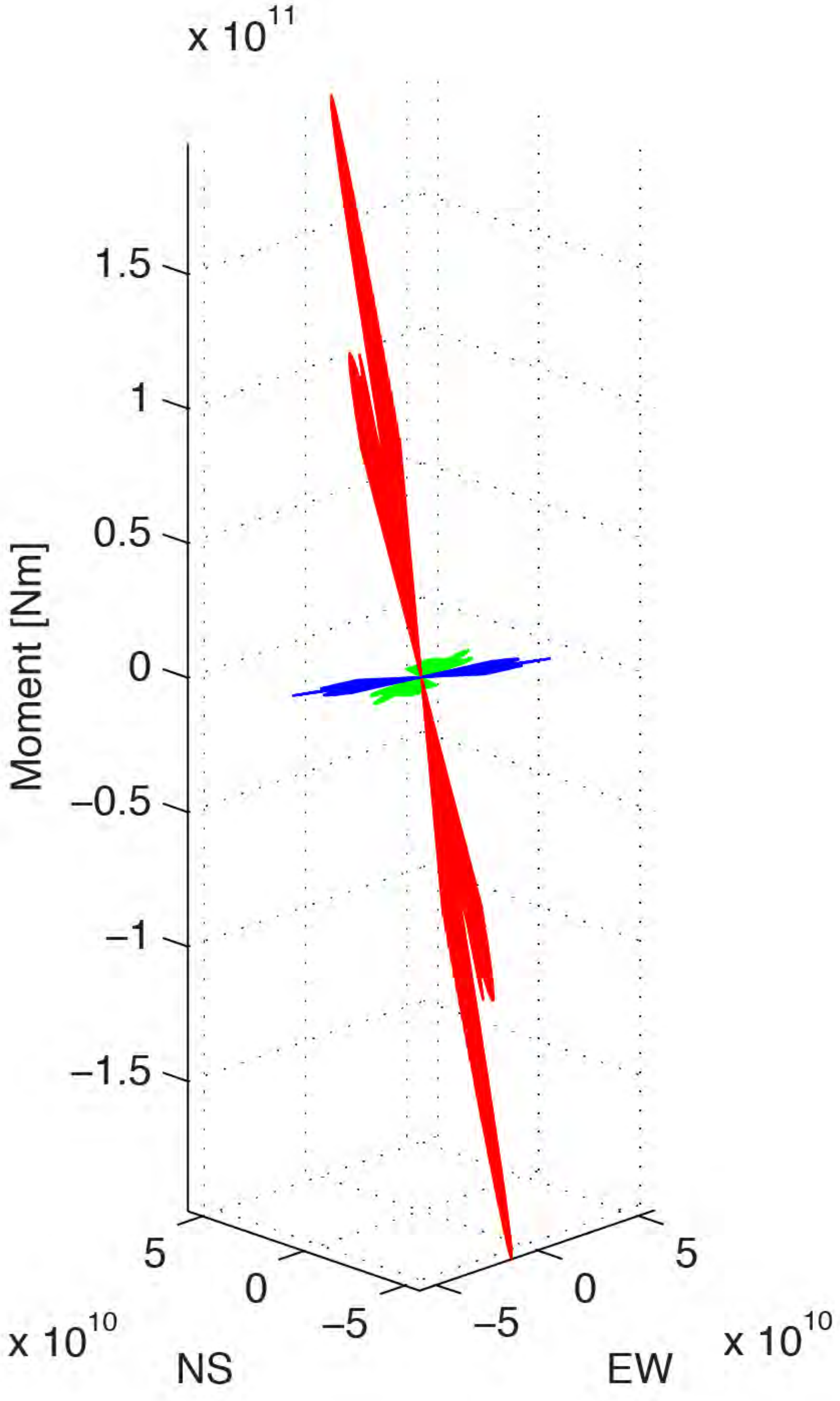

Moment tensor eigenvectors, scaled by eigenvalues

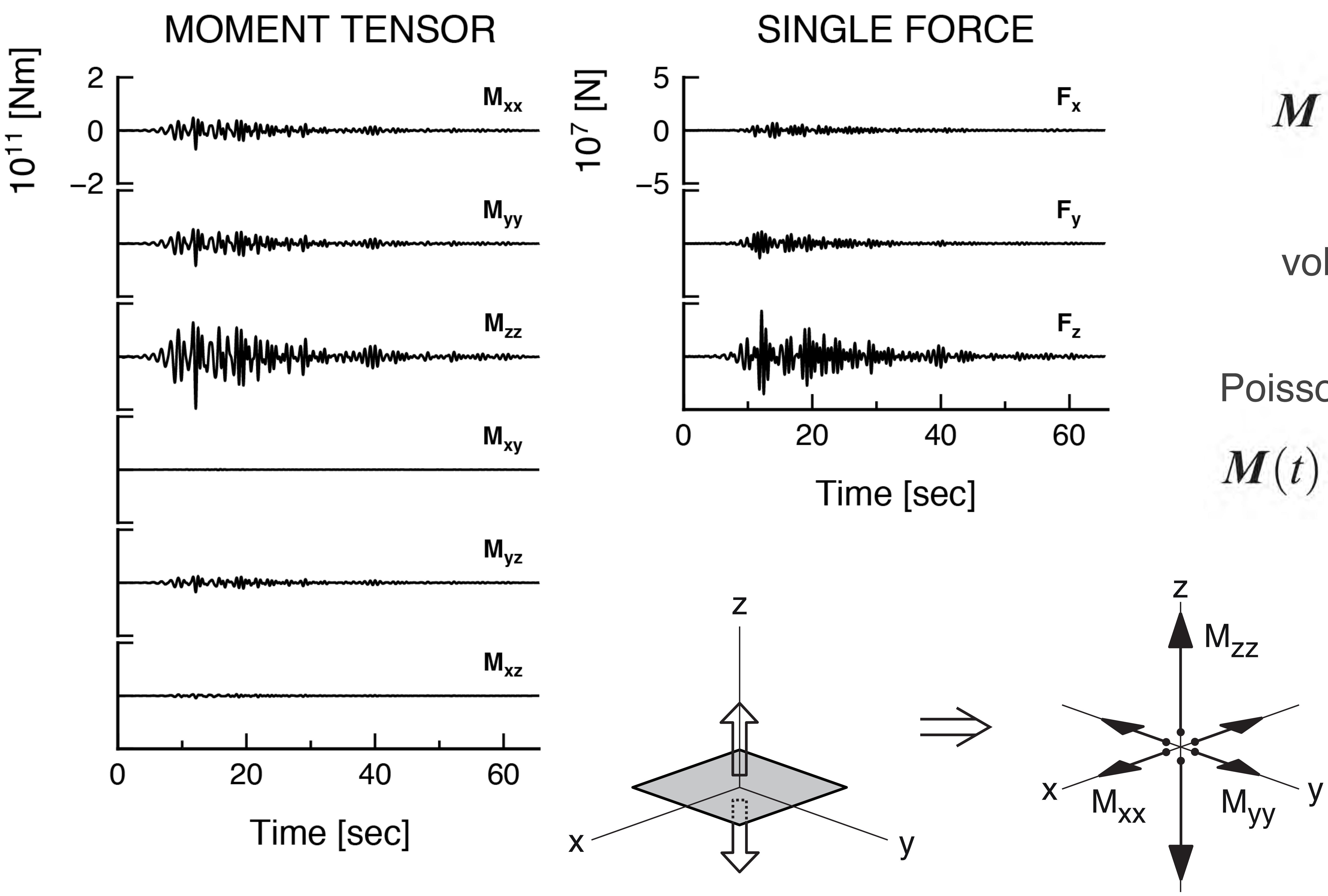

Horizontal crack moment-tensor:

$$\boldsymbol{M} = \underbrace{\Delta V}_{\text{volume change}} \begin{pmatrix} \lambda & 0 & 0 \\ 0 & \lambda & 0 \\ 0 & 0 & \lambda + 2\mu \end{pmatrix}$$

Poisson solid ($\lambda = \mu$):

$$\boldsymbol{M}(t) = 2\mu \underbrace{LWu(t)}_{\text{e.g., rectangular crack } L \times W} \begin{pmatrix} 1 & 0 & 0 \\ 0 & 1 & 0 \\ 0 & 0 & 3 \end{pmatrix}$$

Matoza et al. [2015]

Interpretation

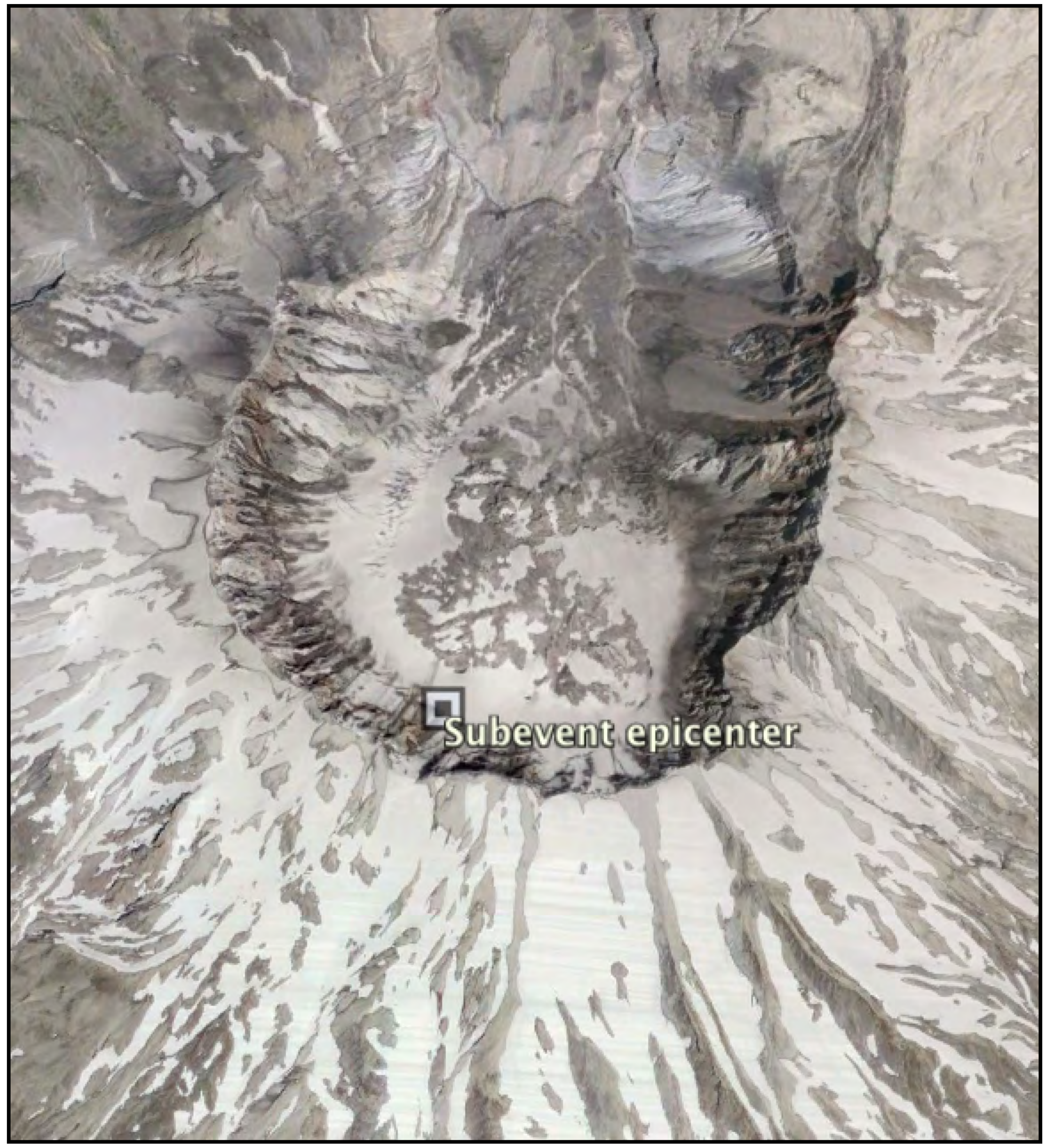

- Interaction point between shallow hydrothermal system and cool meteoric water in outer flank, e.g., snow melt
- Sudden condensation of metastable steam [*Thiéry and Mercury,* 2009]
- Horizontal structure feasible
- ~500 m depth below pre-1980 summit in old volcanic center

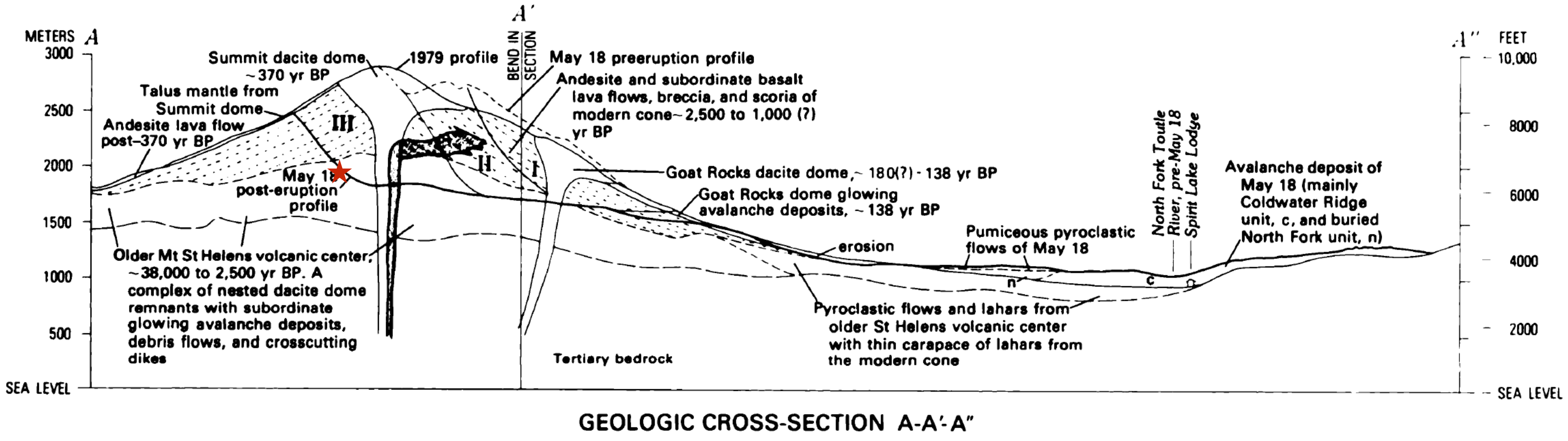

Figure 205.—Cross section A-A" showing August 1979 and May 18 preeruption profiles, and May 18 posteruption profile. Geology of cone from C. A. Hopson, based on unpublished pre–May 18 mapping and inspection of amphitheater. Slide boundaries I (red), II (blue), and III (black) are approximately located, but precise configuration at depth is uncertain. Dacite intrusion of March–May 1980 indicated by light-red pattern.

Voight et al. [1981]

Velocity structure

- Waite and Moran [2008]: simple structure in shallow subsurface with spatial heterogeneities on the order of ~1 km
- Waveform inversions limited to <2 Hz [*Waite et al.*, 2008; *Matoza et al.* 2015]
- Source depth below crater floor: LP events ~200 m; subevents ~30 m [*Waite et al.*, 2008; *Matoza et al.* 2015]

G.P. Waite, S.C. Moran / Journal of Volcanology and Geothermal Research 182 (2009) 113–122

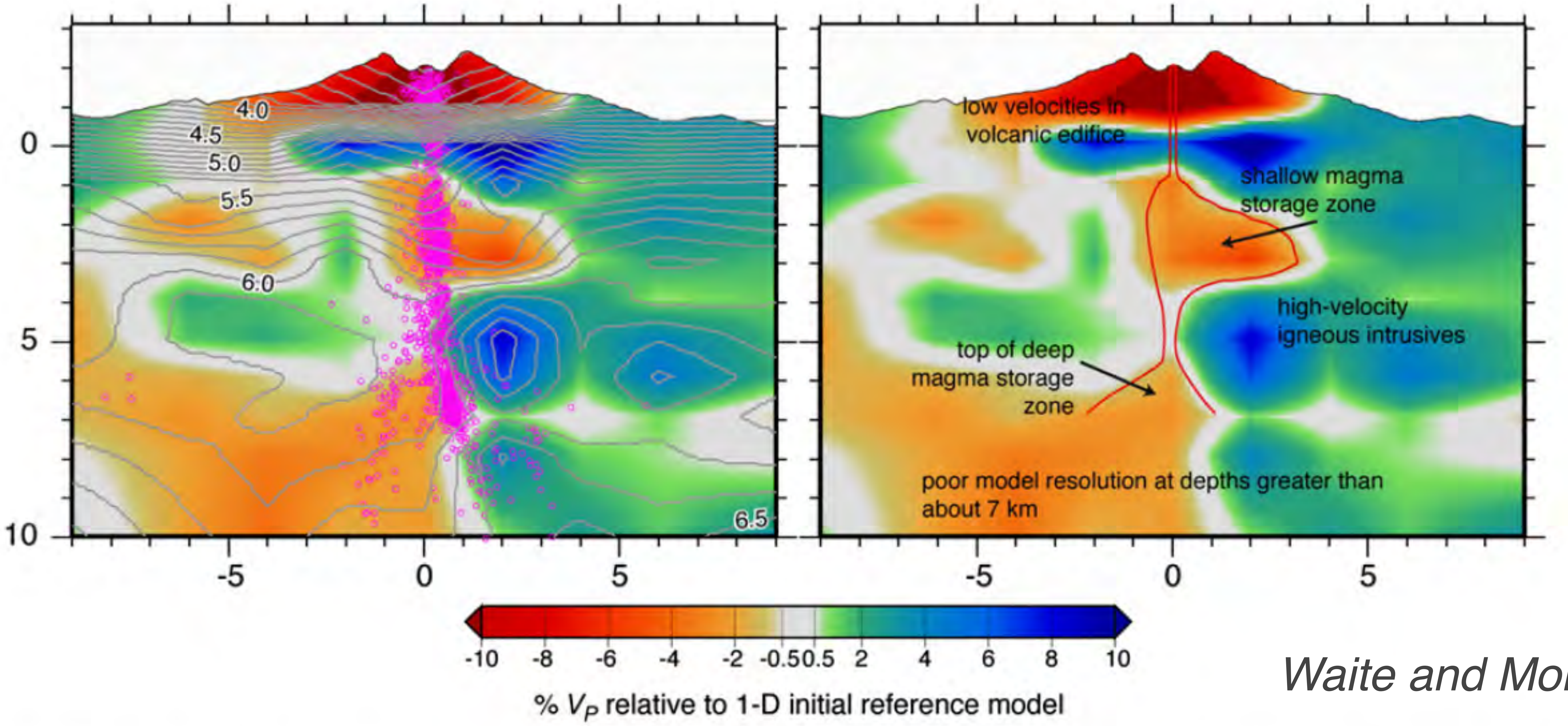

Waite and Moran [2008]

Fig. 7. A west–east cross section through a single fine-grid model highlights the low velocity anomaly directly beneath the volcano. There is no vertical exaggeration.

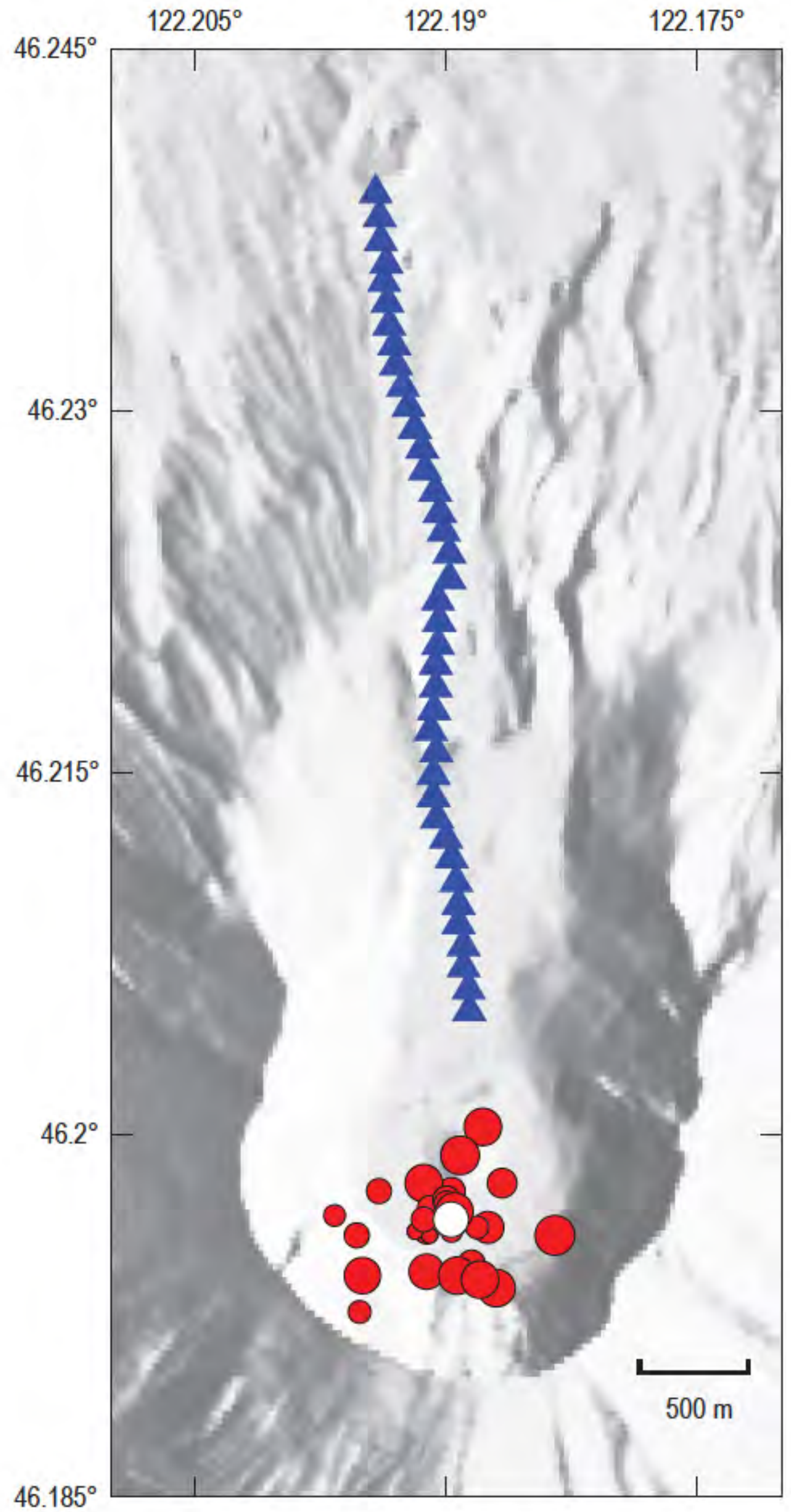

Figure 14. Instrument layout (blue triangles) with earthquake epicenters (red dots) used for P-wave inversion. Epicenter of primary earthquake used in inversion is shown by white dot.

<2 km 1D *P*-wave model
Thelen et al. [2008]

Future Work: Better imaging of near-surface velocity structure

- Improved knowledge of shallow subsurface velocity structure at volcanoes (upper 500 m, within edifice)
- Resolve controversies about source vs. path effects
- Better constrained full-waveform inversion of smaller and higher frequency sources

seismogram: $w(t) = s(t) * l(t) * g(t)$

excitation/trigger — $s(t)$; crack/conduit resonance — $l(t)$; path & site effects — $g(t)$

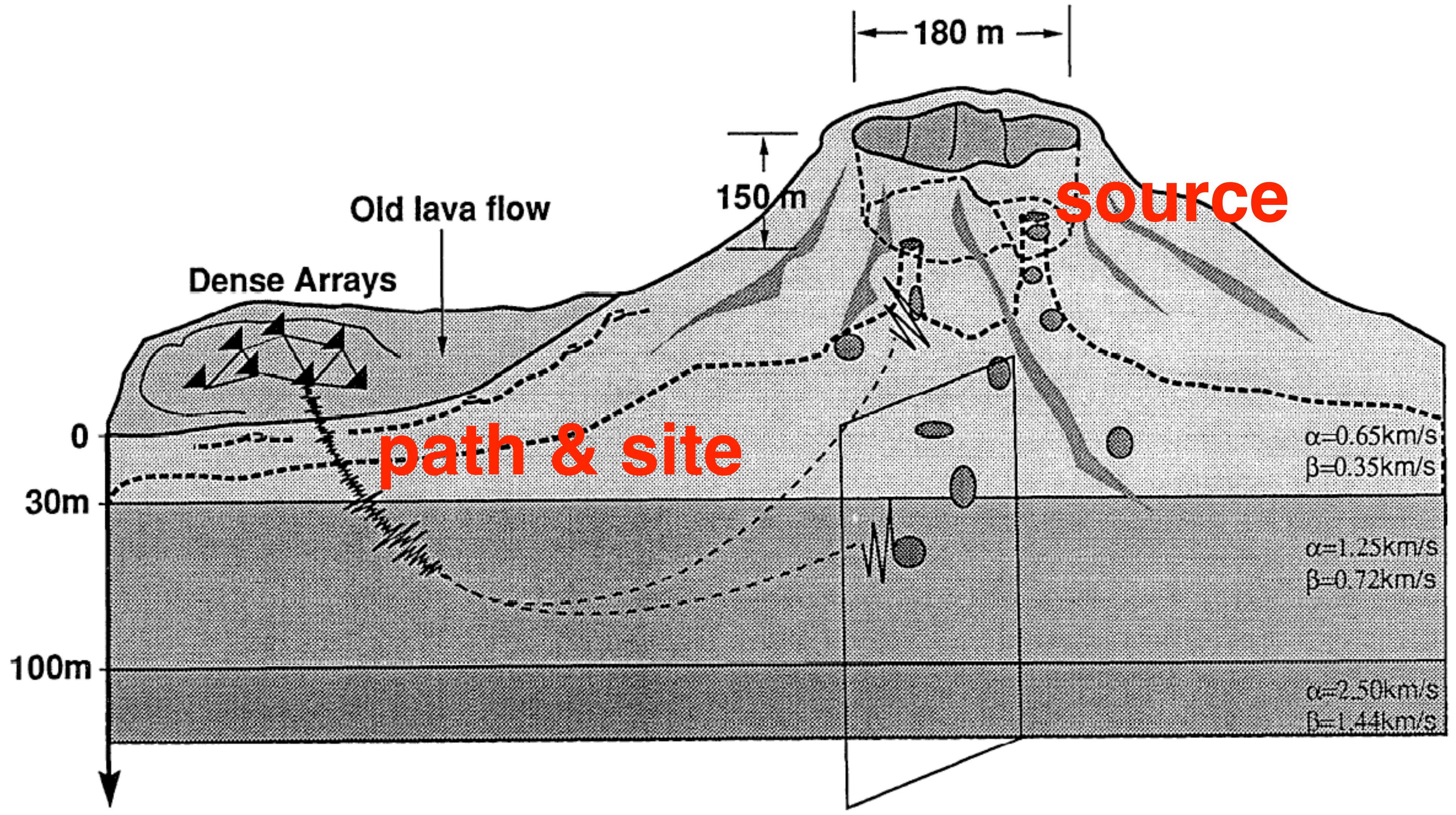

Goldstein and Chouet [1994]

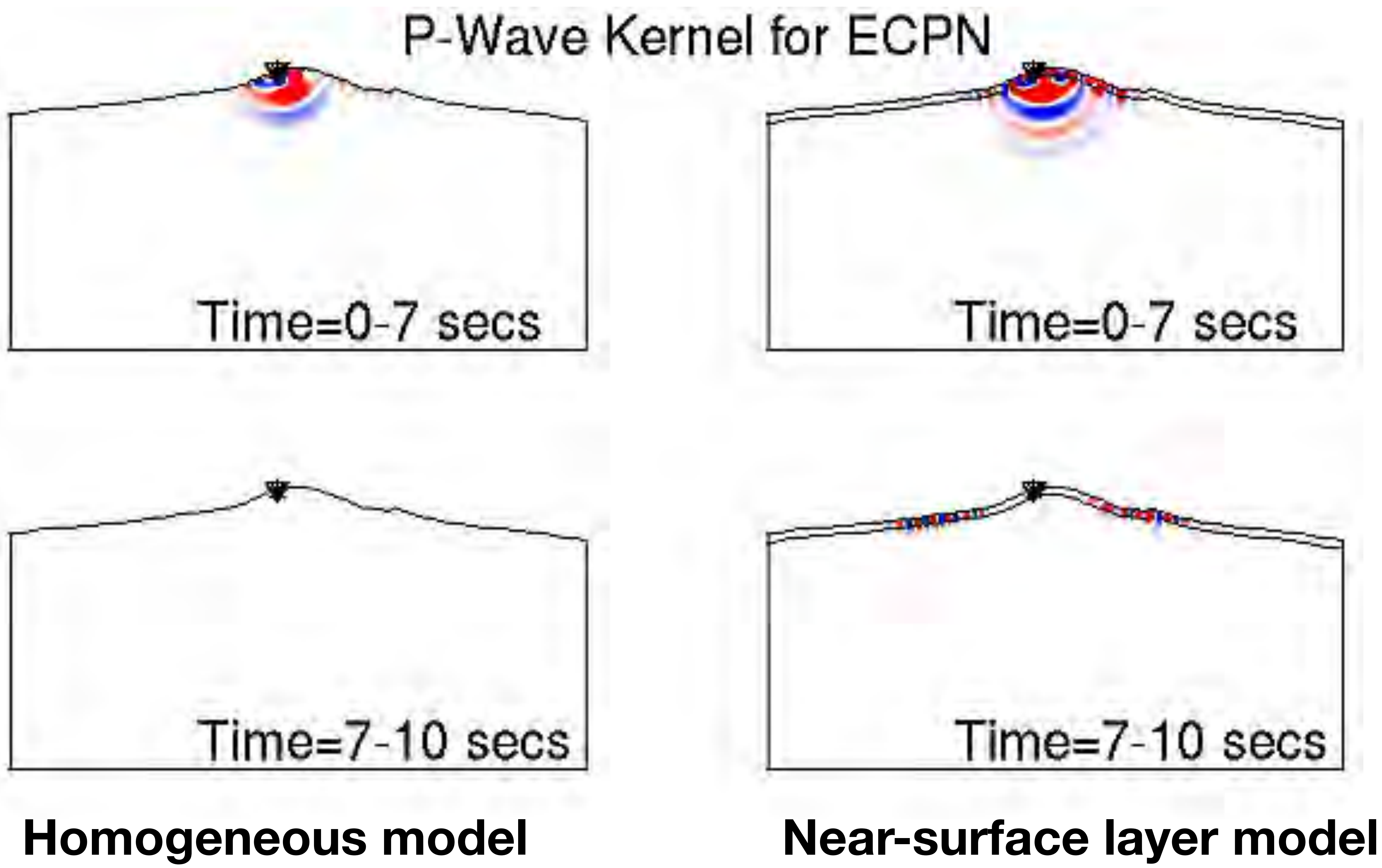

Bean et al. [2008]

Yasur Volcano, Vanuatu, July 2016

- Frequently active and accessible, ~300 m edifice
- “Strombolian” style activity: high-amplitude explosions every ~1–5 minutes from 2–3 main eruptive vents
- Regularly recorded at International Monitoring System infrasound station IS22, New Caledonia (400 km)

image: A. Austin

Collaborative multi-parametric field experiment

26 July to 2 August 2016

Seismic data

- 11 broadband seismometers (Trillium Compact 120 s; Omnirecs DATA-CUBE digitizer)

Infrasound data

- 6 single infrasound sensors (Chaparral C60V)
- 7 small-aperture 3-element infrasound arrays
- 2 tethered balloon infrasound systems

Gas geochemistry data

- FTIR
- 2 scanning Flyspecs (SO_2)

Imaging data

- High-frame rate DSLR
- UAV DJI Phantom
- Go-Pro cameras
- FLIR (infrared)

Geologic samples

- Scoria and ash samples for petrologic analysis

Seismo-acoustic network

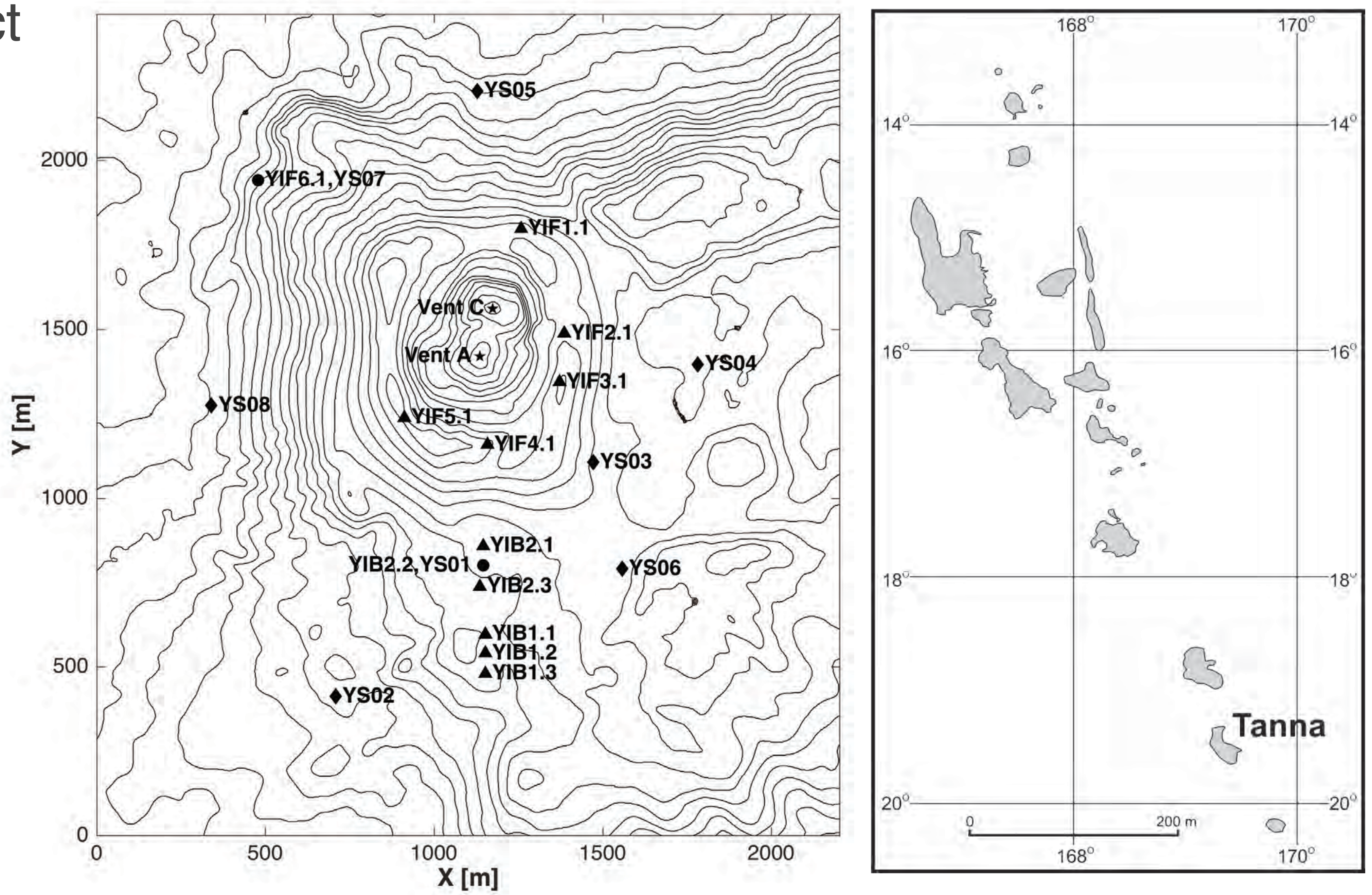

YS: seismic; **YI**: infrasound
Contour interval: 20 m

University of California, Santa Barbara; GNS New Zealand; University of Alaska Fairbanks; University of Canterbury, New Zealand

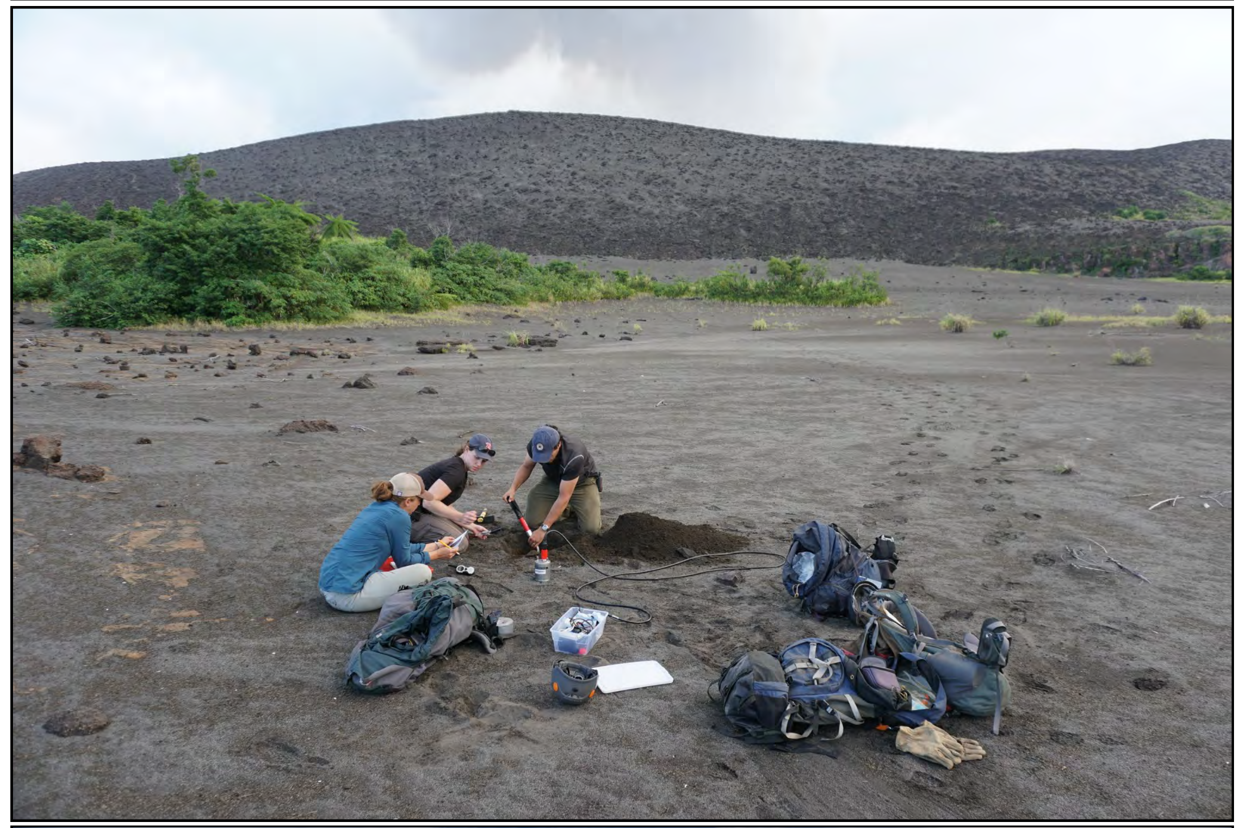

Rapid deployment of broadband network

- Nanometrics Trillium Compact 120-s post-hole
- Omnirecs DATA-CUBE digitizer
- 8 x D-Cell battery pack per 4 days

image: D. Fee

Seismo-acoustic data

26 July to 2 August 2016

- First order event detection with network-coincident STA/LTA automatic triggering
- 6-day dataset, >8,400 infrasound explosions, >10,400 seismic events
- ~1–2 events per minute

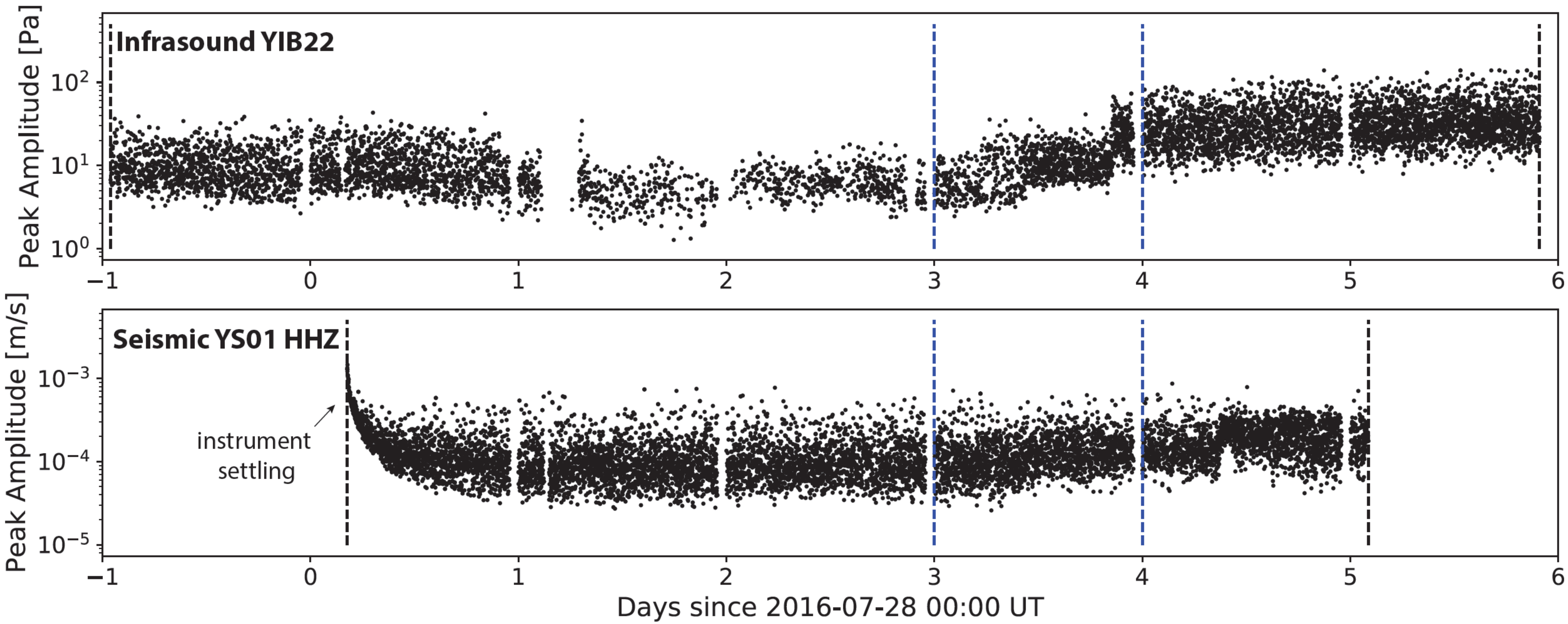

Seismo-acoustic data

26 July to 2 August 2016

- First order event detection with network-coincident STA/LTA automatic triggering
- 6-day dataset, >8,400 infrasound explosions, >10,400 seismic events

Infrasound

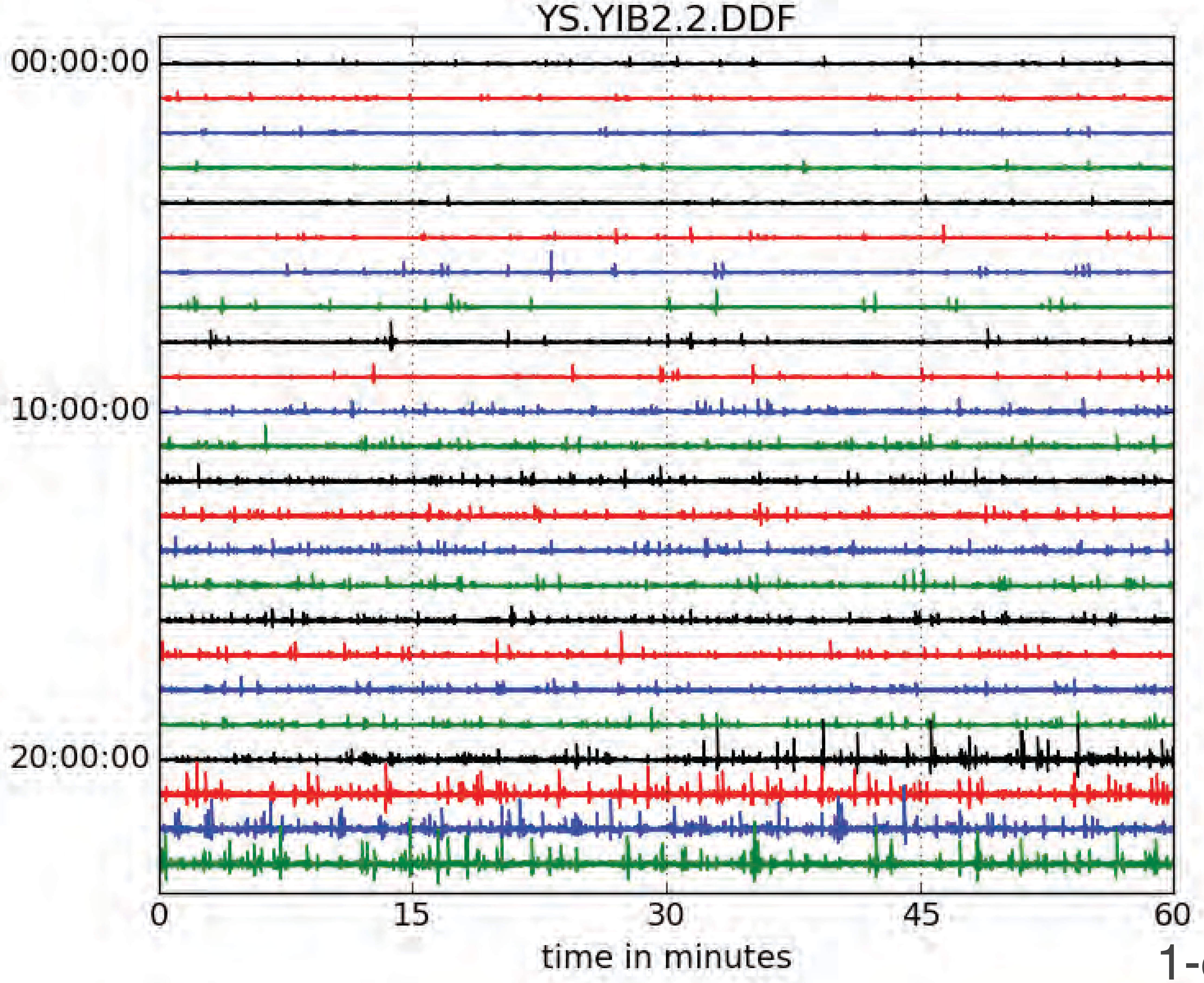

Seismic

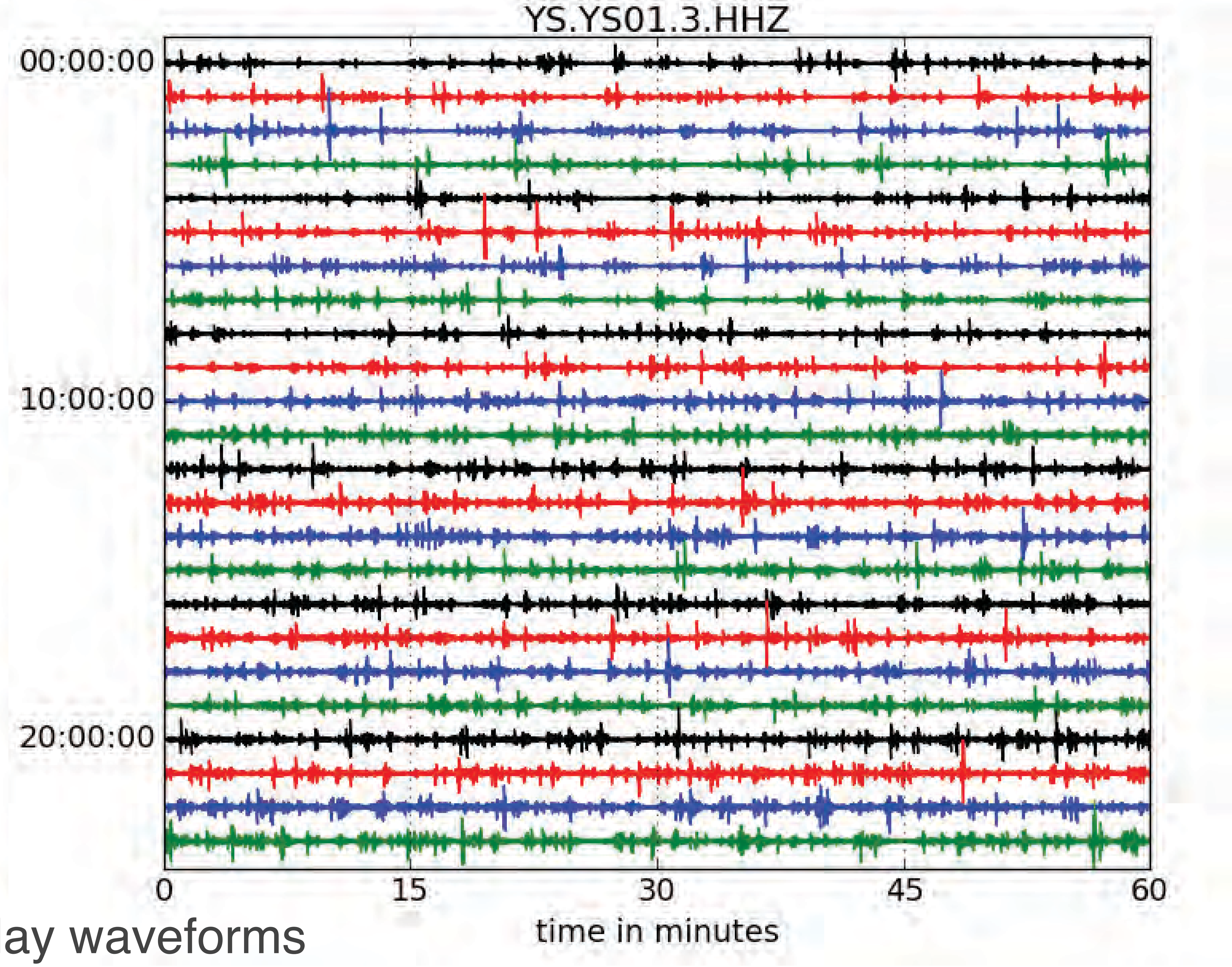

1-day waveforms

Seismo-acoustic waveforms

Infrasound

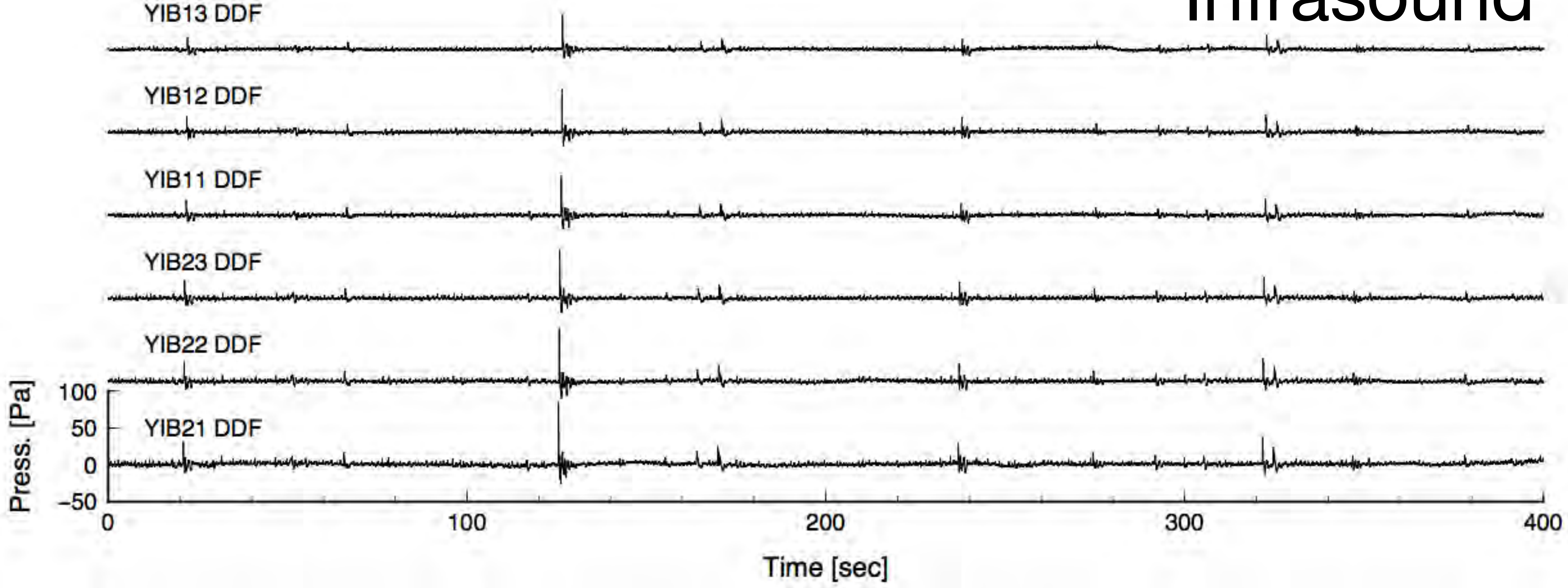

Seismic

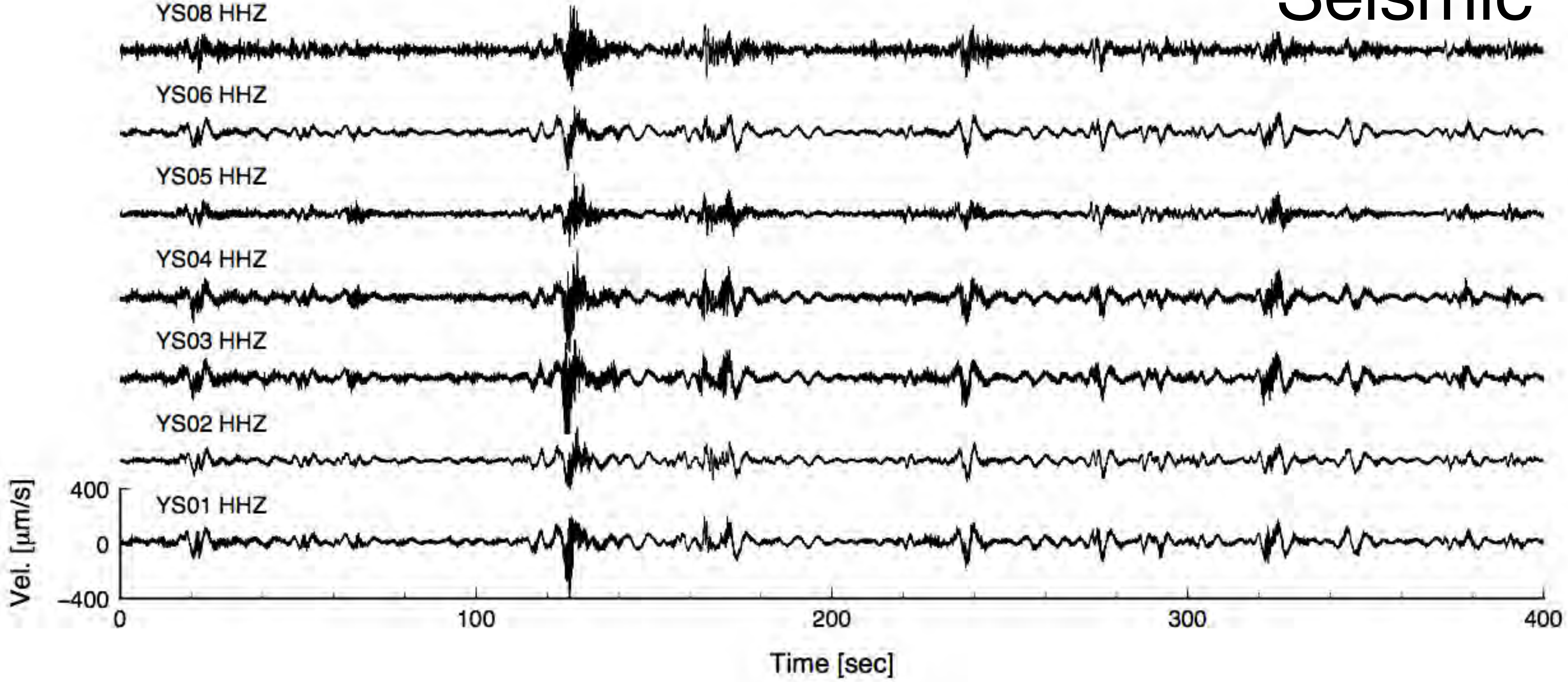

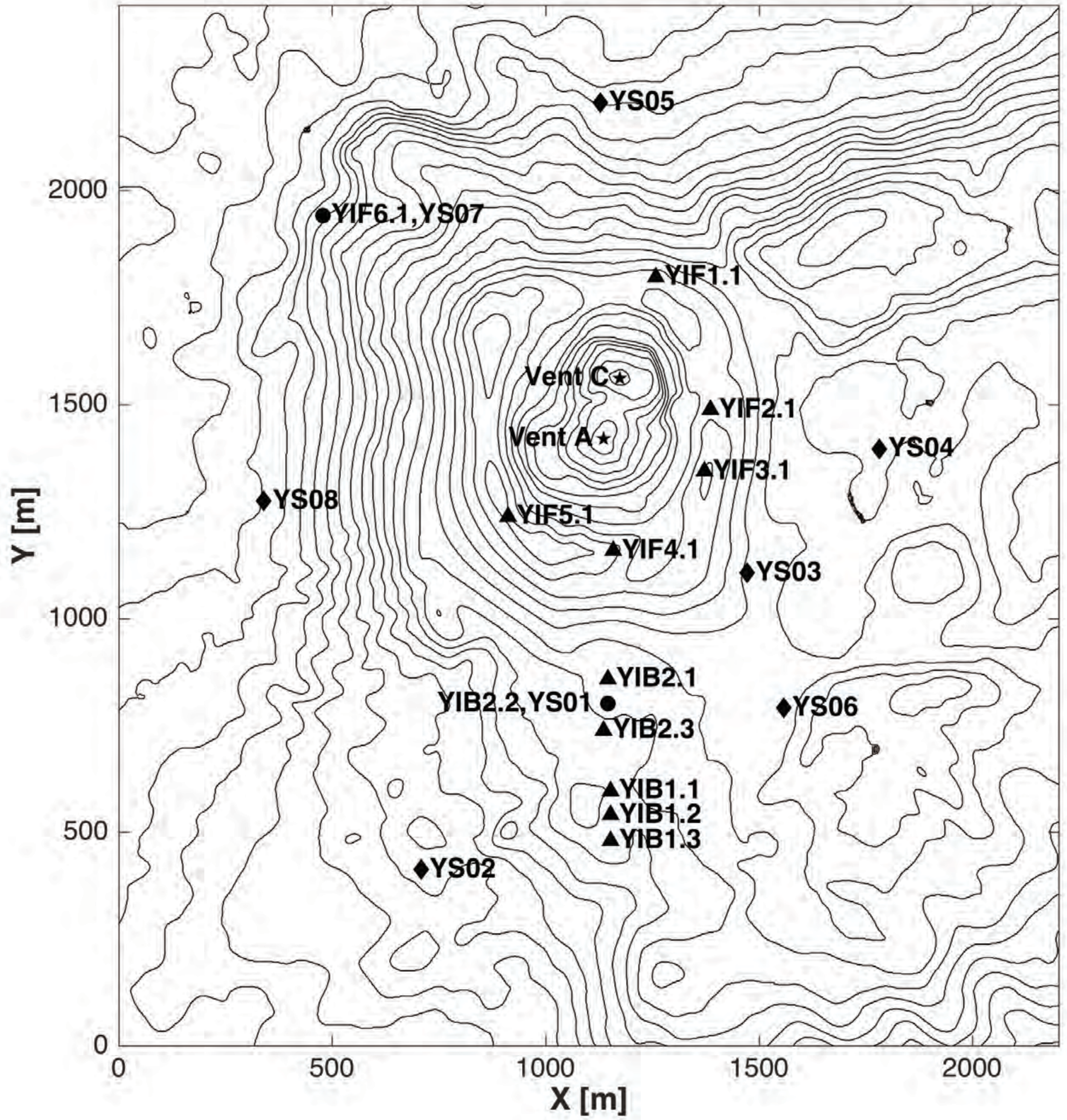

YS: seismic; **YI**: infrasound
Contour interval: 20 m

Seismo-acoustic waveforms

Infrasound

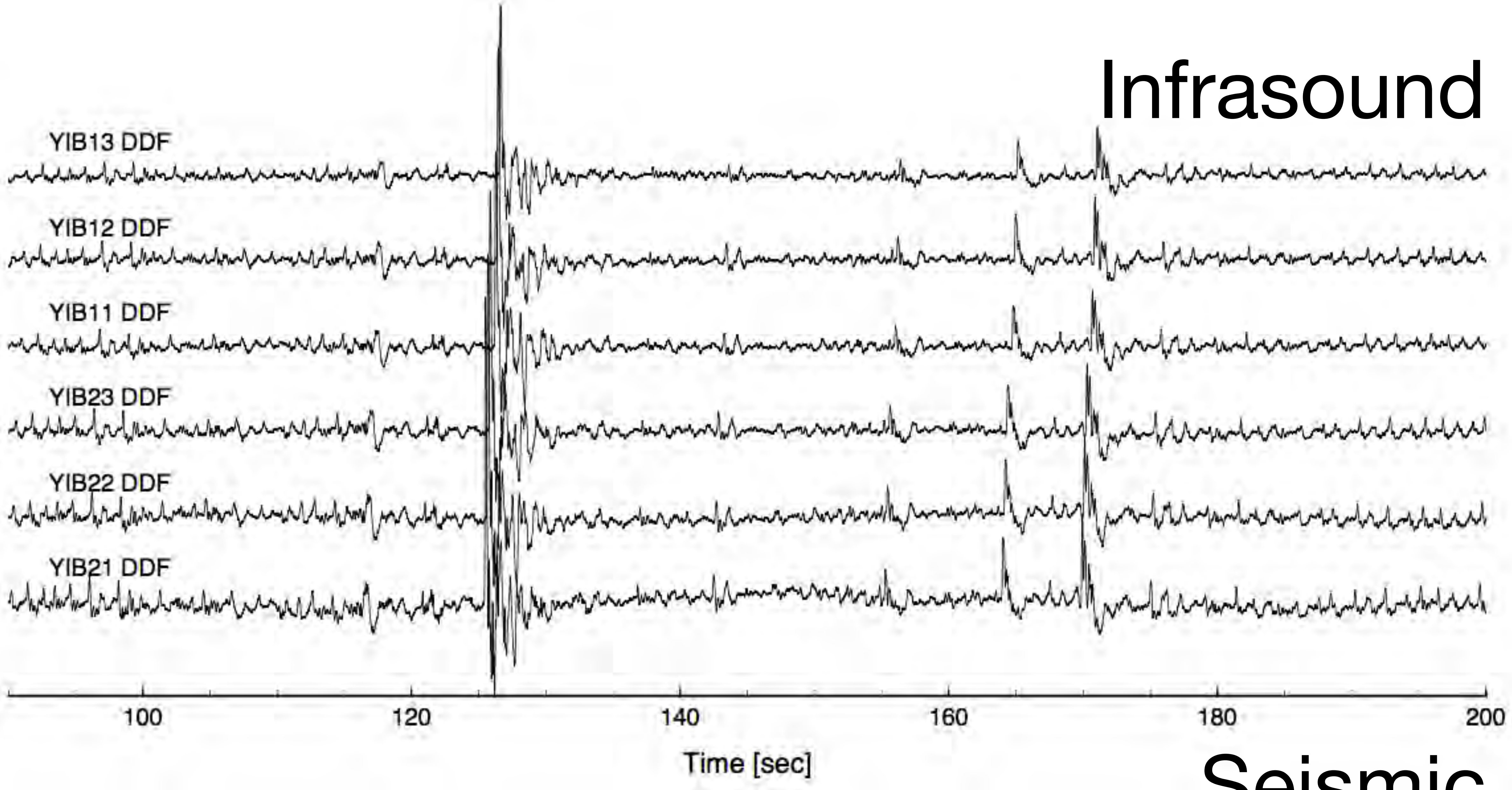

- Short-duration asymmetric explosion waveforms
- Near-continuous broadband infrasonic tremor consisting of repetitive positively skewed pulses

[*Marchetti et al.*, 2013; *Meier et al.*, 2016; *Spina et al.*, 2016]

Seismic

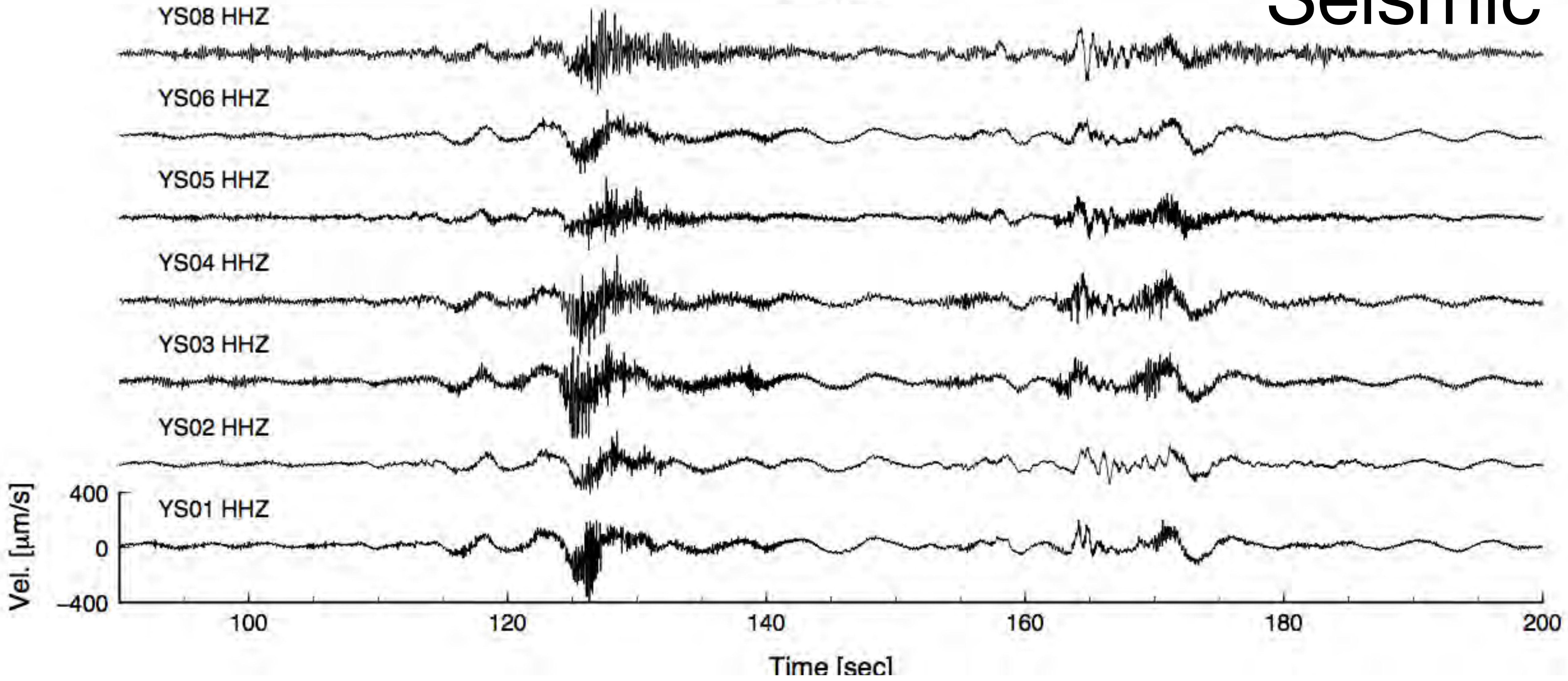

- Numerous repetitive long-period (LP) events
- Underlain by very-long-period (VLP) signals with periods of ~10 s

[*Kremers et al.*, 2013; *Battaglia et al.*, 2012; 2016]

LP: 0.5–5 Hz (0.2–2 s period)
VLP: 0.01–0.5 Hz (2–100 s period)

Full-waveform inversion of VLP seismic events

- Frequency of inversion: 0.002 to 2 Hz
- Perform a grid search over trial source nodes with increasing spatial density (3 stages down to 20-m spacing)
- Define solution with the minimum E_2 residual error

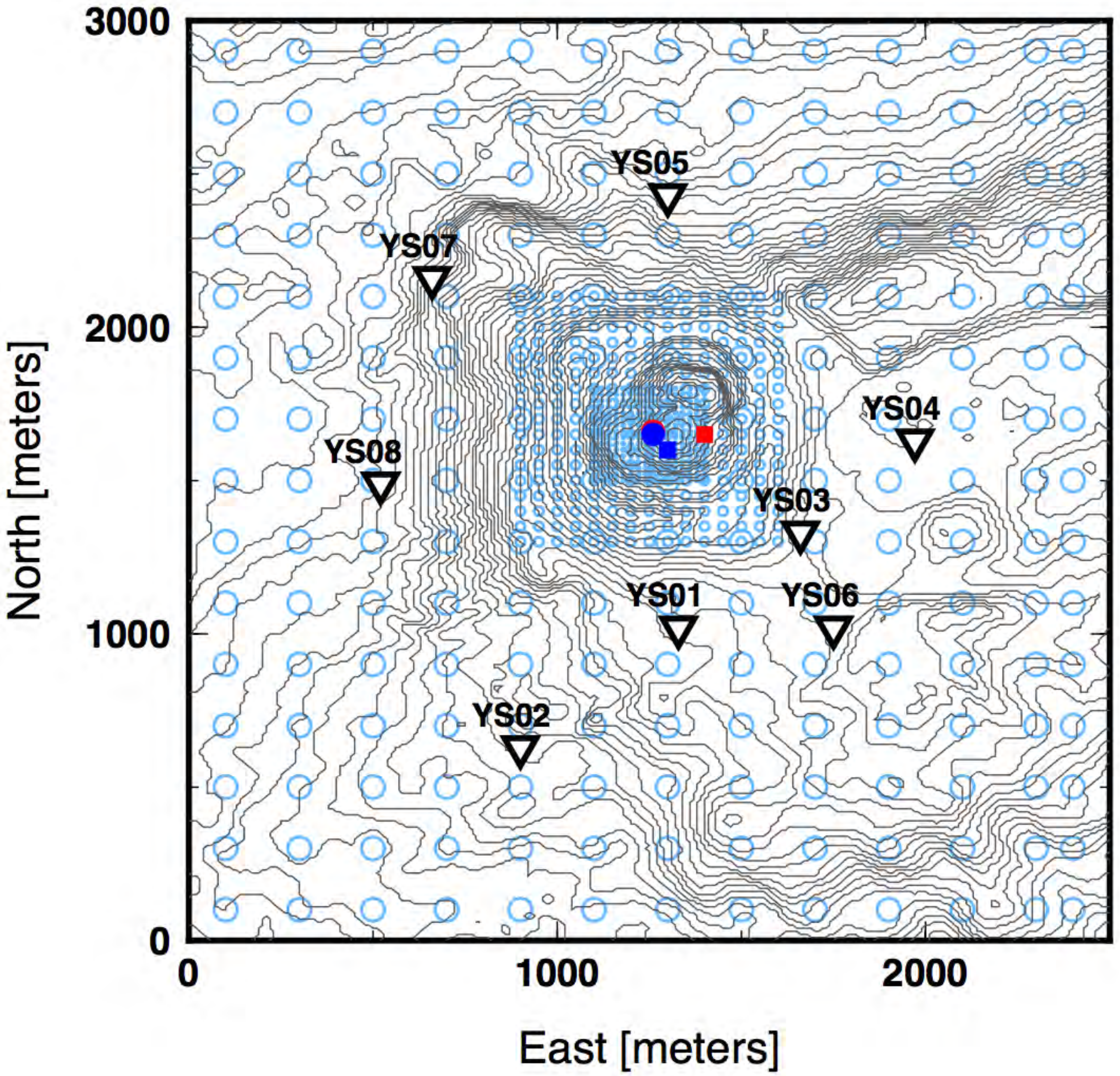

$$E_2 = \frac{1}{N_r}\sum_{n=1}^{N_r}\left[\frac{\sum_{j=1}^{3}\sum_{p=1}^{N_s}\left(u_{n,j}^{o}(p\Delta t) - u_{n,j}^{s}(p\Delta t)\right)^2}{\sum_{j=1}^{3}\sum_{p=1}^{N_s}\left(u_{n,j}^{o}(p\Delta t)\right)^2}\right]$$

Observed

Synthetic

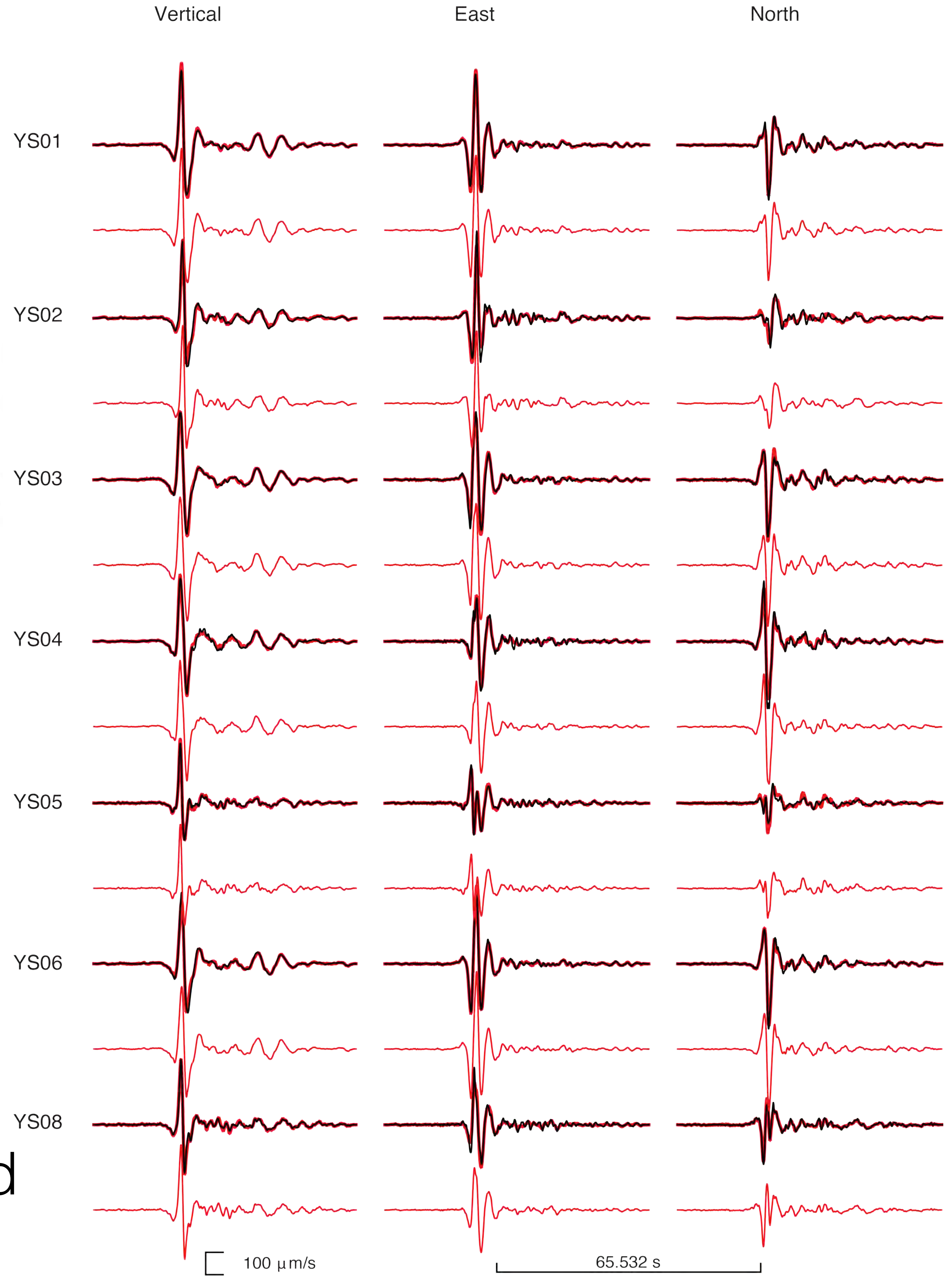

Network-based detection

- Individual VLP seismic events are contaminated by noise from microseisms and from the continuous VLP tremor oscillation
- Employ network-based template matching and stacking to boost the signal-to-noise ratios and isolate the transient VLP waveform signature

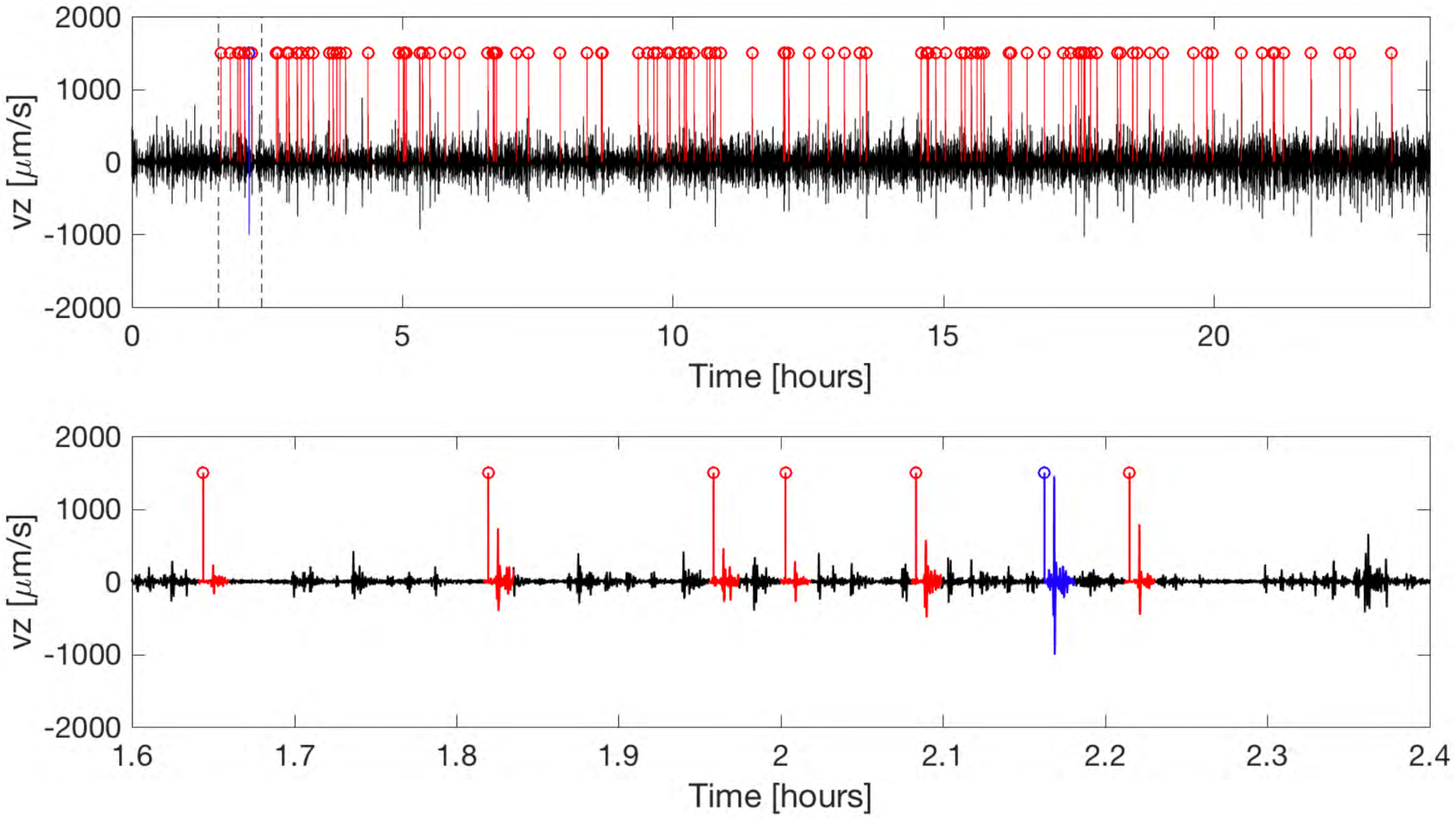

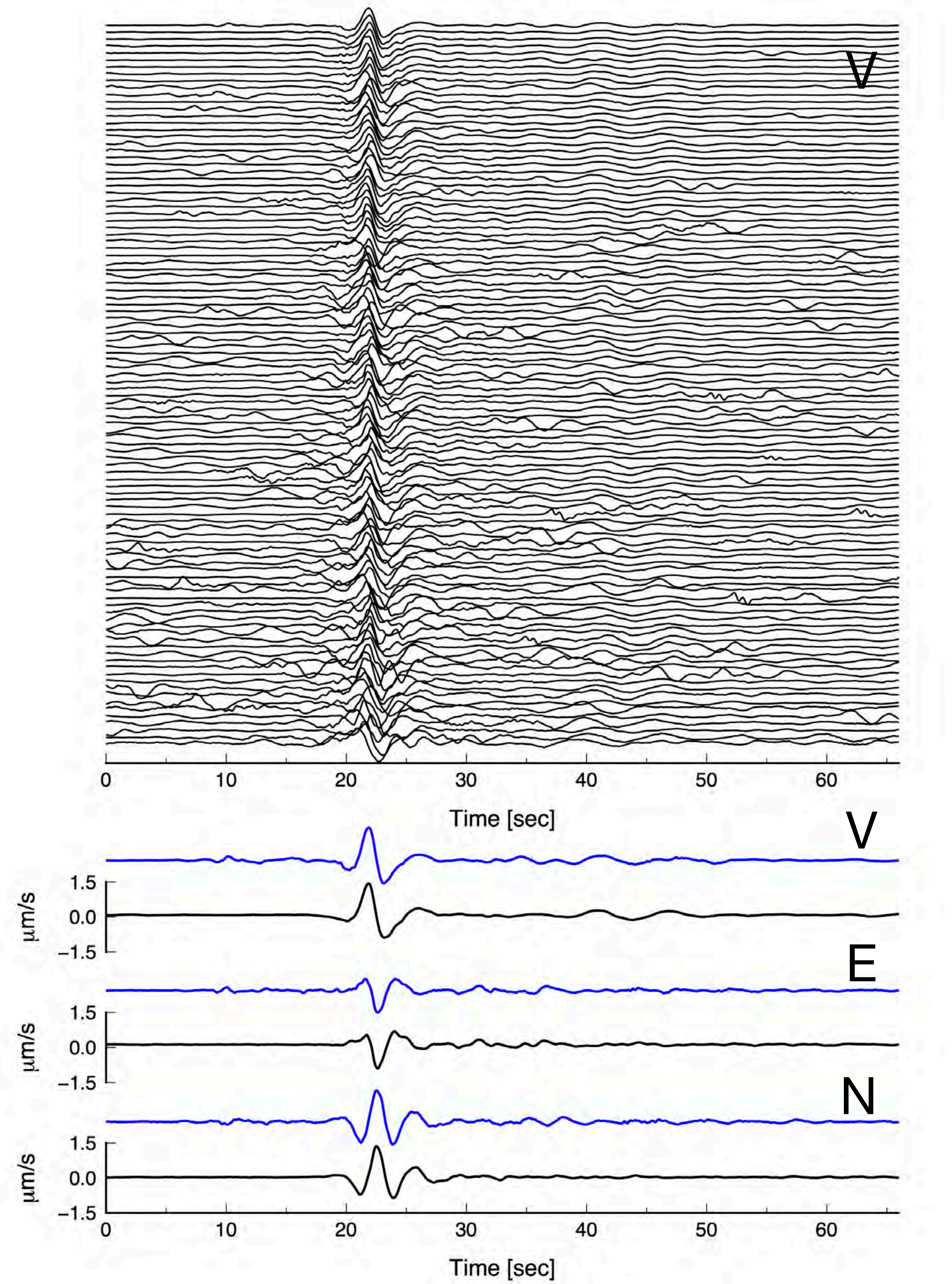

Full-waveform inversion of VLP seismic events

- Derived source location is beneath the main summit vent area at 680 m below sea level (870 m below the topography at this location)

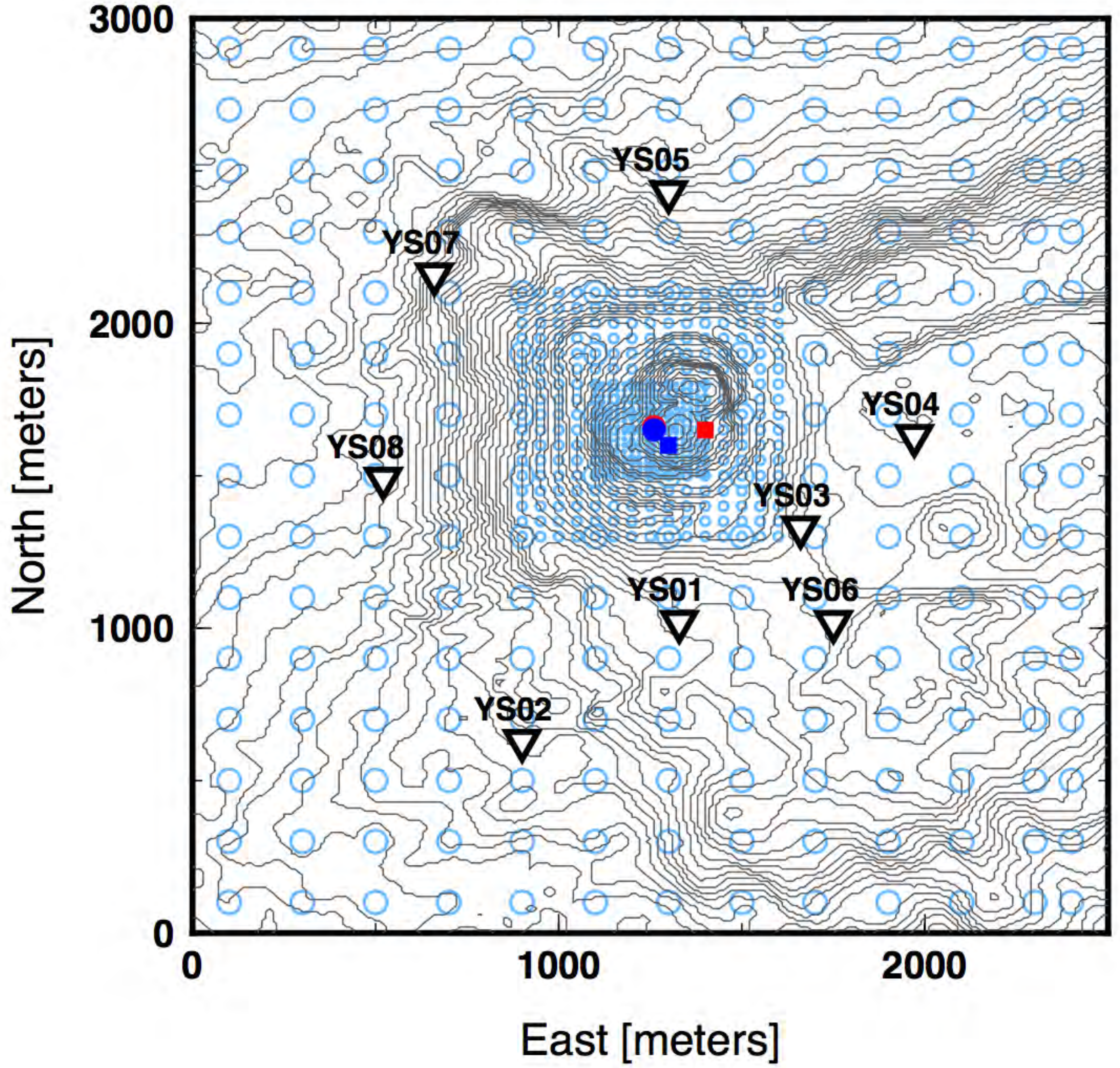

Global minimum E_1 (red) and E_2 (blue)
31 July 2016 (circles) and 29 July 2016 (squares)

E2 error is 4.2% based on the waveform portion from 10 to 50 s; in the band 0.002 to 2 Hz

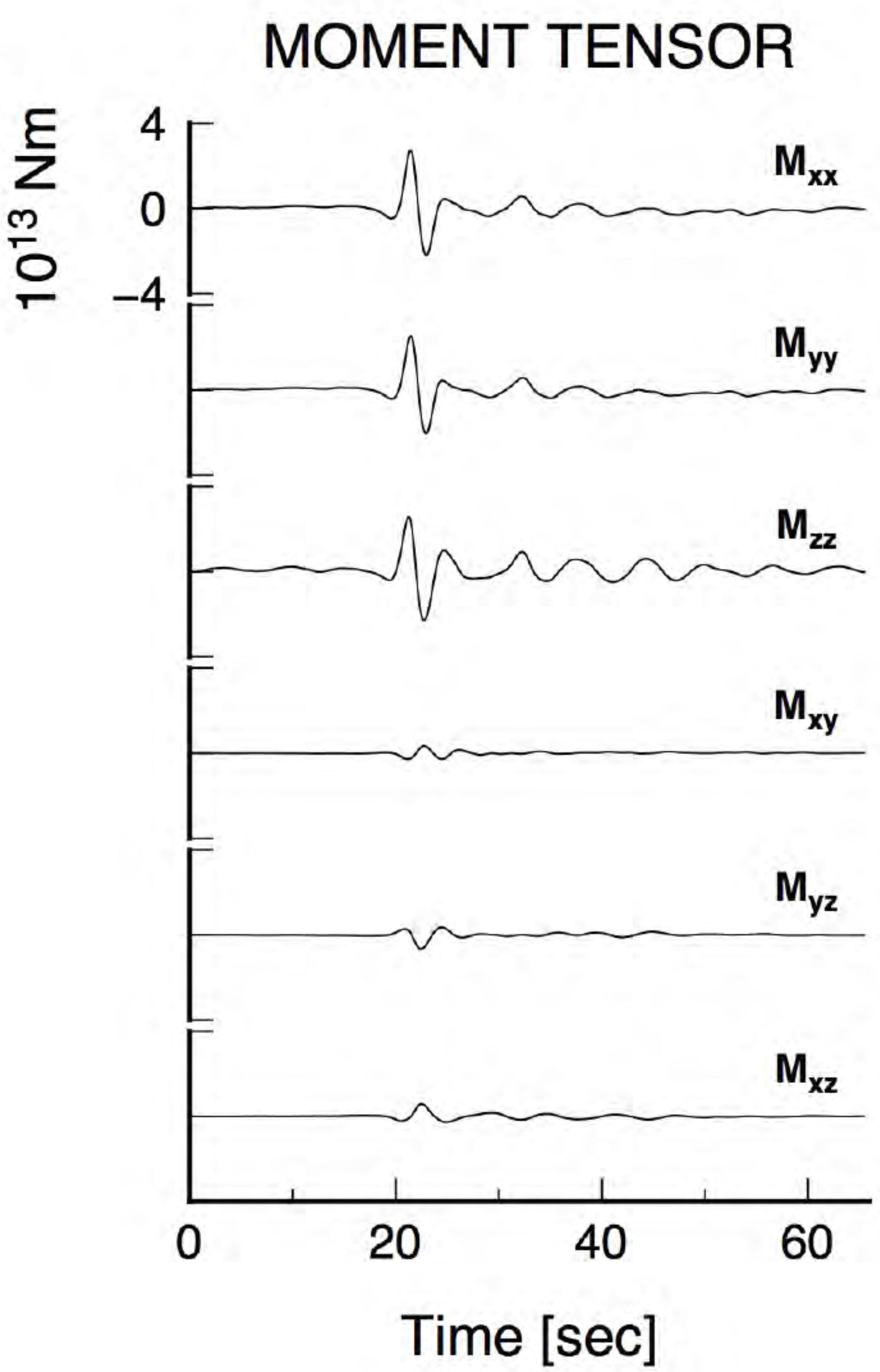

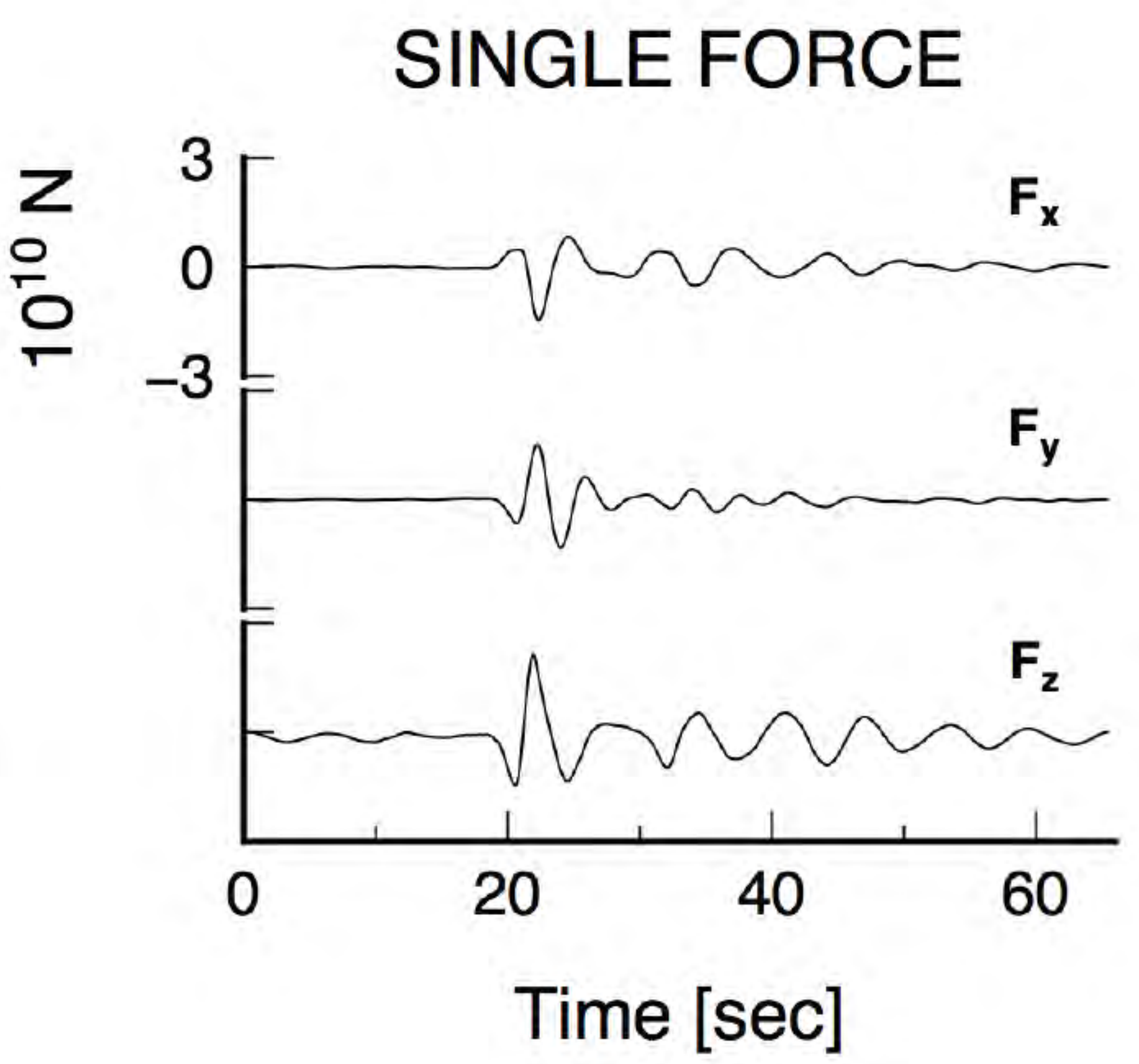

Preliminary results:

- Horizontal sill (80% of moment tensor (volume change) &
  - Two sub-dominant and orthogonal vertical cracks
  - Or a subdominant vertical pipe.

Hawaiian Volcano Observatory (HVO) network

- Hawaii Island: tectonic, VT, and LP earthquakes at a range of depths from mantle to surface; ~5,000-10,000 earthquakes per year
- Digital waveform data available from mid-1980s

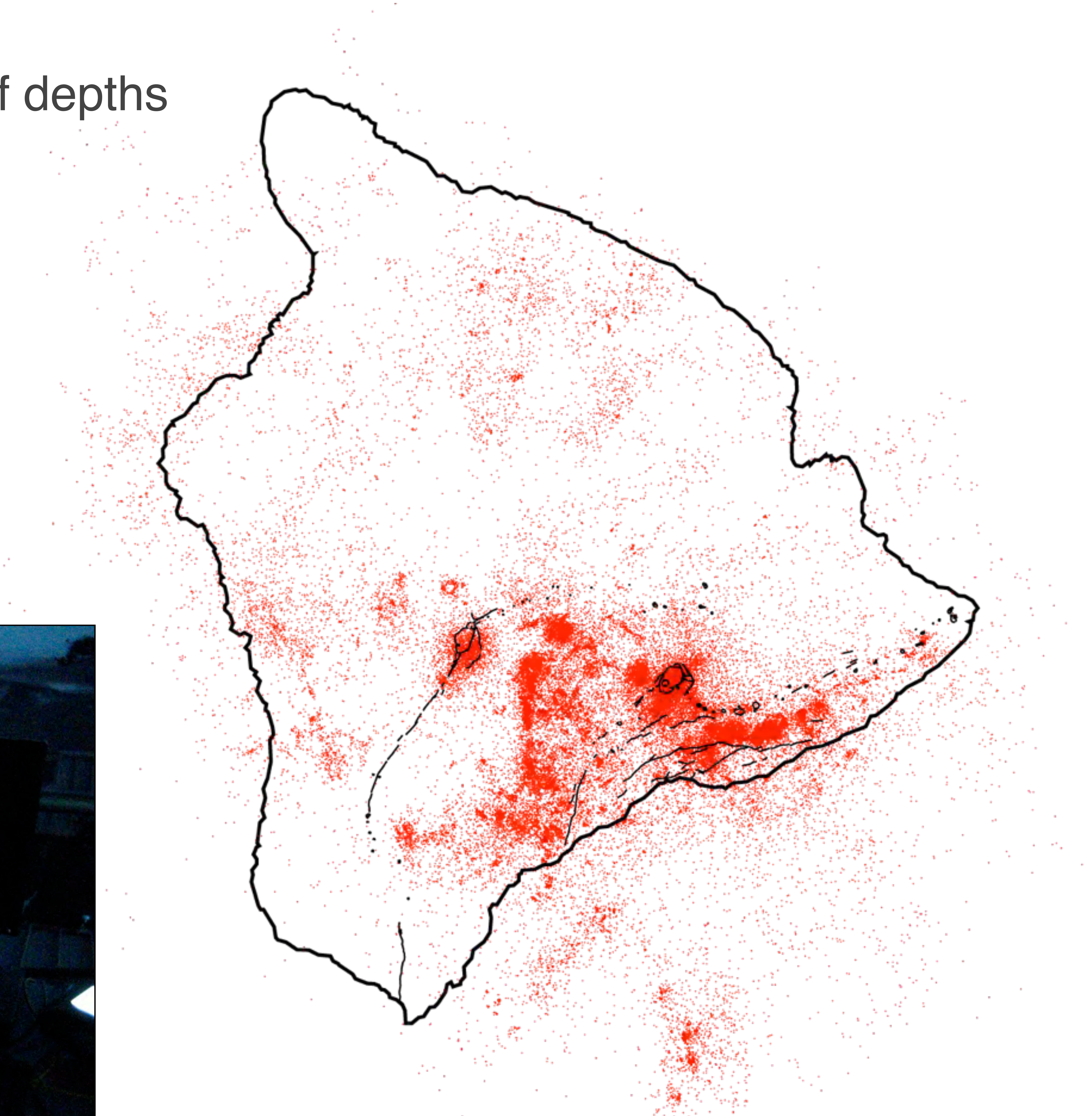

Hawaiian Volcano Observatory (HVO) network

- ~50-station permanent HVO network; mostly short-period, vertical component only 1986–2009
- Systematic analyses (e.g., 198k events 1986-2009; 23 years of data from CUSP system; Matoza et al. [2013], Lin and Okubo [2016])
- Currently working on data post 2009 (AQMS), more broadband stations; continuous waveform data

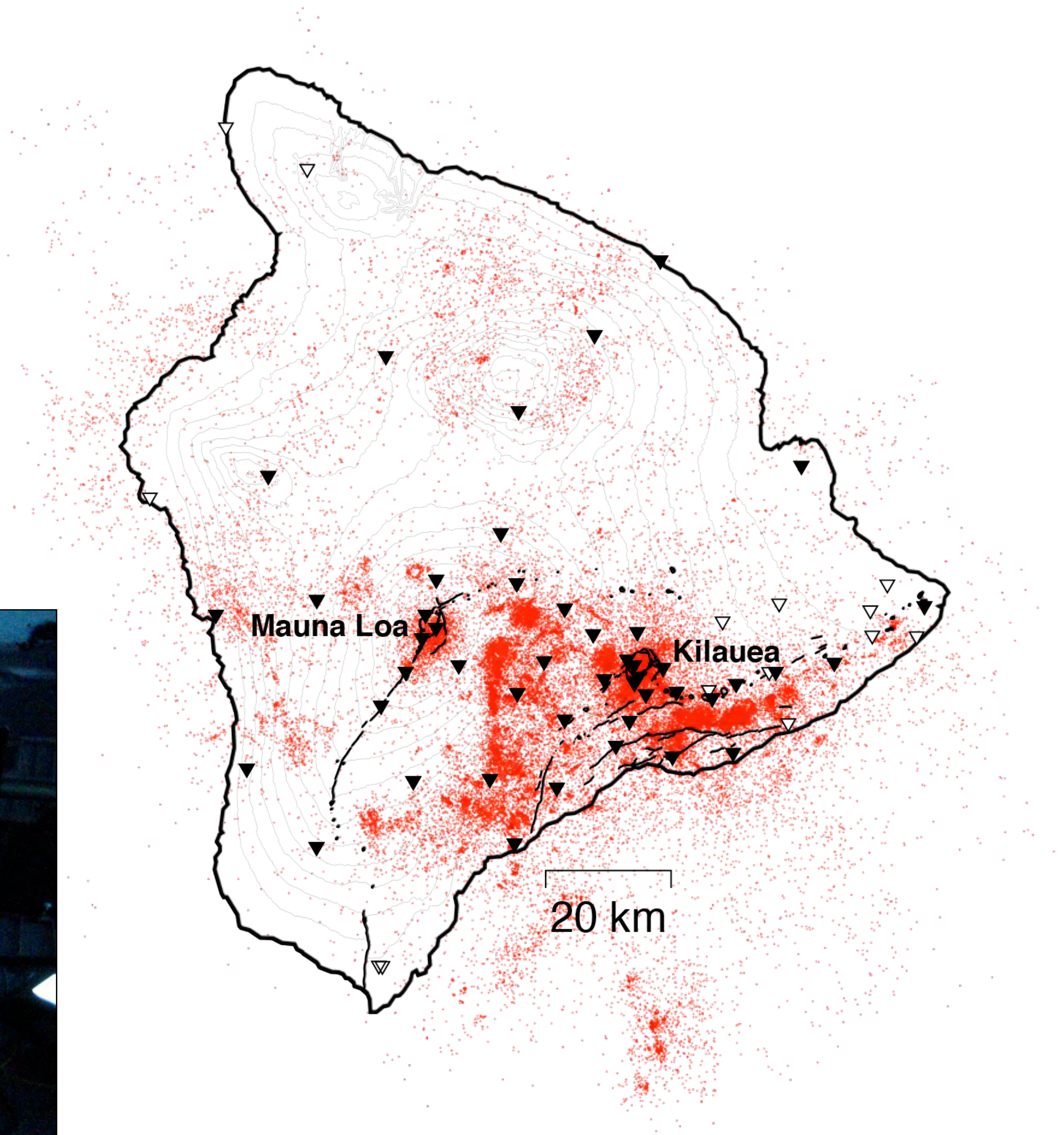

Relative event location

- Solve for relative location between nearby events
- Without solving for complex 3D velocity structure
- Waveform cross correlation dramatically reduces phase pick uncertainty

- Considered waveforms for 198k events, 23 years
- Time-domain cross correlations computed for ~71 million event pairs, *P*- and *S*-waves, 243 million differential times
- Combined cluster analysis and relative relocation using grid-search *L*1-norm method
- Relocated 157k (79%)
- Based on methods developed for Southern California

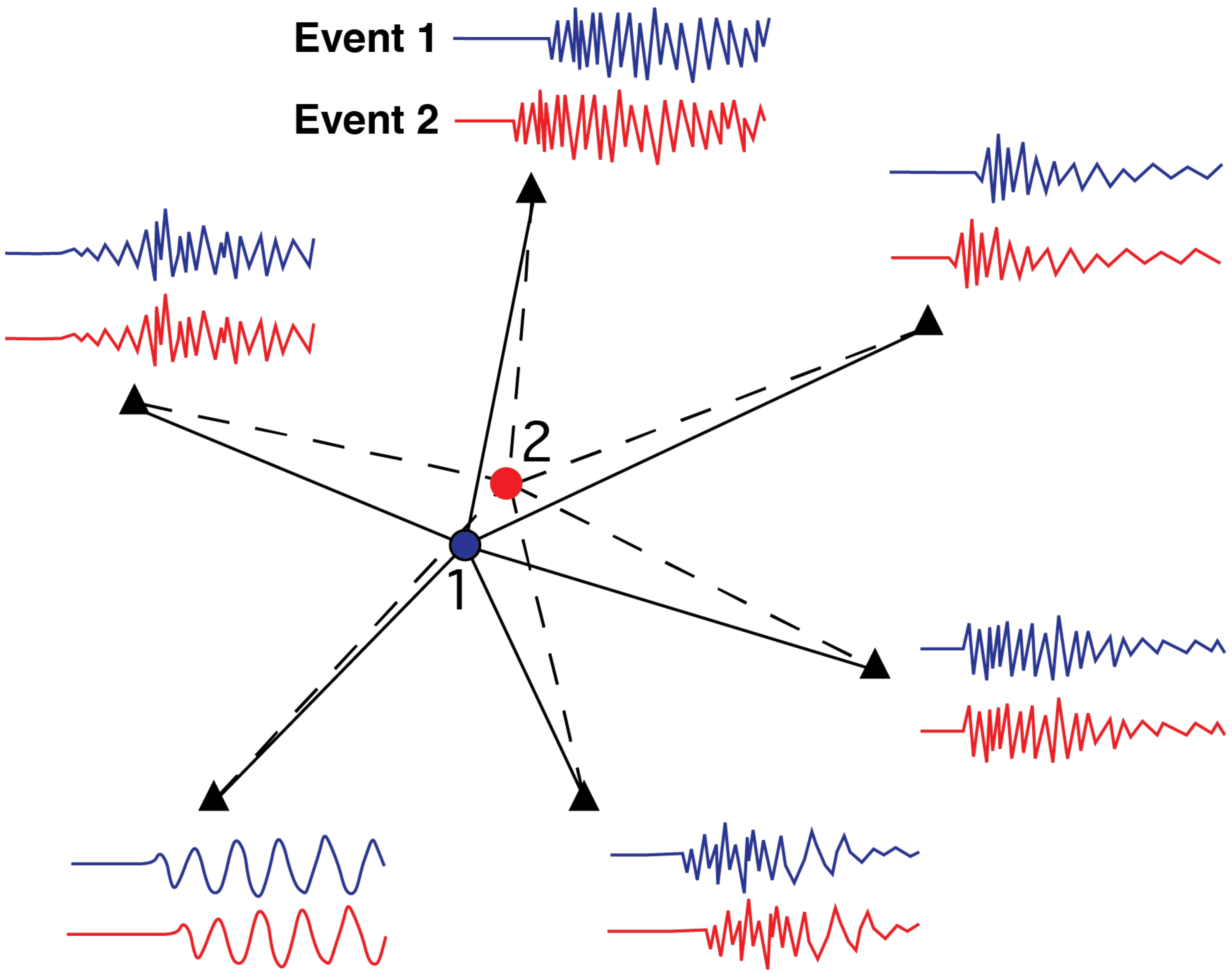

Relative event location

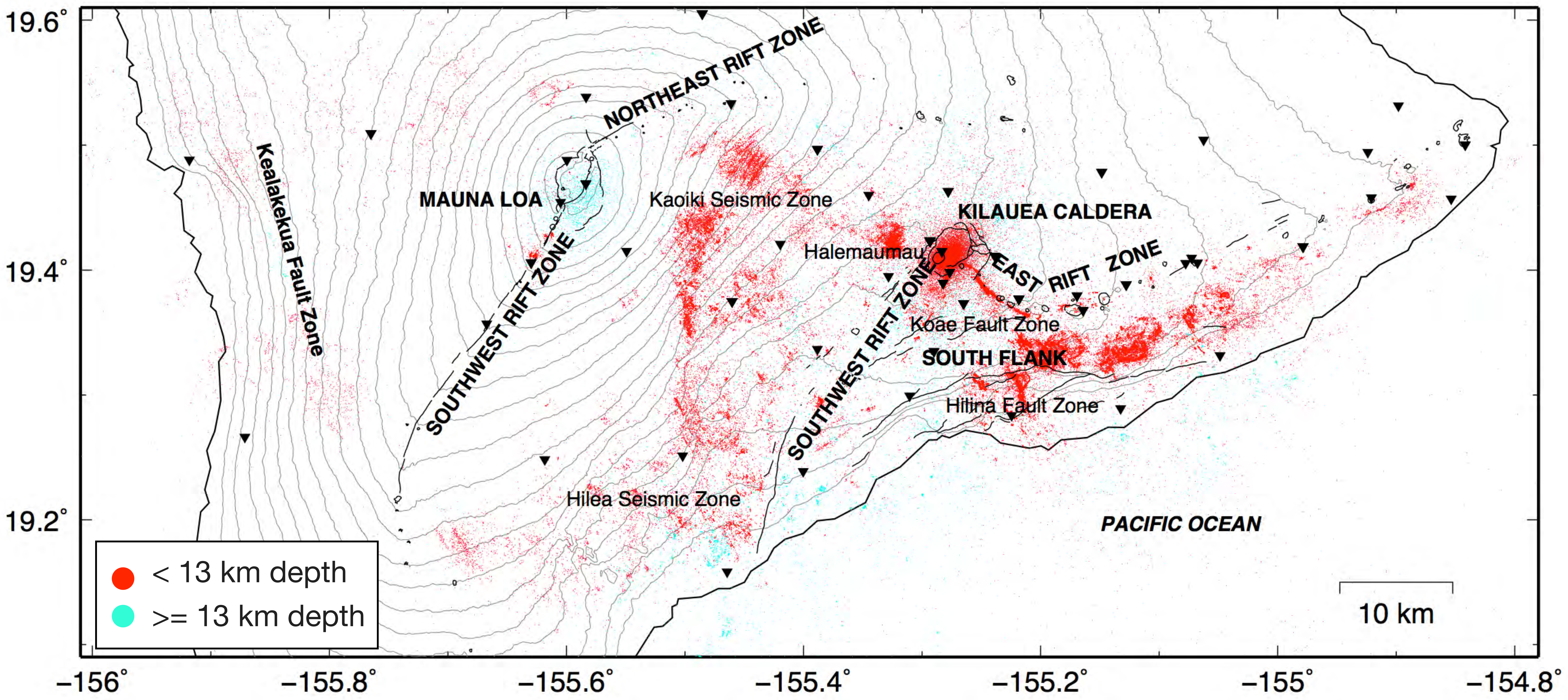

- Sharpening of earthquake clustering along faults, streaks, rift zones, rings, and magmatic features
- Generally consistent with previous relocation studies, but many more events

Matoza et al., [2013]

Relative event location

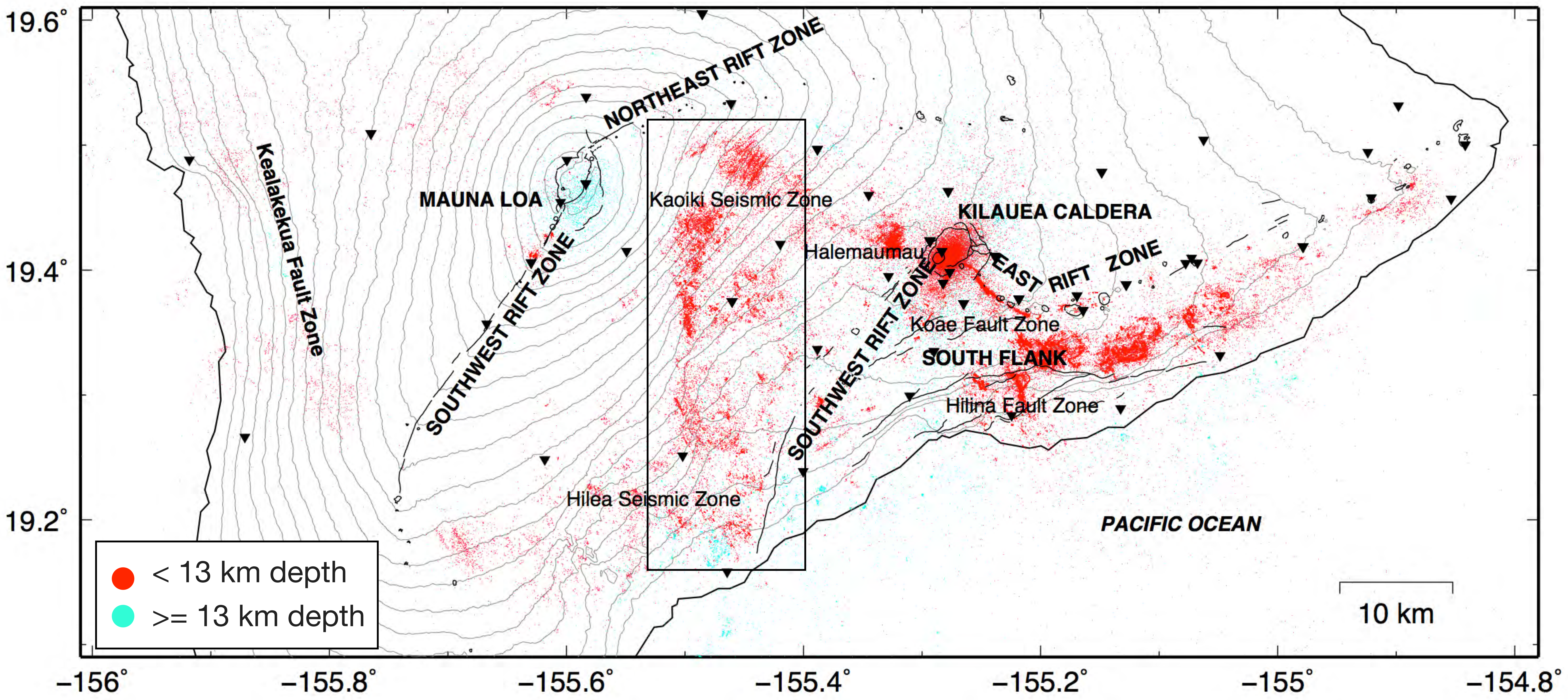

- Sharpening of earthquake clustering along faults, streaks, rift zones, rings, and magmatic features
- Generally consistent with previous relocation studies, but many more events

Matoza et al., [2013]

Relative event location

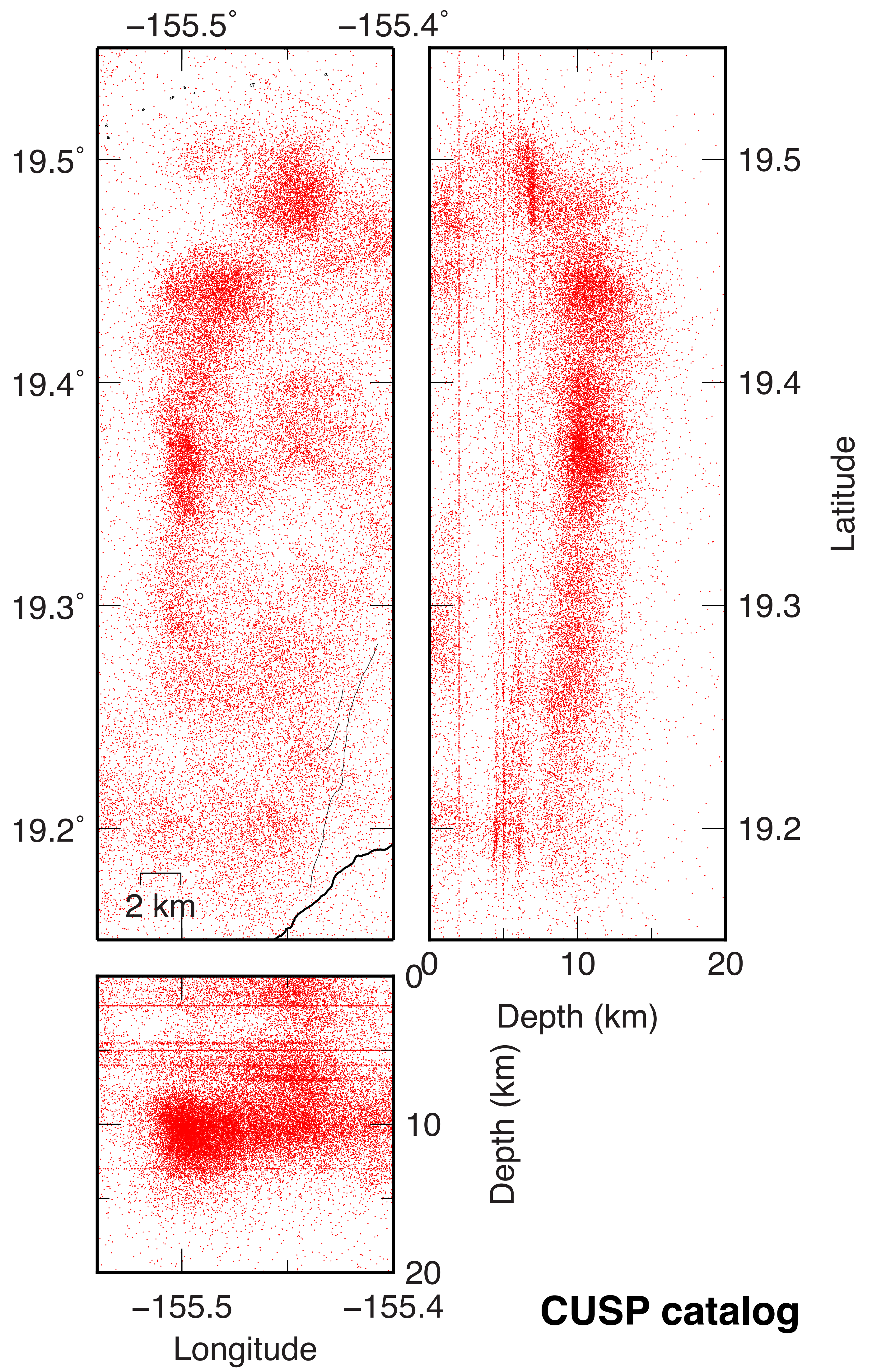

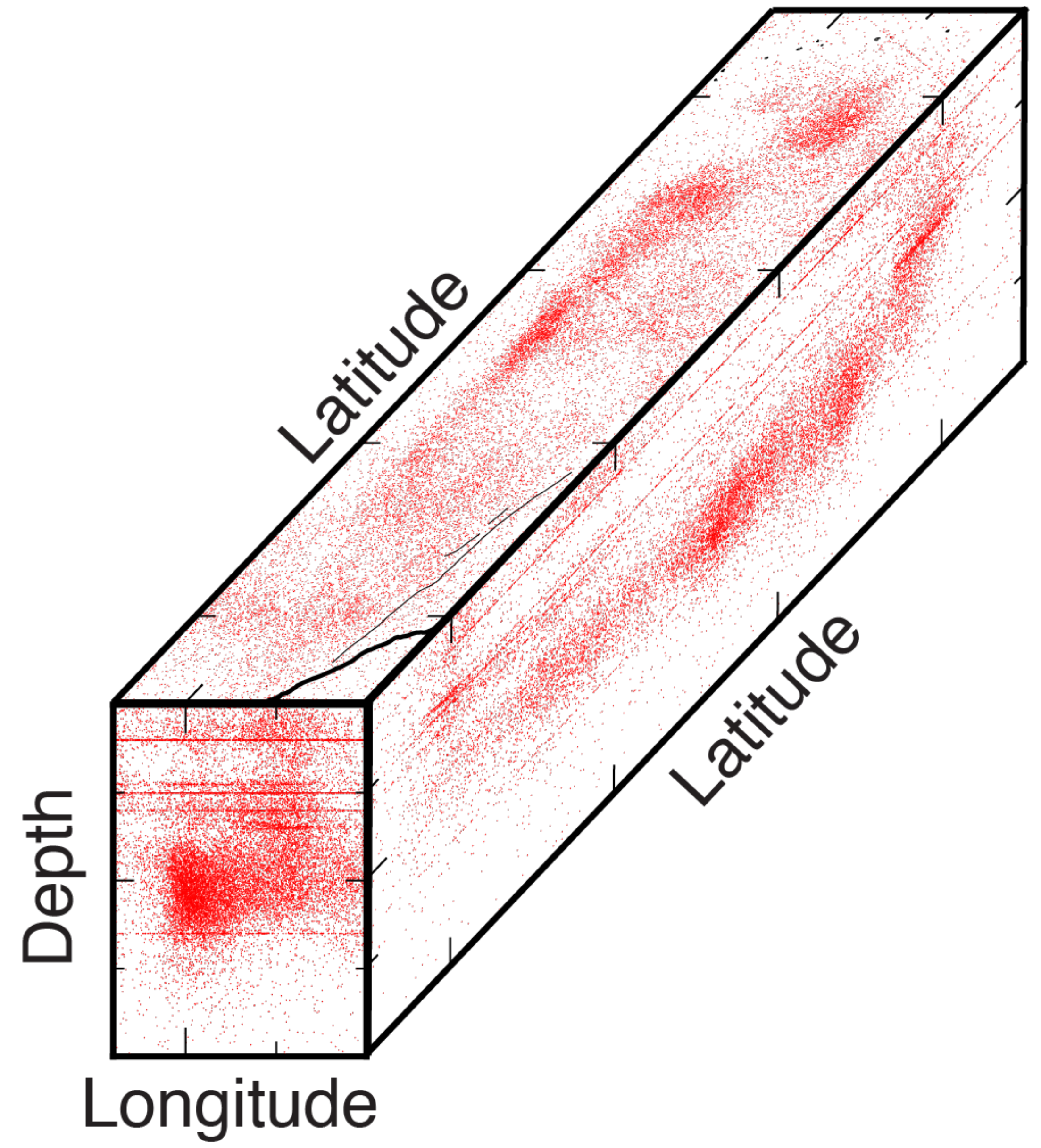

Matoza et al., [2013]

Relative event location

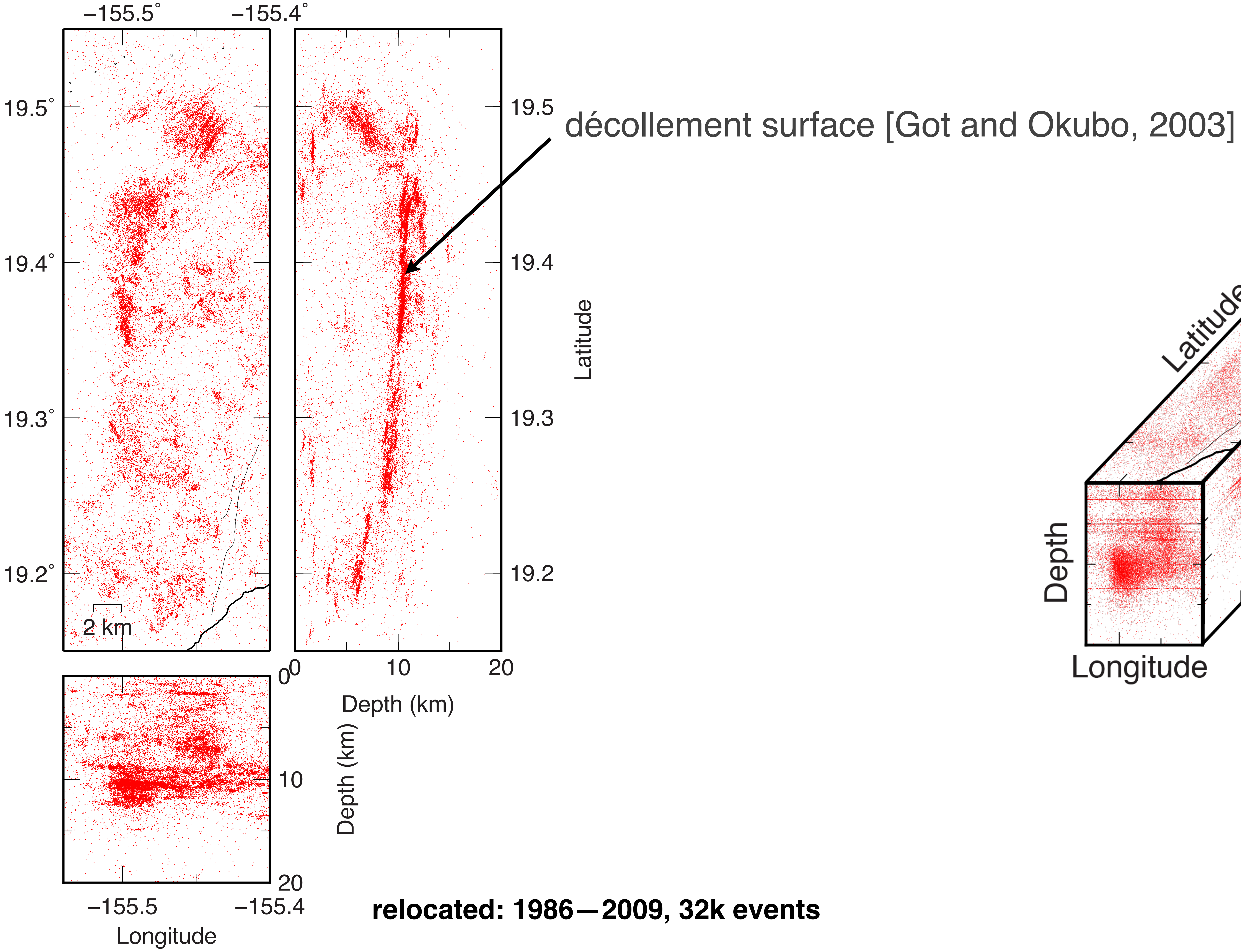

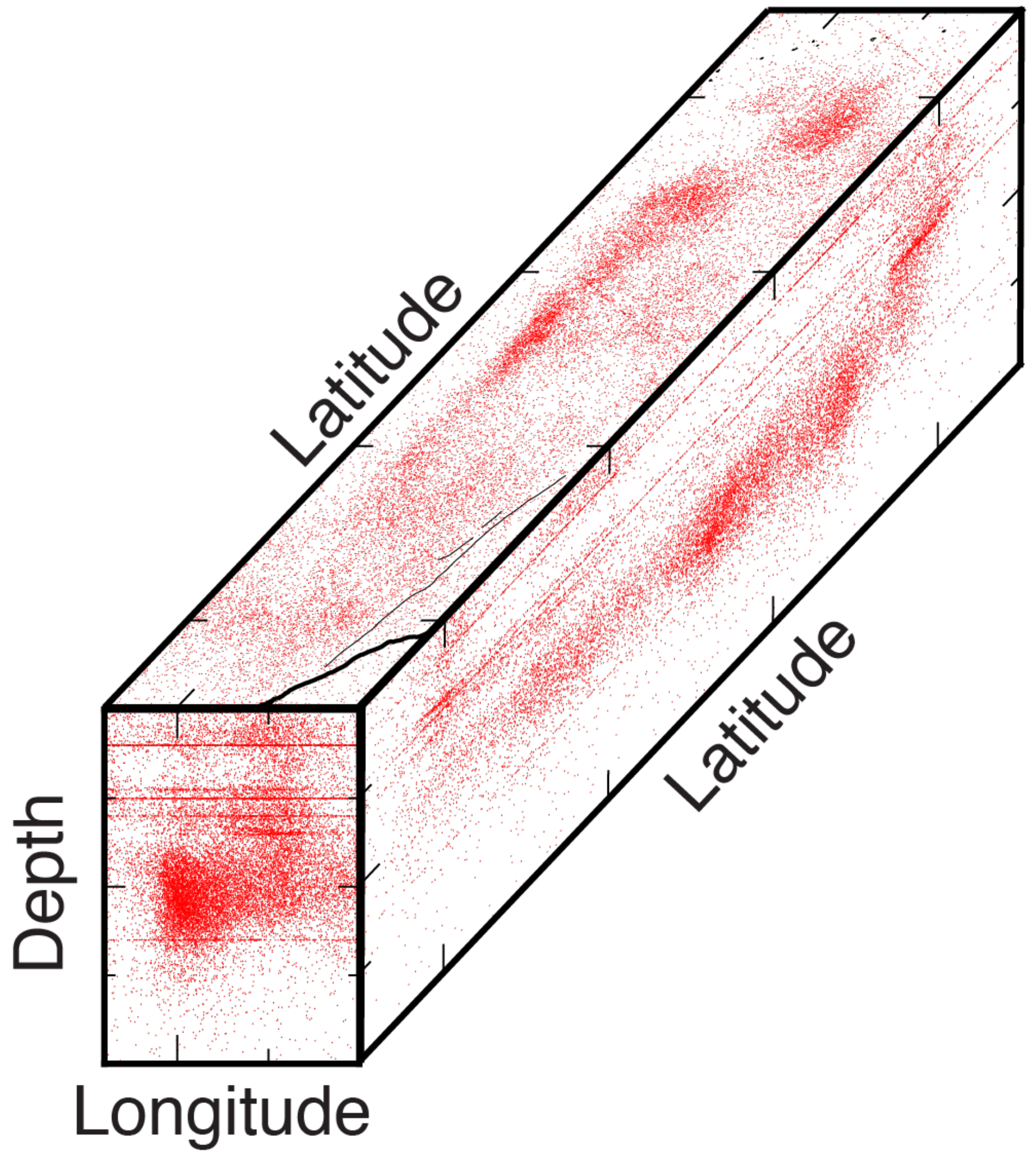

relocated: 1986—2009, 32k events

Matoza et al., [2013]

Volcano seismology and acoustics

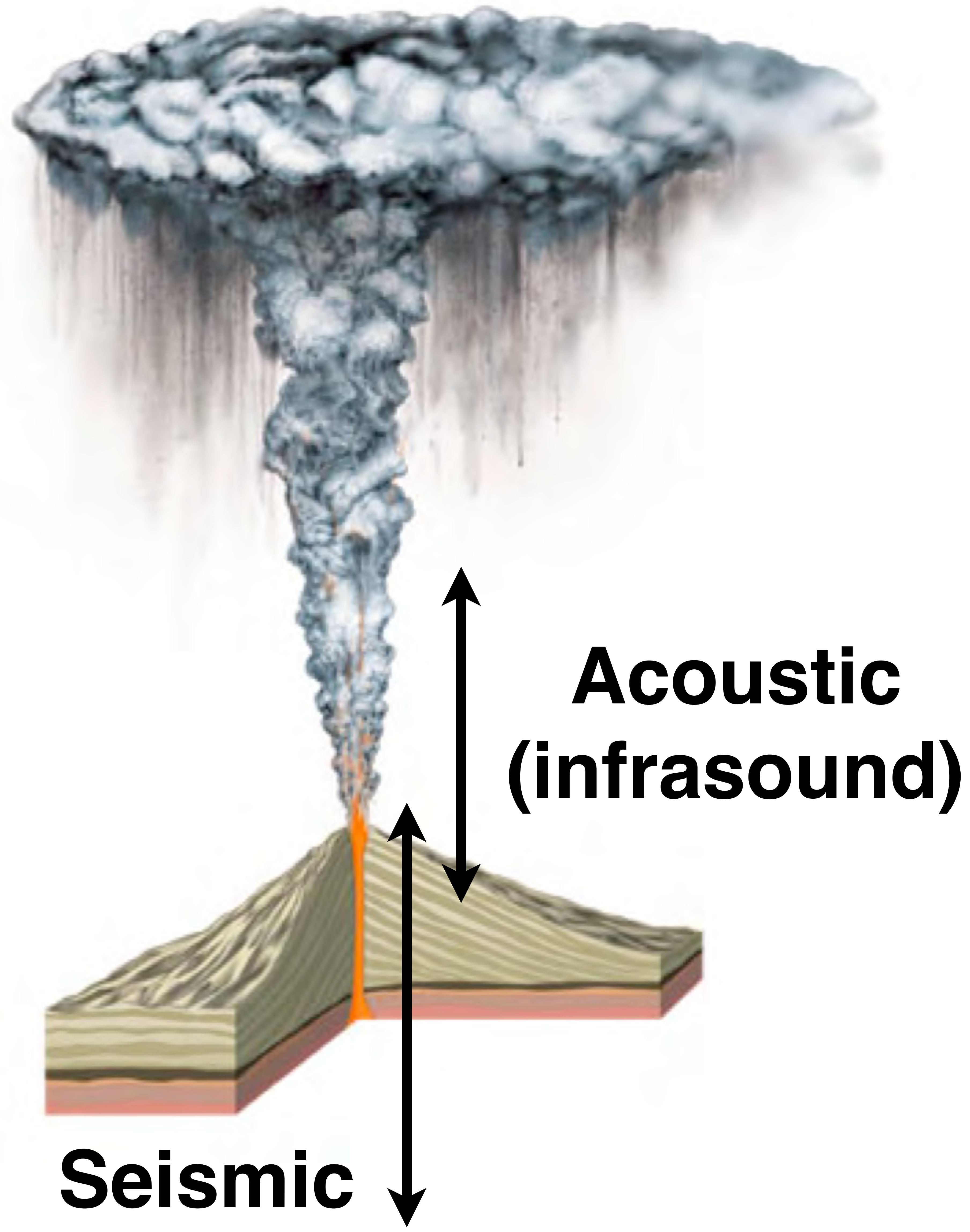

Acoustic

- Atmospheric acoustics (infrasound): ~0.01-20 Hz
- Variety of shallow and subaerial sources
- Explosive volcanism: powerful signals

Seismic

- Migration of fluid from mantle depths to surface
- Faulting & fluid transport in the solid earth
- Limited propagation < few hundred km

Volcano seismology and acoustics

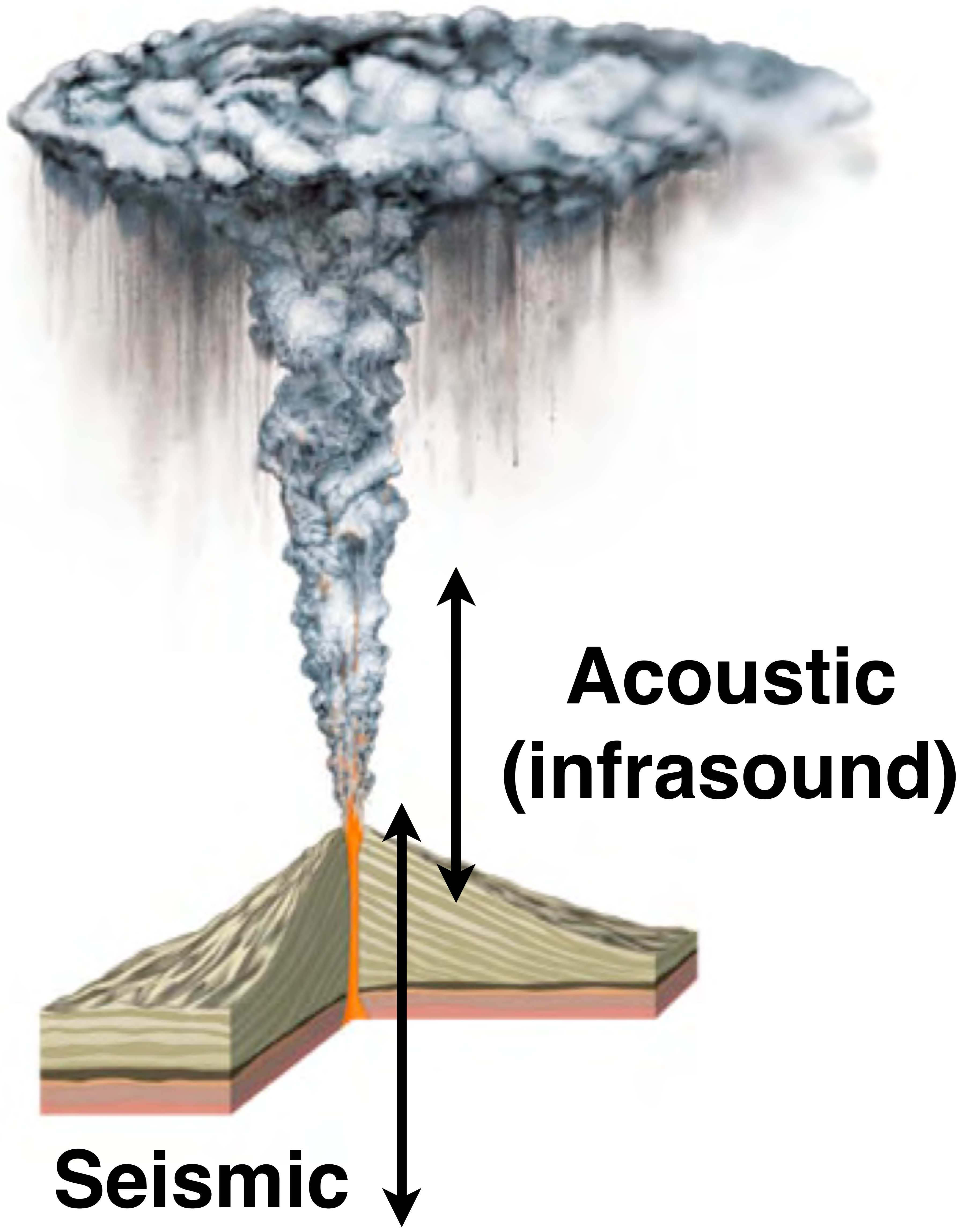

Acoustic

- Atmospheric acoustics (infrasound): ~0.01-20 Hz
- Variety of shallow and subaerial sources
- Explosive volcanism: powerful signals
- Can propagate thousands of kilometers

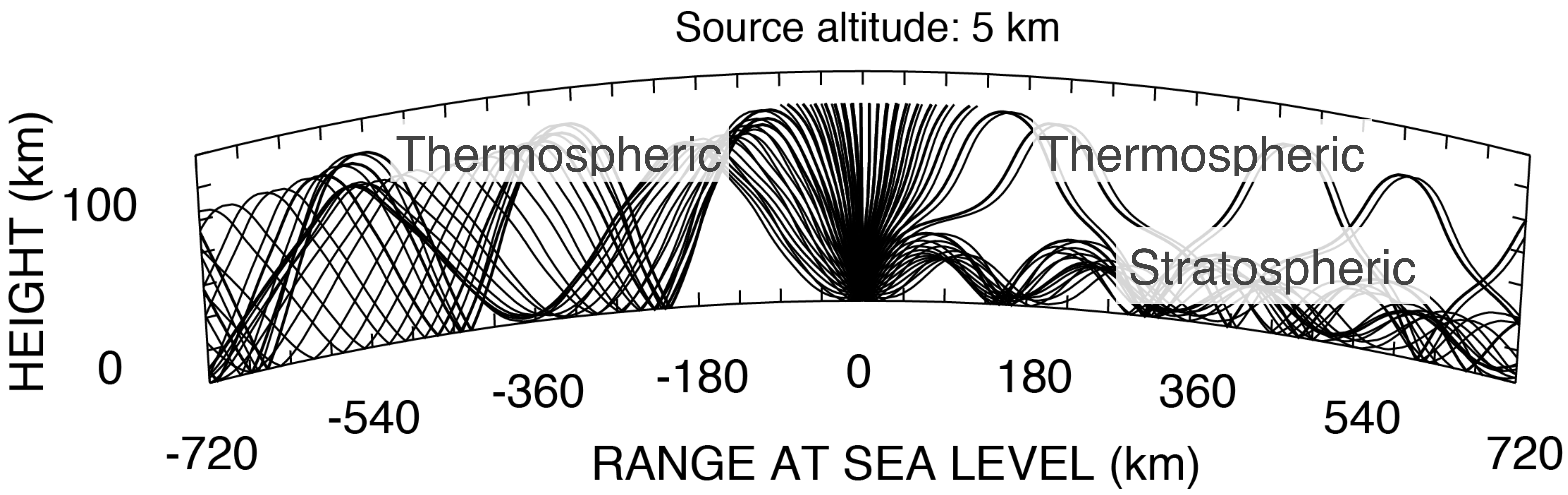

Ray-tracing with HARPA code [Jones et al. 1986]

International Monitoring System (IMS)

- CTBTO IMS: Growing global network of infrasound arrays (50 certified, 60 planned)
- Each station is a 4–8 element infrasound array (2–3 km aperture)
- Average station spacing: ~2,000 km for complete network

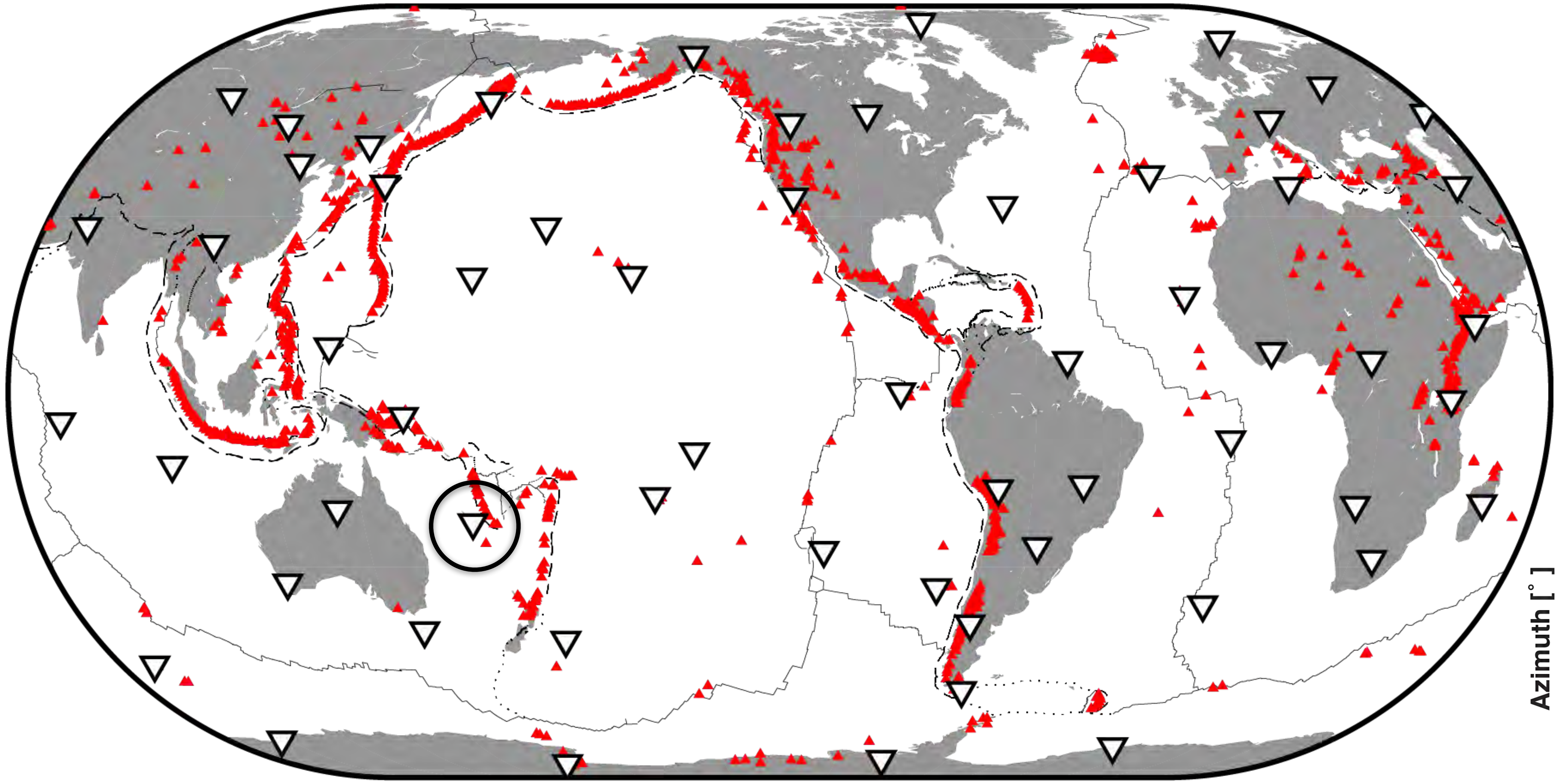

▲ Potentially active volcanoes [*Siebert and Simkin*, 2002-]

▽ IMS infrasound network

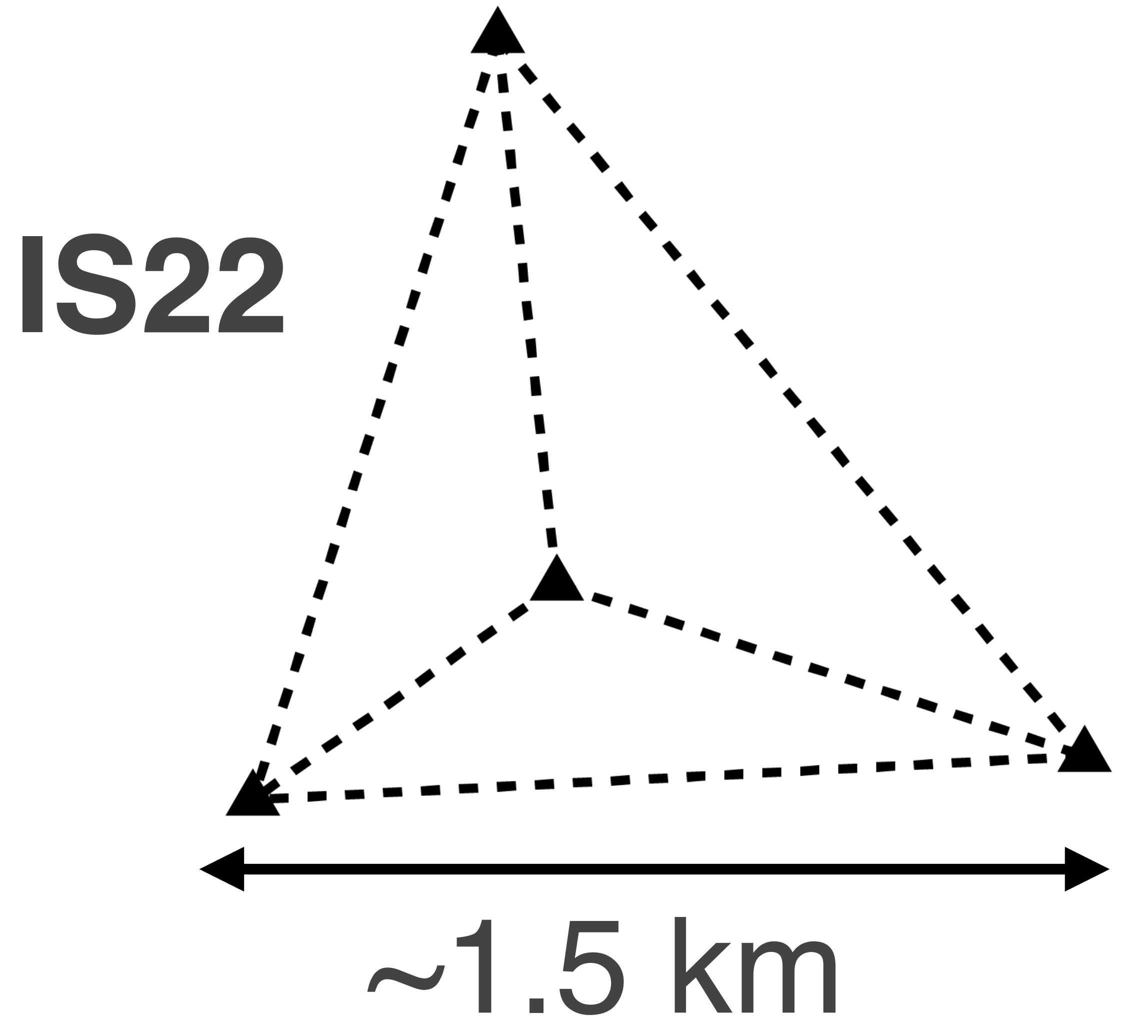

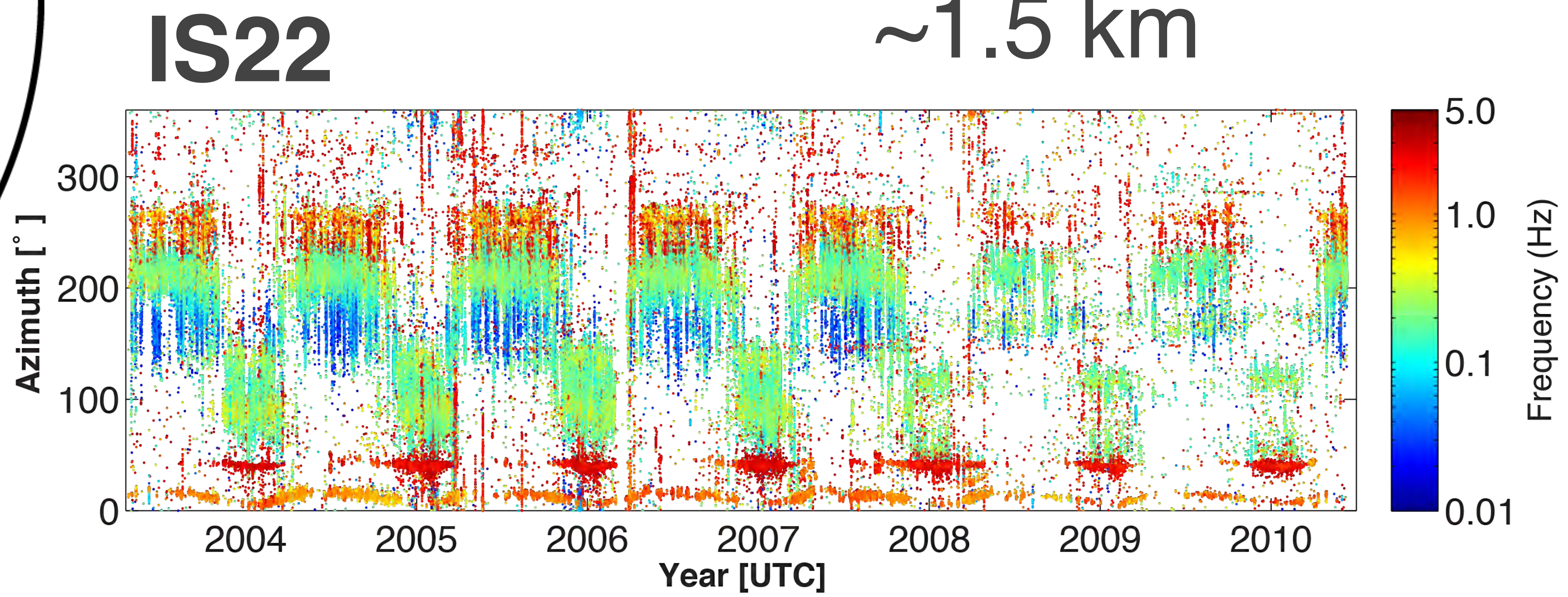

Le Pichon, Matoza, et al. [2010]

June 2009 Eruption of Sarychev Peak, Kuriles

- Infrasound 640-6,400 km from Sarychev Peak
- Only ground-based data (remote location, no local monitoring)

International Monitoring System Infrasound network

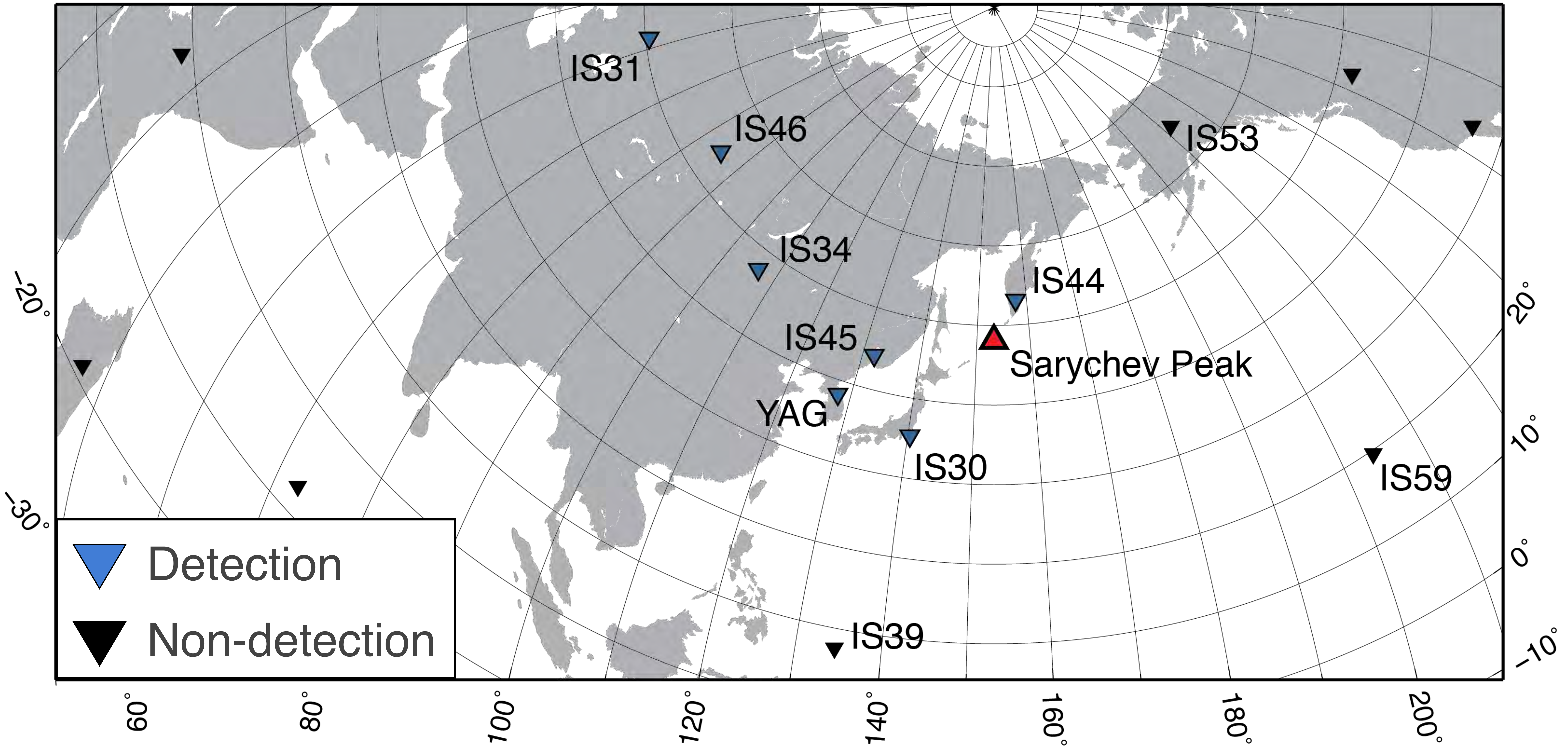

Matoza et al. [2011]

Neal et al. [2009]

NASA Earth Observatory

June 2009 Eruption of Sarychev Peak, Kuriles

- **We can:** Detect, locate, and provide chronologies of explosive volcanism
- **Caveat:** Latency ~15 minutes per 250 km; IS44 ~35 minute latency.

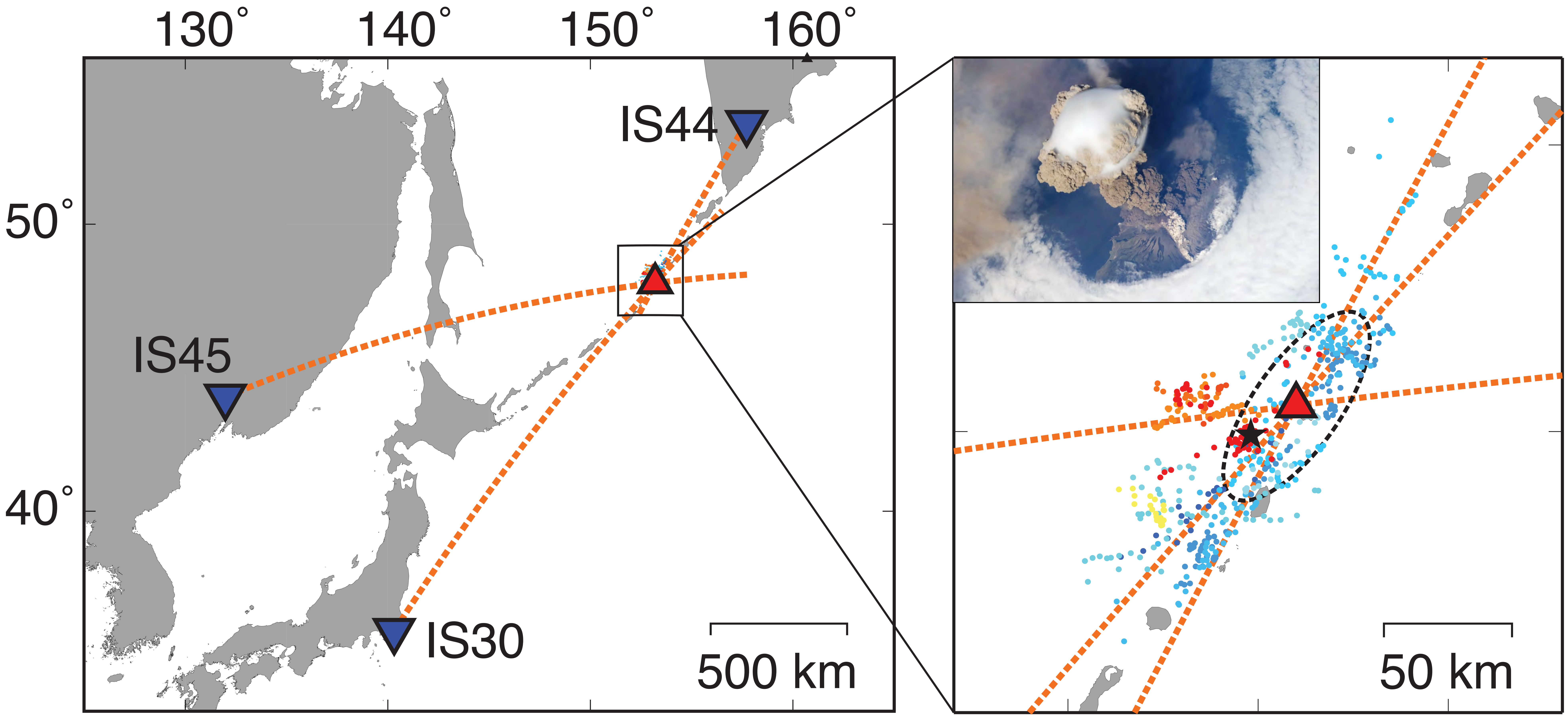

Matoza et al. [2011]

June 2009 Eruption of Sarychev Peak, Kuriles

- **We can:** Detect, locate, and provide chronologies of explosive volcanism

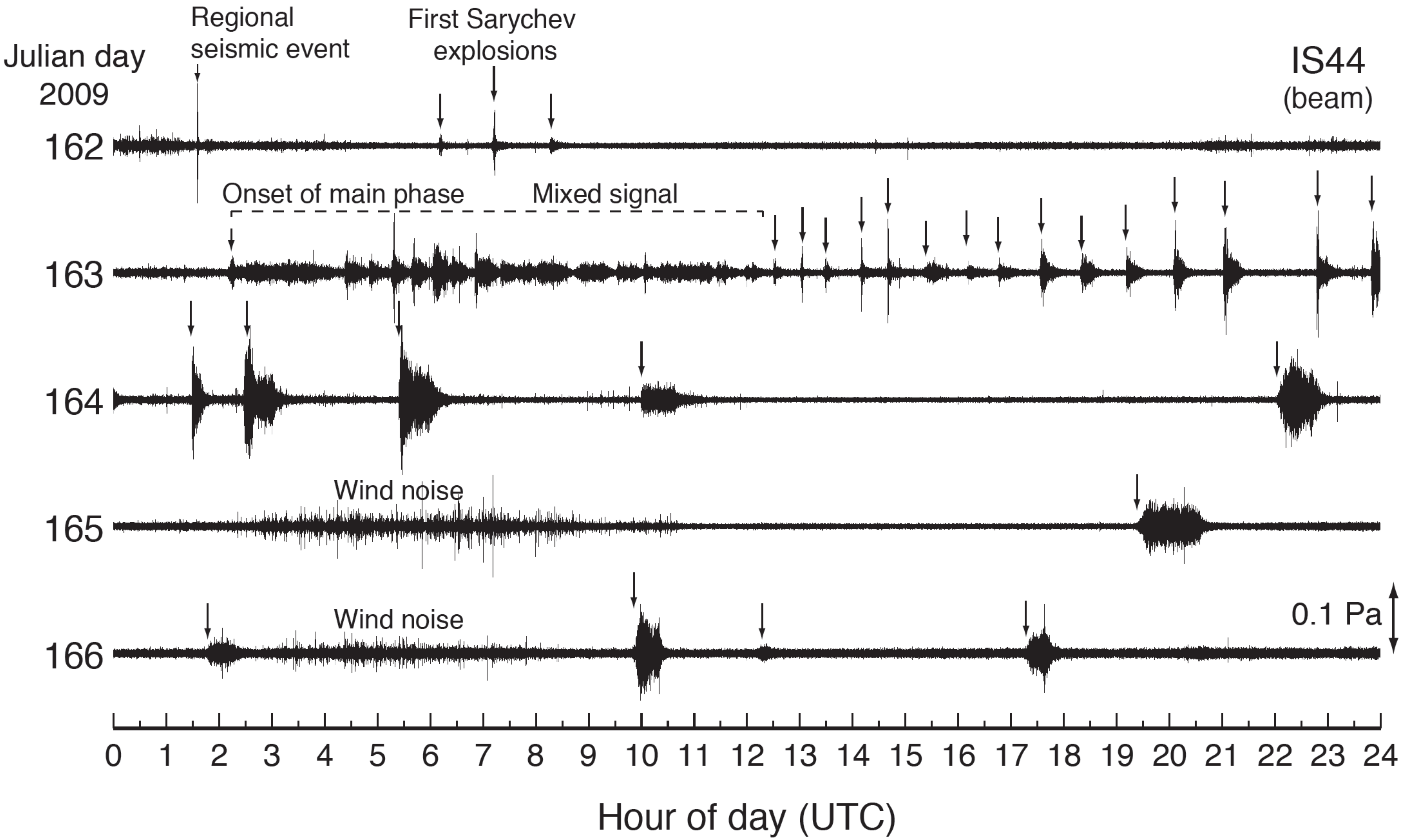

Matoza et al. [2011]

Automated global volcano acoustic cataloging

- Systematic search of IMS data for eruption infrasound
- Aim: build a global quantitative acoustic catalog of explosive volcanism

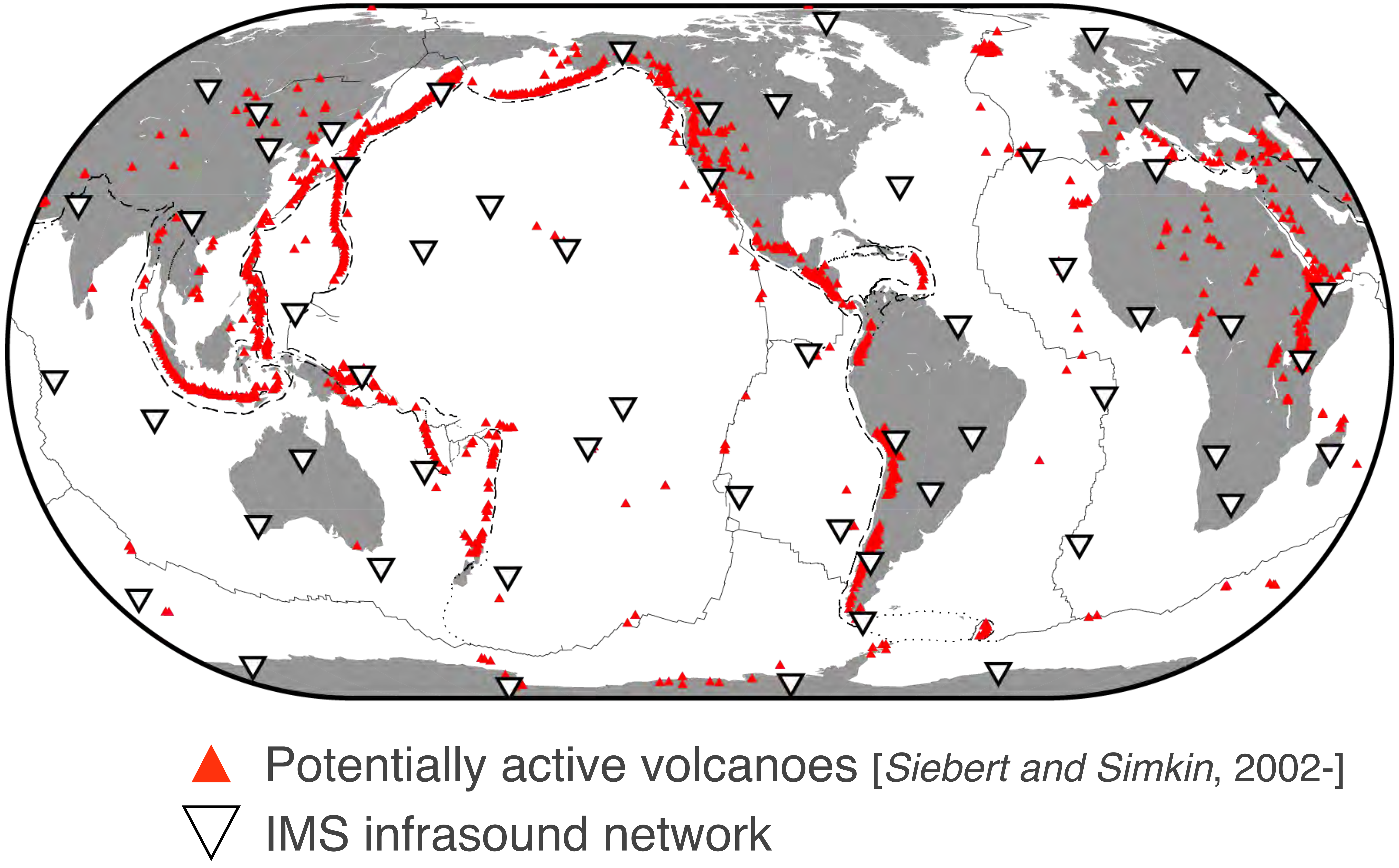

Matoza et al., [2017]

Automated global volcano acoustic cataloging

1. Go backwards from infrasound data, blind search for eruption signals
2. Analyze all IMS data globally, not just individual case studies or regions

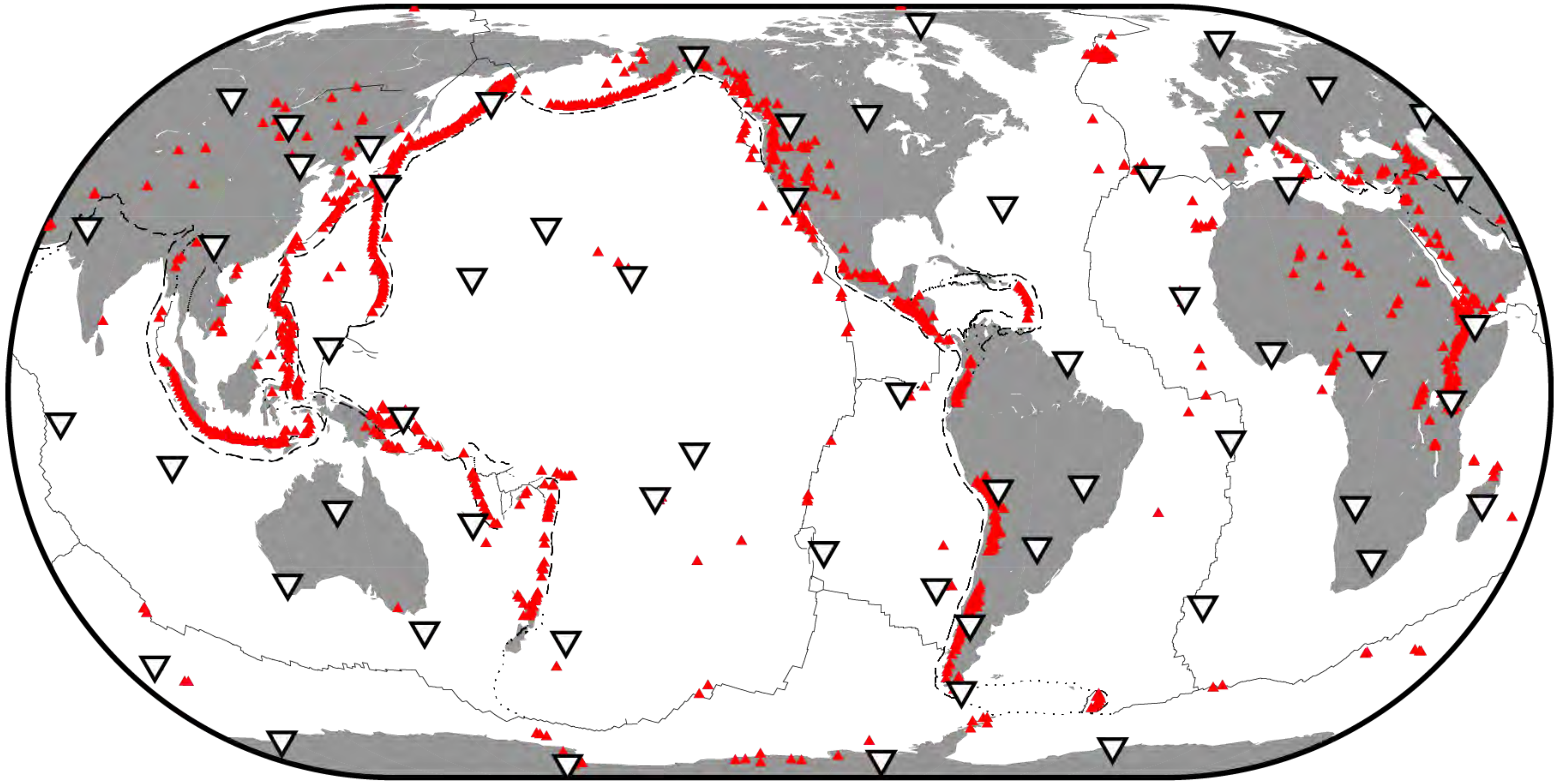

▲ Potentially active volcanoes [*Siebert and Simkin*, 2002-]

▽ IMS infrasound network

Matoza et al., [2017]

IMS-vAsc: association and location

Combined association and location: brute-force, grid-search, cross-bearings approach

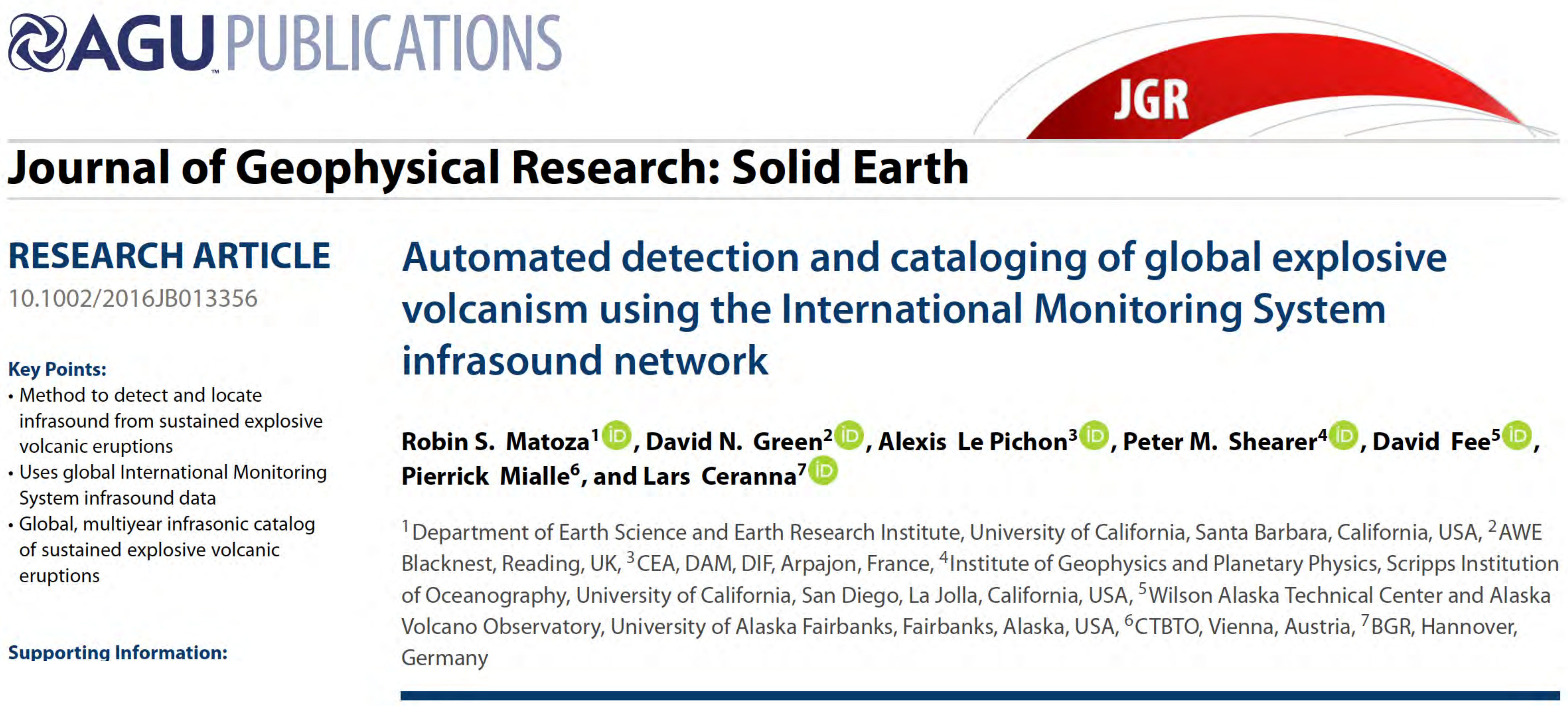

AGU PUBLICATIONS

JGR

Journal of Geophysical Research: Solid Earth

RESEARCH ARTICLE

10.1002/2016JB013356

Key Points:
- Method to detect and locate infrasound from sustained explosive volcanic eruptions
- Uses global International Monitoring System infrasound data
- Global, multiyear infrasonic catalog of sustained explosive volcanic eruptions

Supporting Information:

Automated detection and cataloging of global explosive volcanism using the International Monitoring System infrasound network

Robin S. Matoza[1], David N. Green[2], Alexis Le Pichon[3], Peter M. Shearer[4], David Fee[5], Pierrick Mialle[6], and Lars Ceranna[7]

[1]Department of Earth Science and Earth Research Institute, University of California, Santa Barbara, California, USA, [2]AWE Blacknest, Reading, UK, [3]CEA, DAM, DIF, Arpajon, France, [4]Institute of Geophysics and Planetary Physics, Scripps Institution of Oceanography, University of California, San Diego, La Jolla, California, USA, [5]Wilson Alaska Technical Center and Alaska Volcano Observatory, University of Alaska Fairbanks, Fairbanks, Alaska, USA, [6]CTBTO, Vienna, Austria, [7]BGR, Hannover, Germany

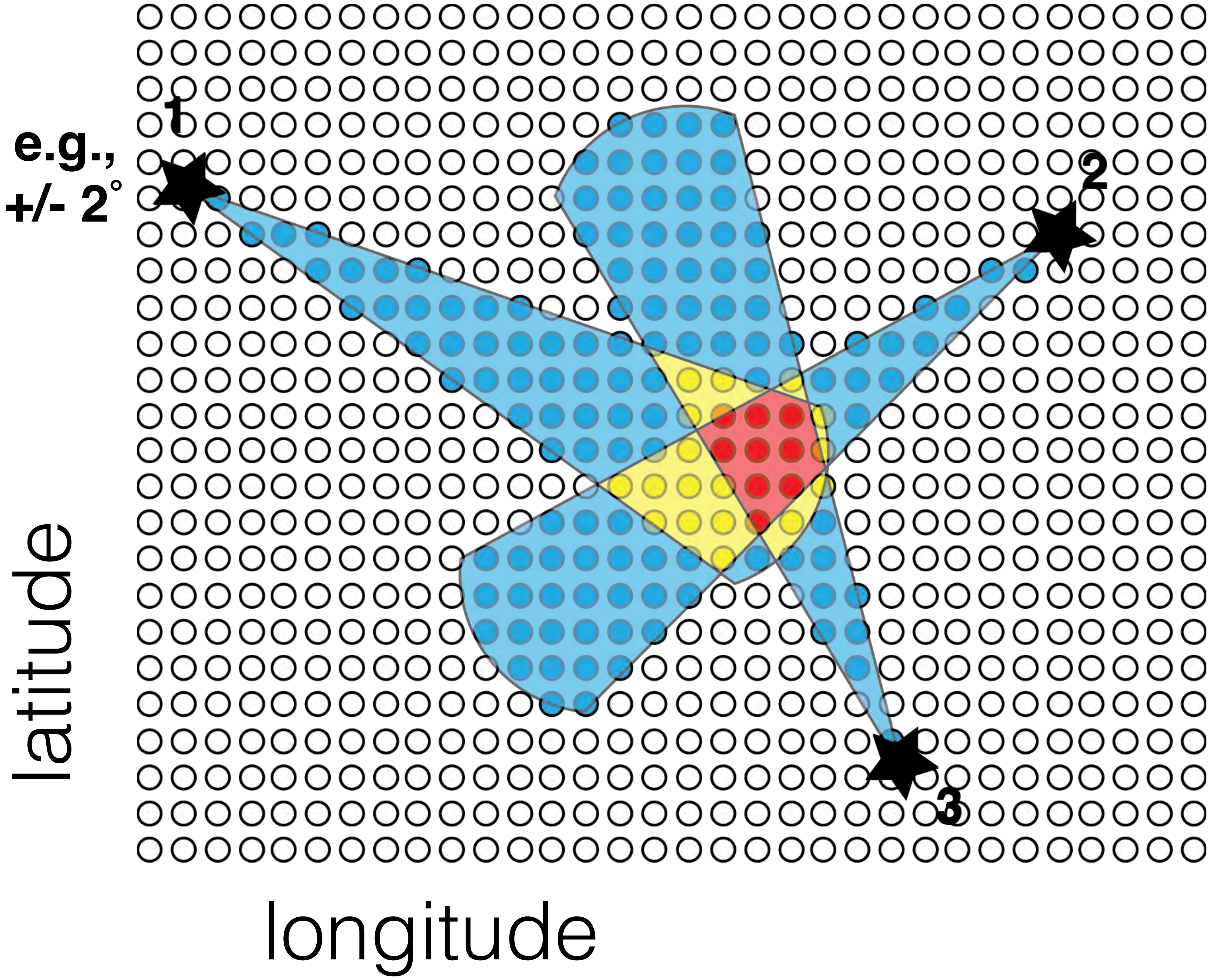

- Link each station to a grid of trial source nodes based on backazimuth
- No atmospheric propagation correction

Planned: Public release of Fortran 90 code

Matoza et al. [2017]

Example grid function: Sarychev Peak 2009

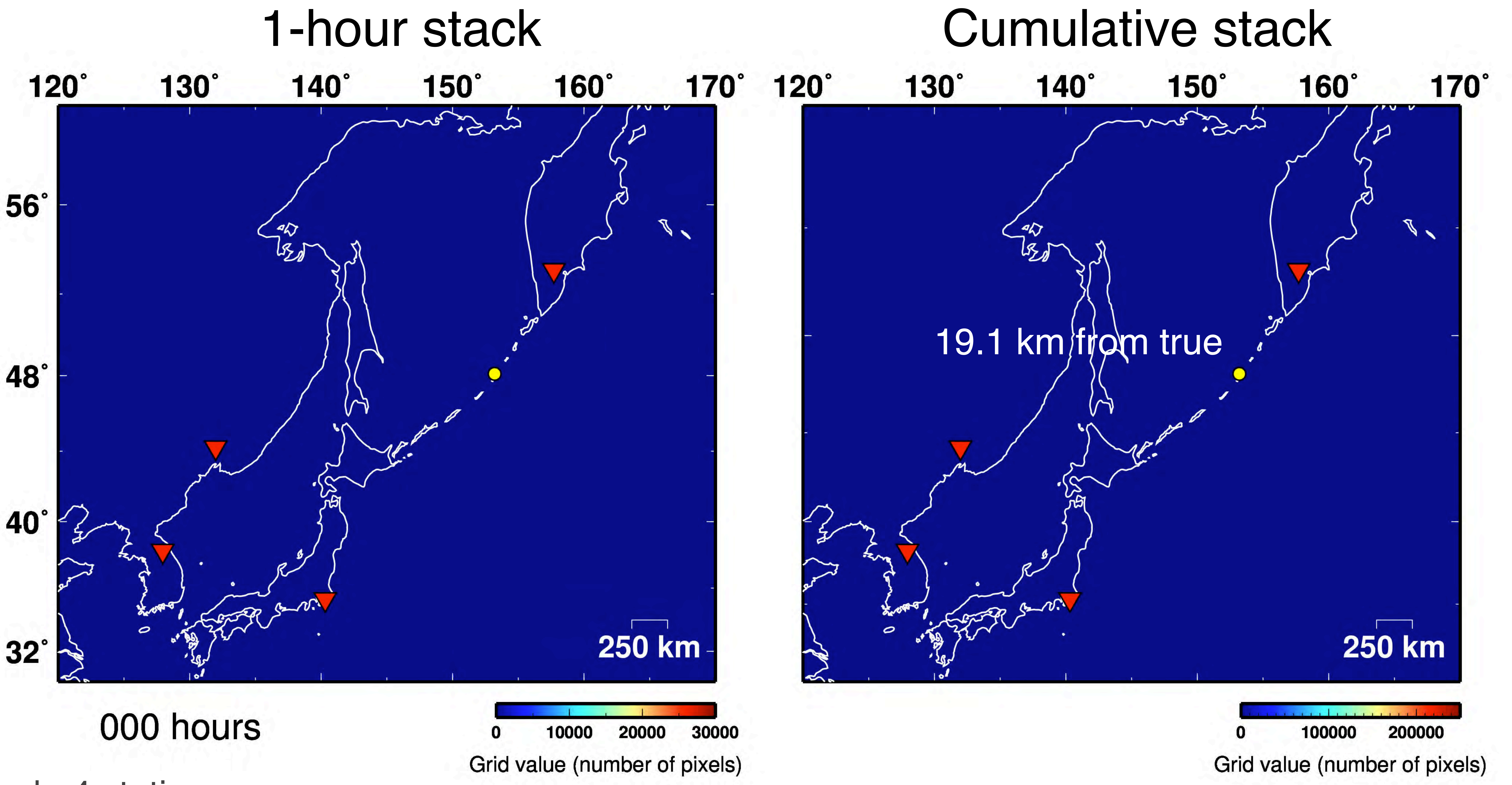

- Sarychev Peak, 4 stations
- 11–16 June 2009

Matoza et al. [2017]

IMS-vAsc: association and location

Combined association and location: brute-force, grid-search, cross-bearings approach

Sarychev Peak 4 stations

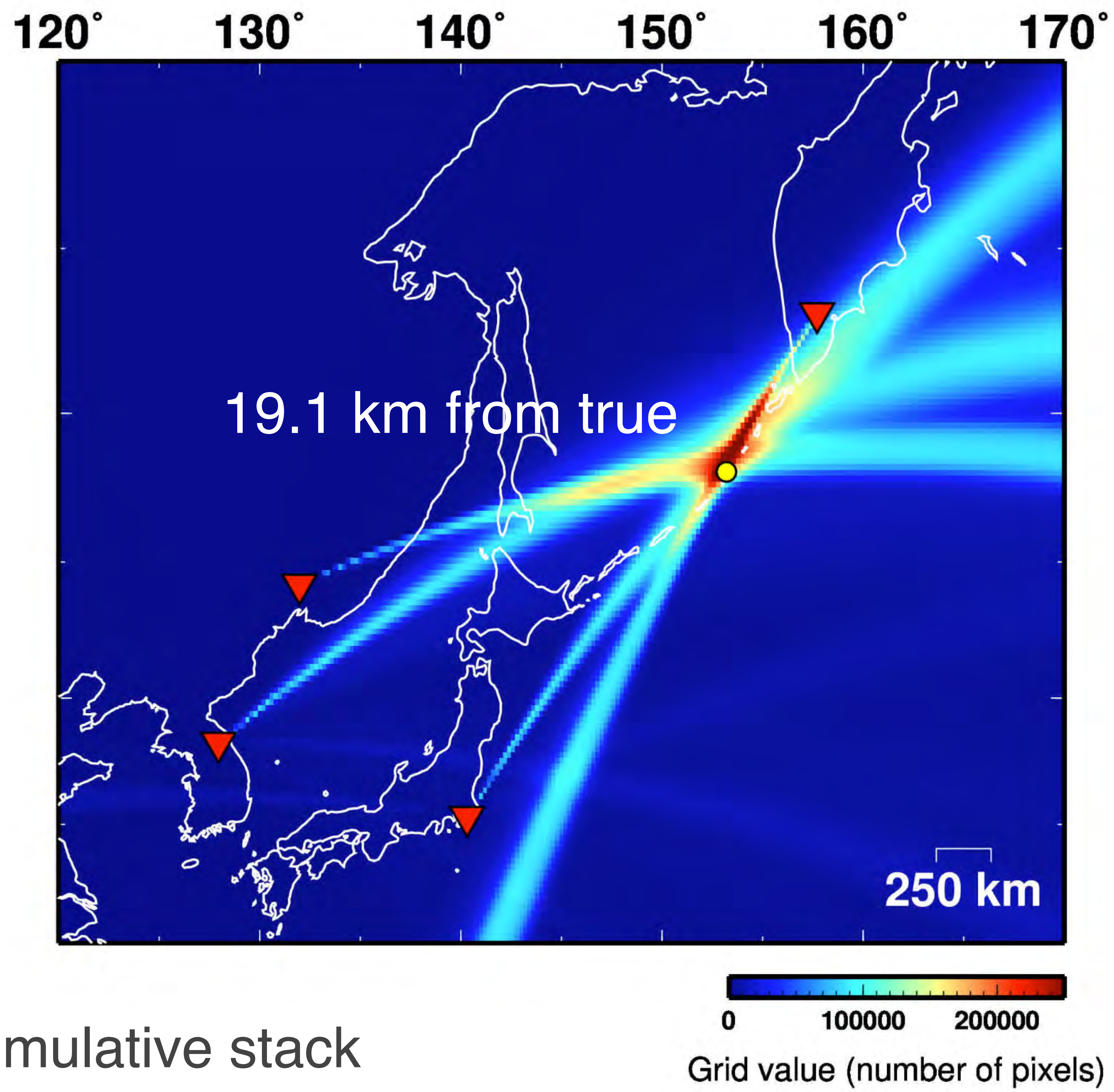

- 5-day cumulative stack
- 11–16 June 2009

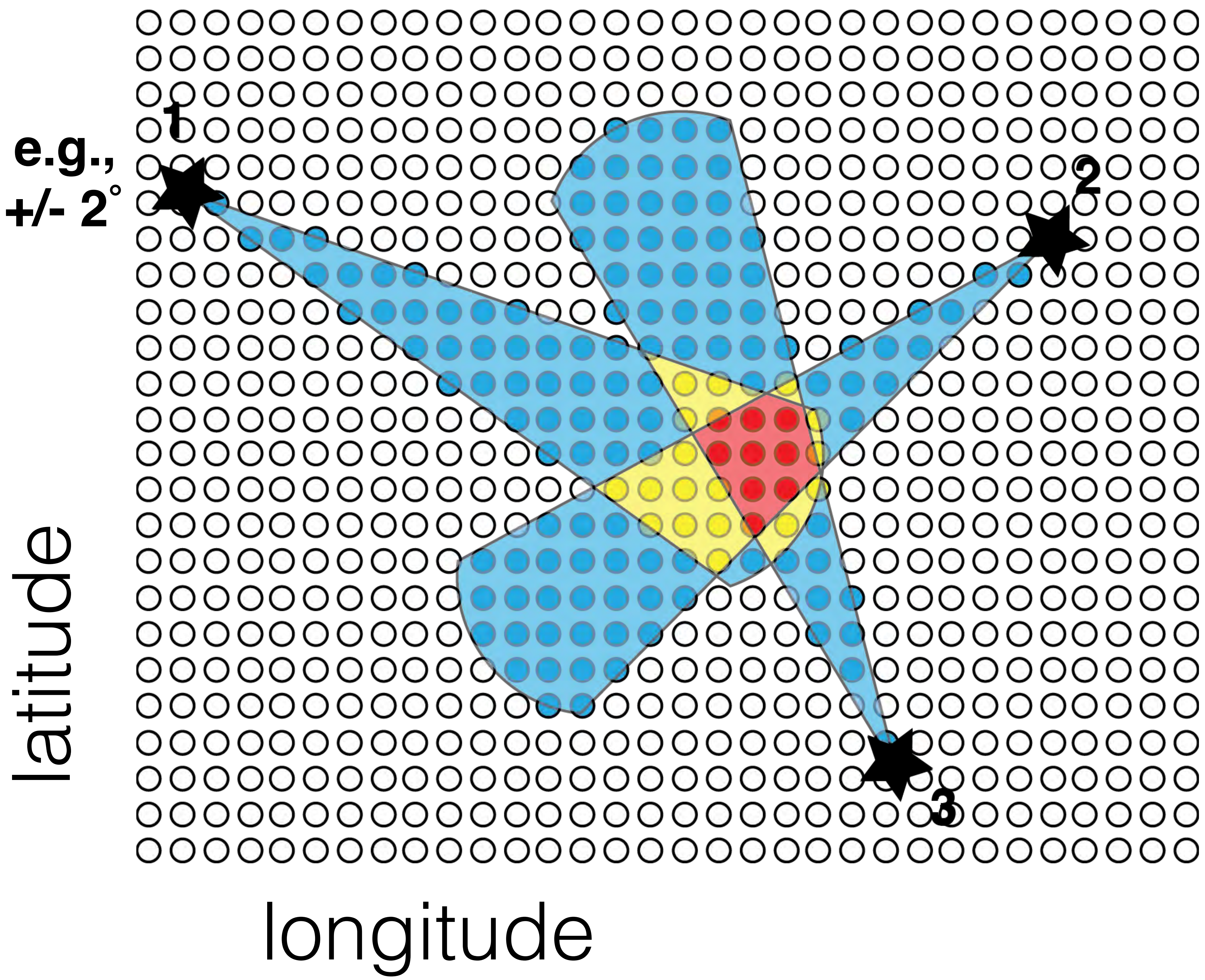

- Link each station to a grid of trial source nodes based on backazimuth
- No atmospheric propagation correction

Matoza et al. [2017]

Results: 2005–2017

- Matoza et al. [2017]; Data from 2005–2010: IMS under construction, 2/3 complete
- Results with more recent data 2005–2017, more complete network (in progress)

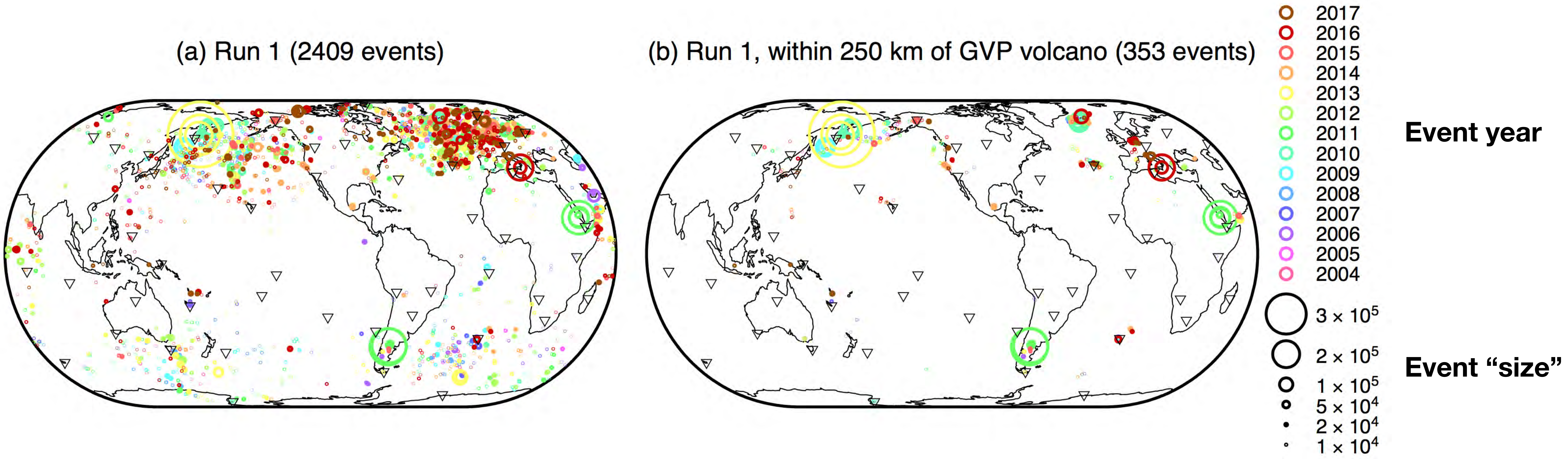

Results: 2005–2017

- Results with more recent data 2005–2017, more complete network (in progress)

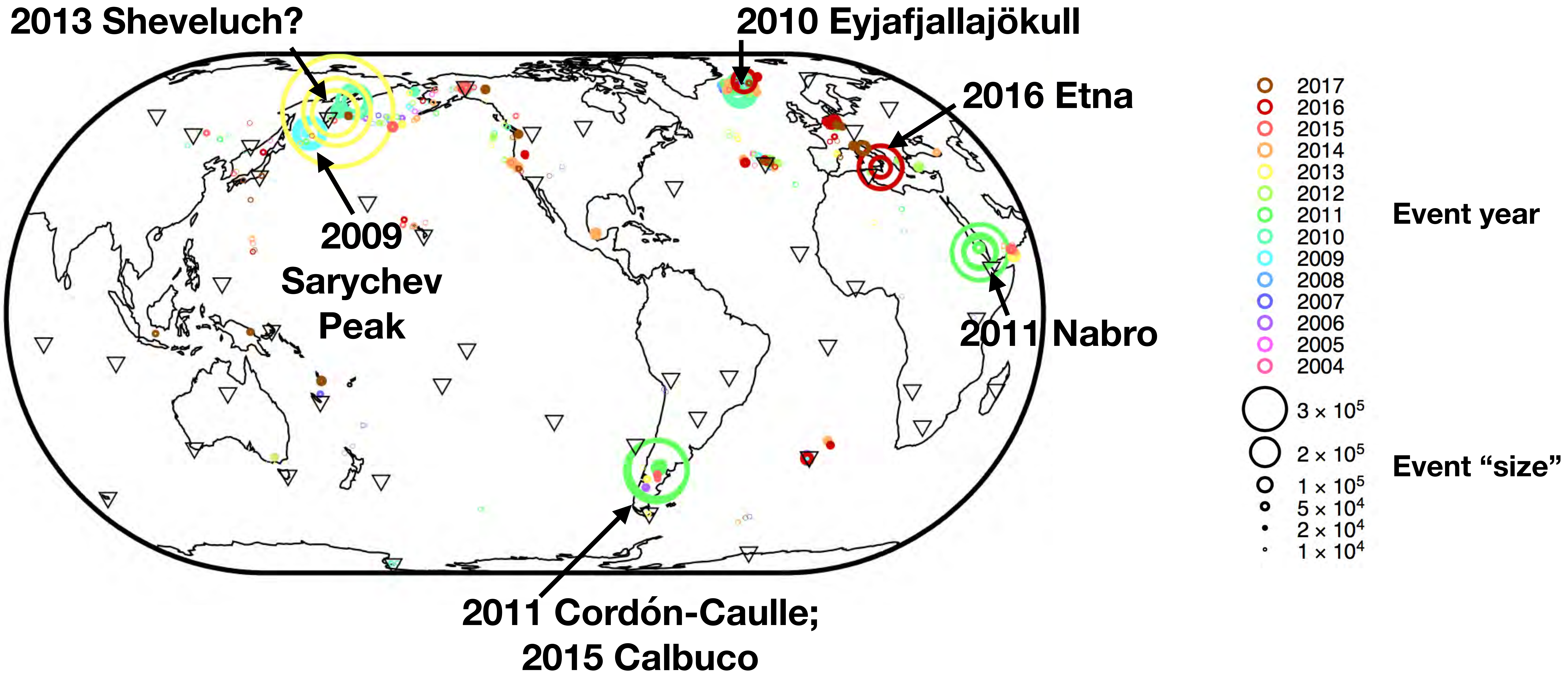

IMS network and global volcano monitoring

- Detection capability improves as IMS network nears completion
- Utility of additional infrasound stations in regions of dense volcanism [e.g., *Guilbert et al.*, 2005; *Matoza et al.*, 2007; *Garces et al.*, 2008; *De Angelis et al.*, 2012; *Taisne et al.*, 2012; *Tailpied et al.*, 2013]
- Add more infrasound sensors to existing regional seismic networks

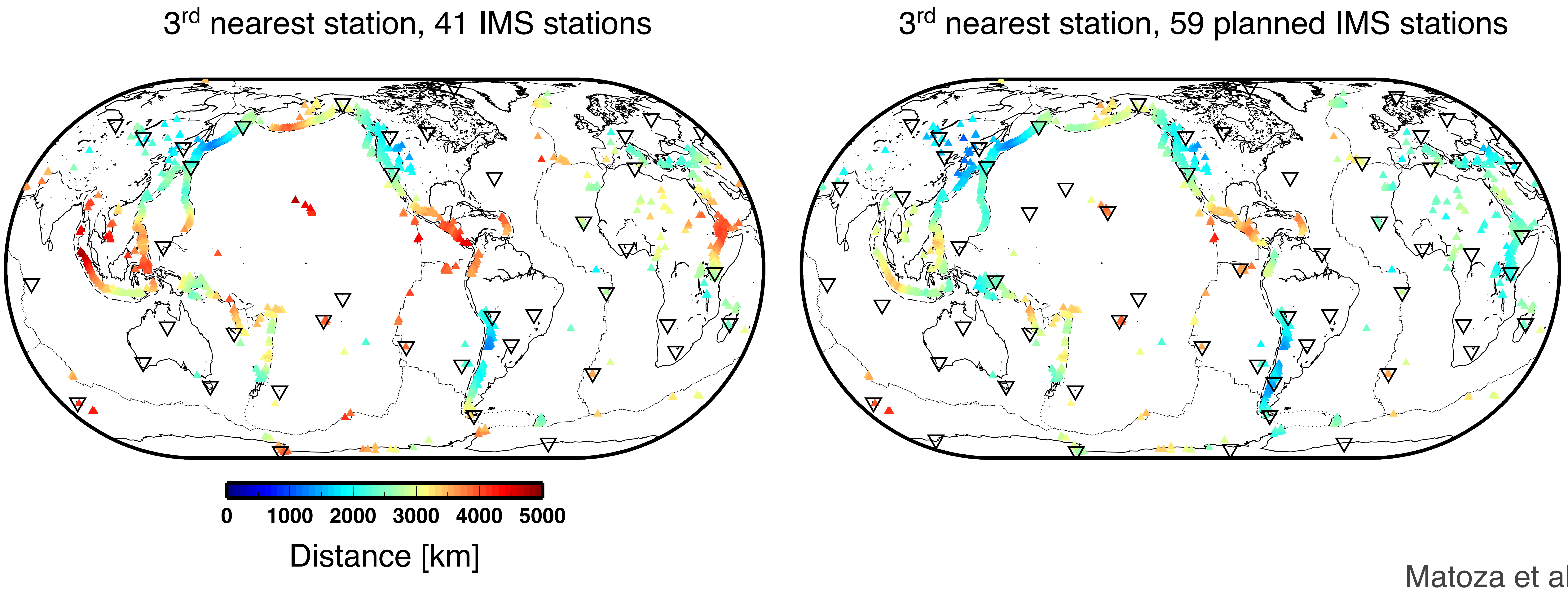

Matoza et al. [2017]

April 2015 eruption of Calbuco

- VEI 4 explosive volcanic eruption in Chile
- 22–23 April 2015; plume heights > 23 km a.s.l.
- Recorded on 5 stations of the IMS network: 1,525 to 5,122 km ranges
- Recorded by local monitoring stations and seismo-acoustic stations across Chile

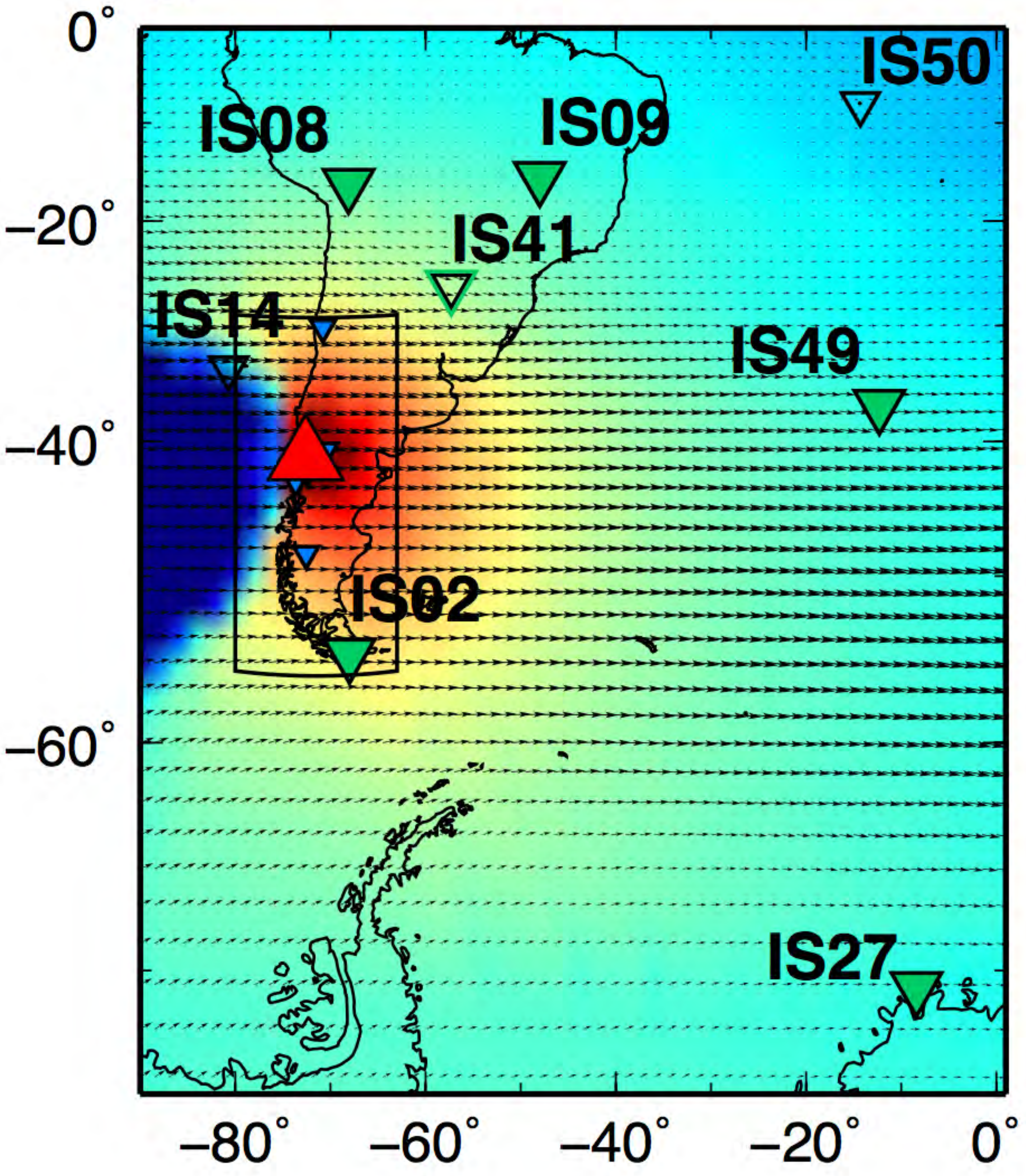

Color: Transmission Loss [dB]

Matoza et al. [2018]

April 2015 eruption of Calbuco

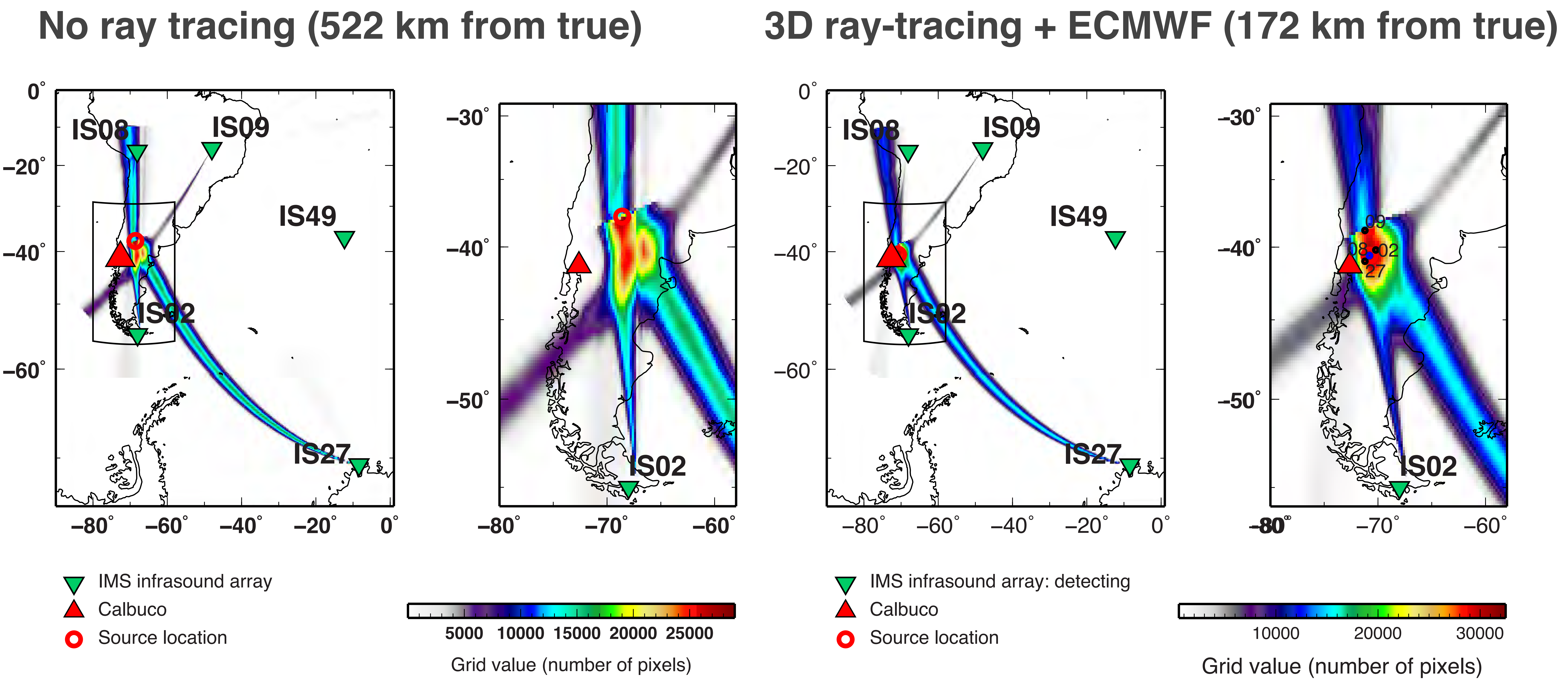

Matoza et al. [2018]

Regional seismo-acoustic observations

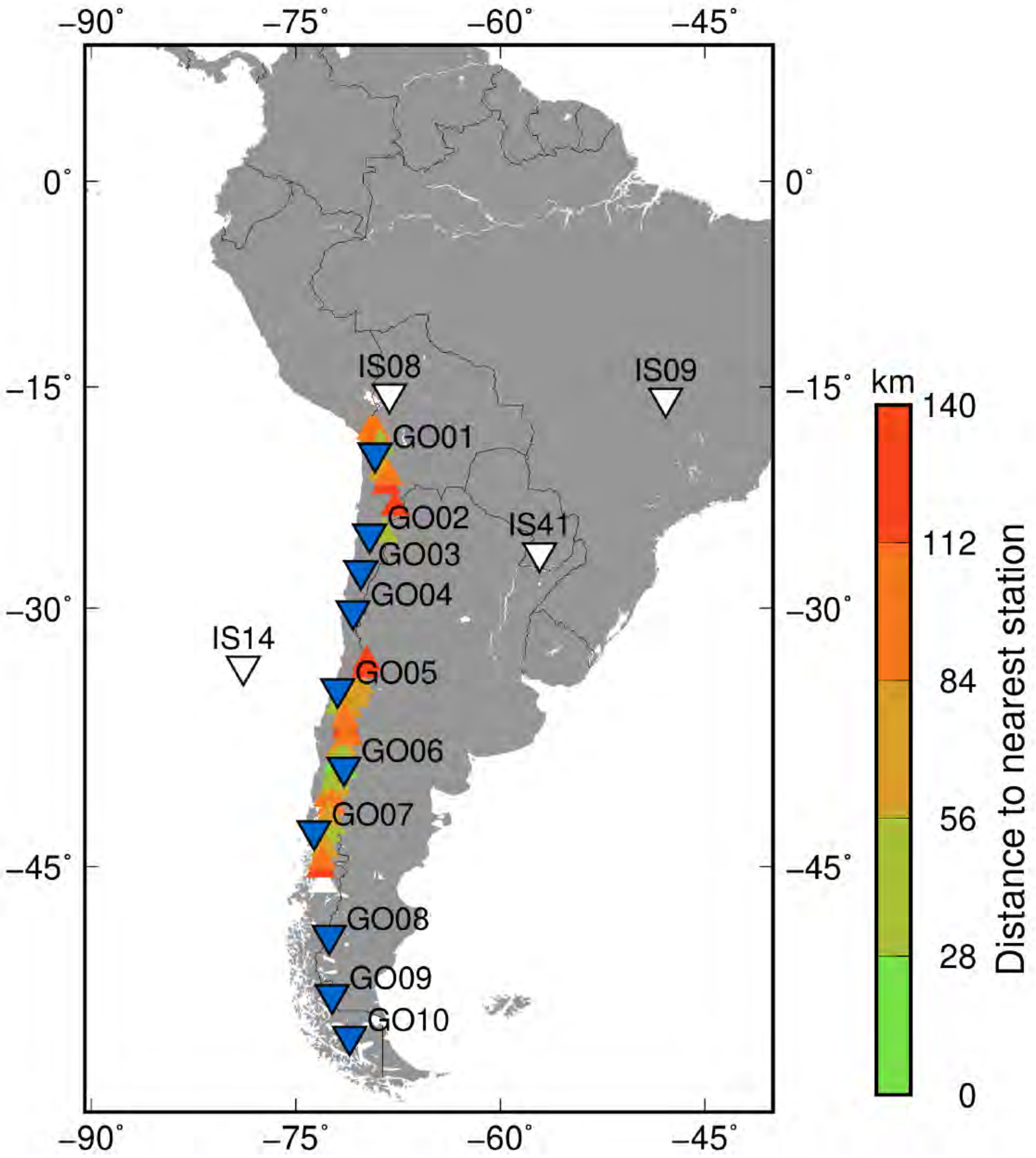

Rodrigo De Negri, UCSB

- Chilean National Seismic Network: 10 seismo-acoustic stations
- Infrasound recorded well on 4 stations out to 1,540 km
- Only 1 station (GO07, 216 km) recorded both infrasound and seismic from Calbuco

Matoza et al. [2018]

Regional seismo-acoustic observations

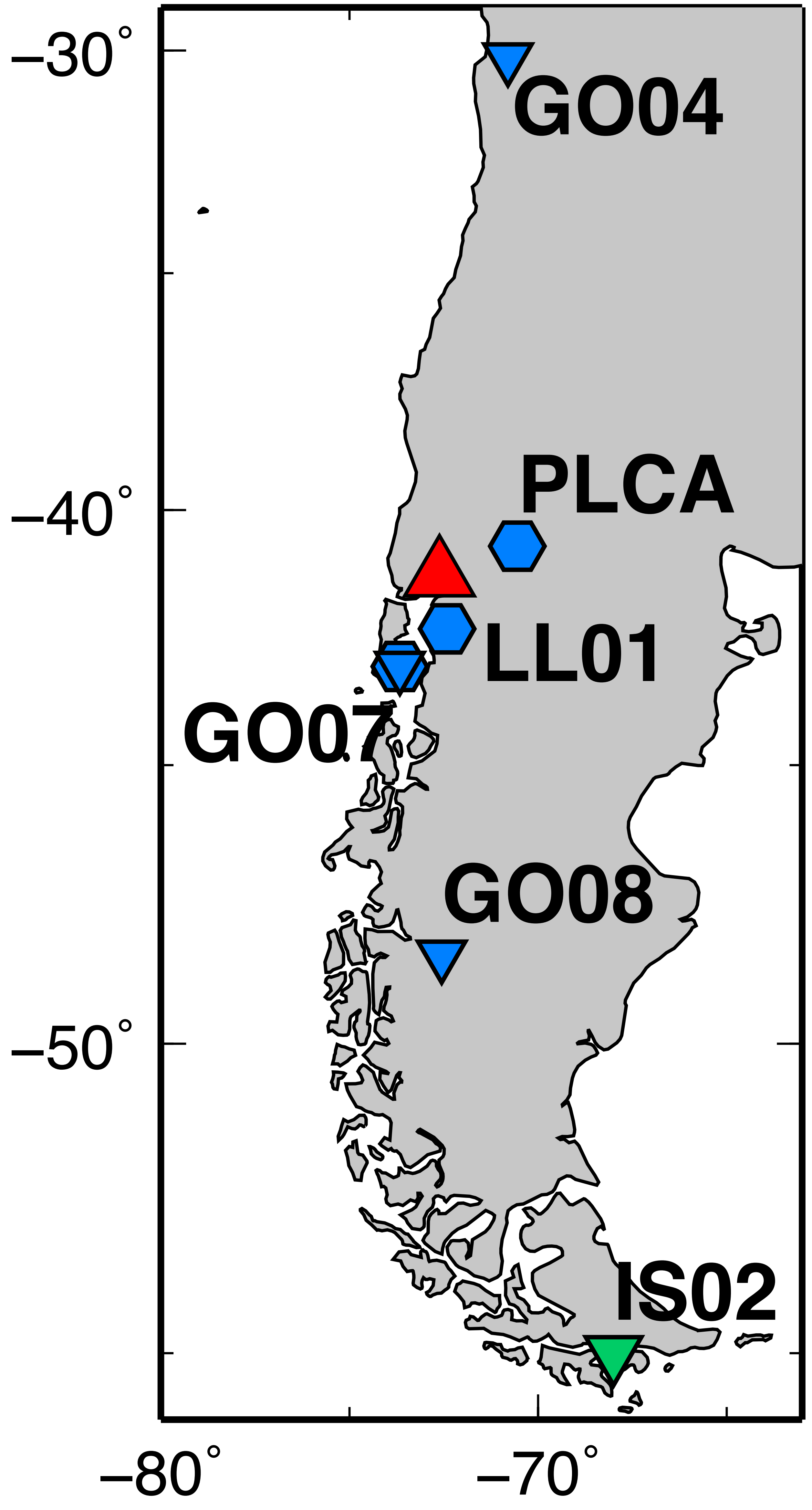

- Seismic signals recorded out to ~250 km
- Combined seismic + air-ground coupled infrasound

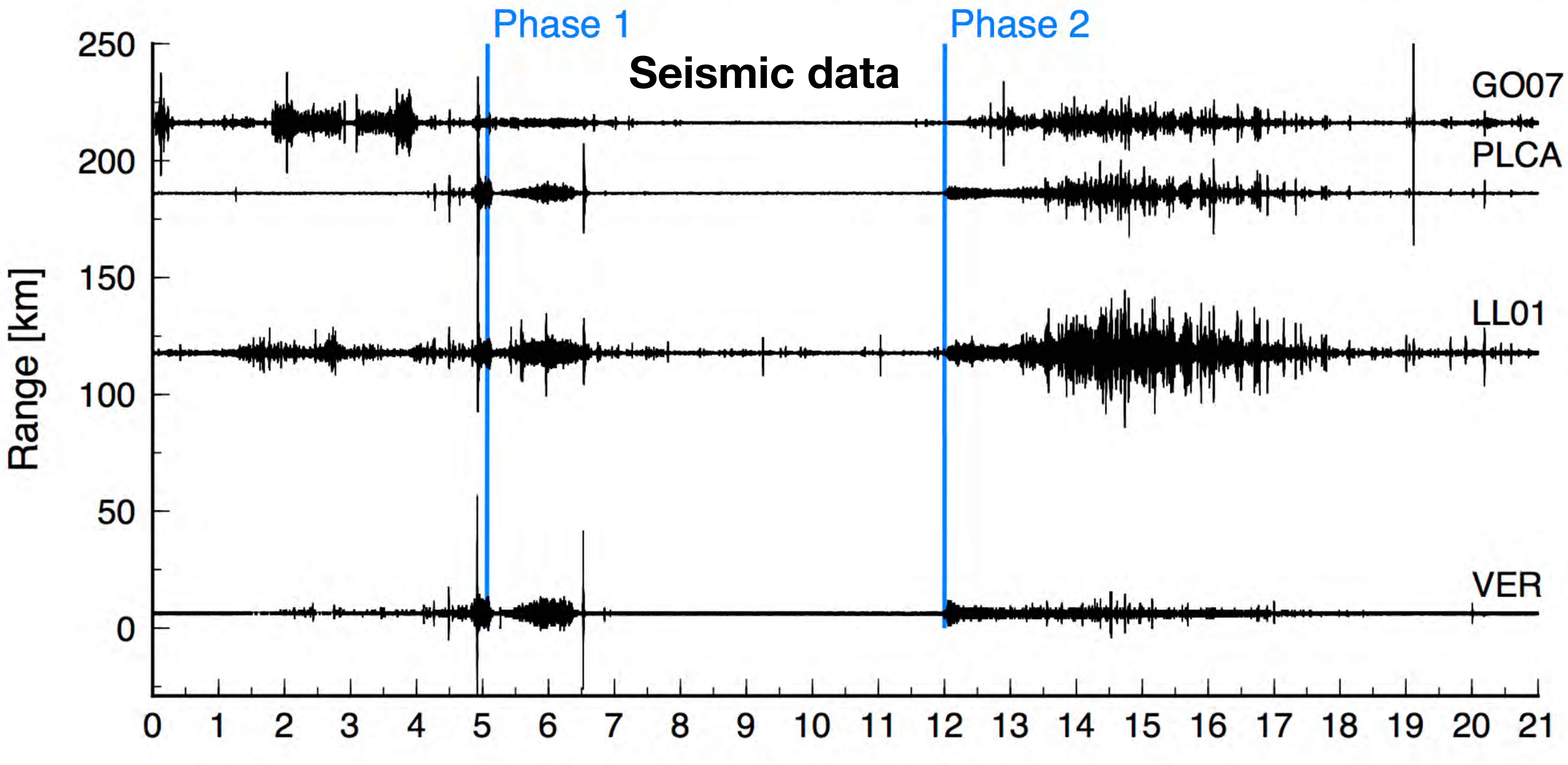

Data from Chilean National Seismic Network, Red Sismologica Nacional, Global Telemetered Seismograph Network. Downloaded via IRIS

Matoza et al. [2018]

Regional seismo-acoustic observations

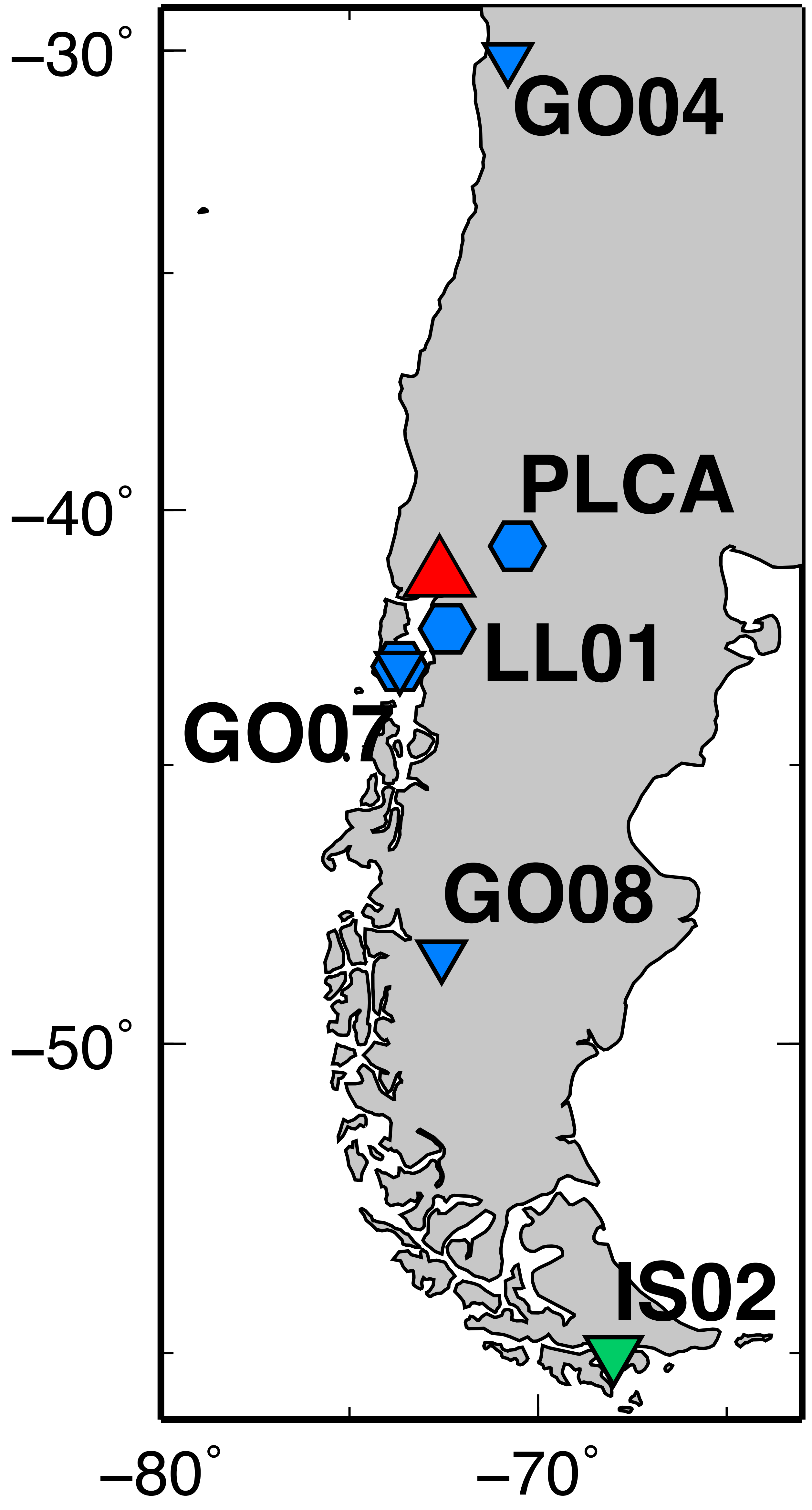

P and *S* phases propagating with move-outs of 6.8 km/s and 3.8 km/s

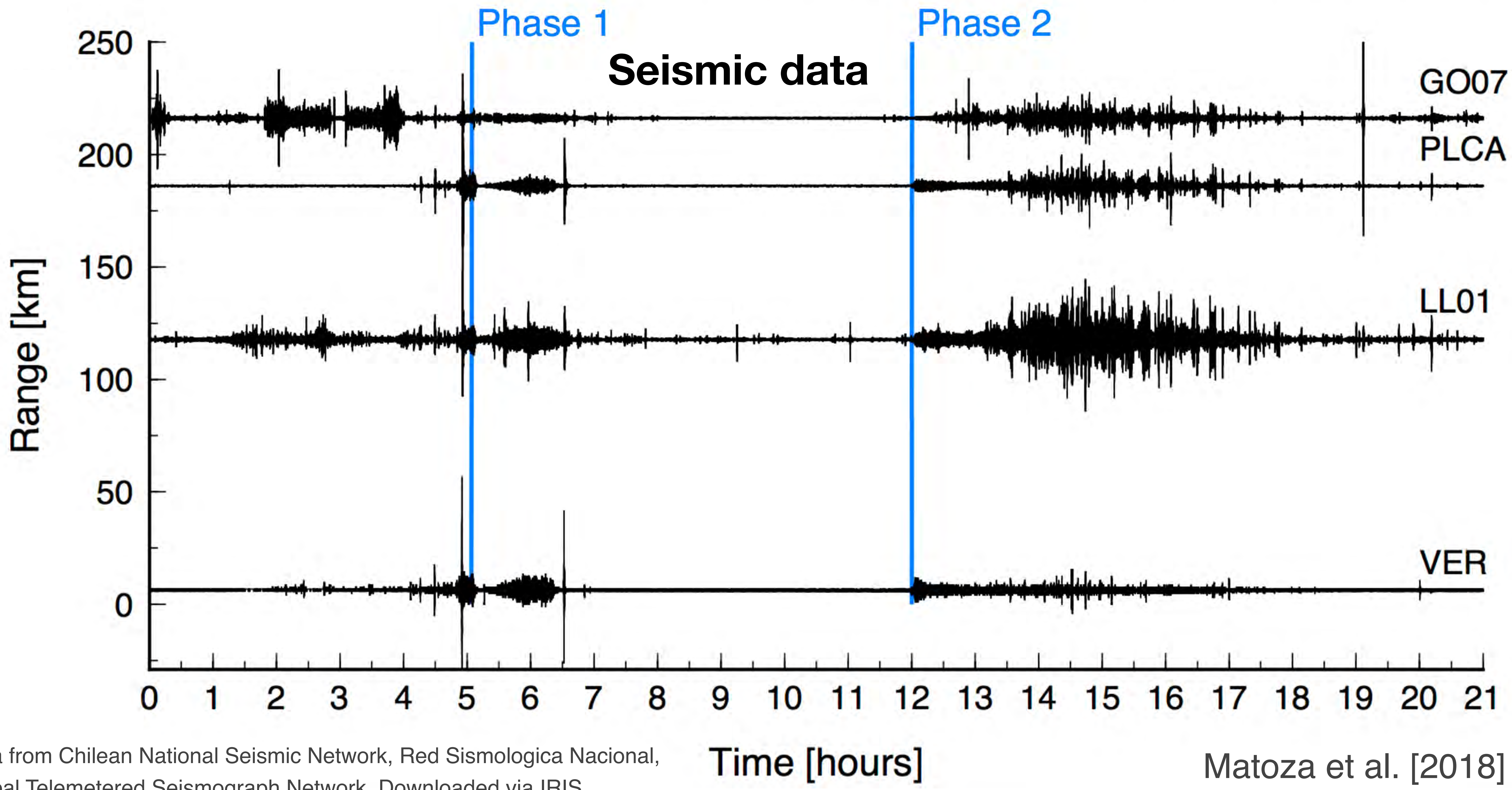

Data from Chilean National Seismic Network, Red Sismologica Nacional, Global Telemetered Seismograph Network. Downloaded via IRIS

Matoza et al. [2018]

Regional seismo-acoustic observations

Also infrasound arrivals ~0.3 km/s move out (celerity)

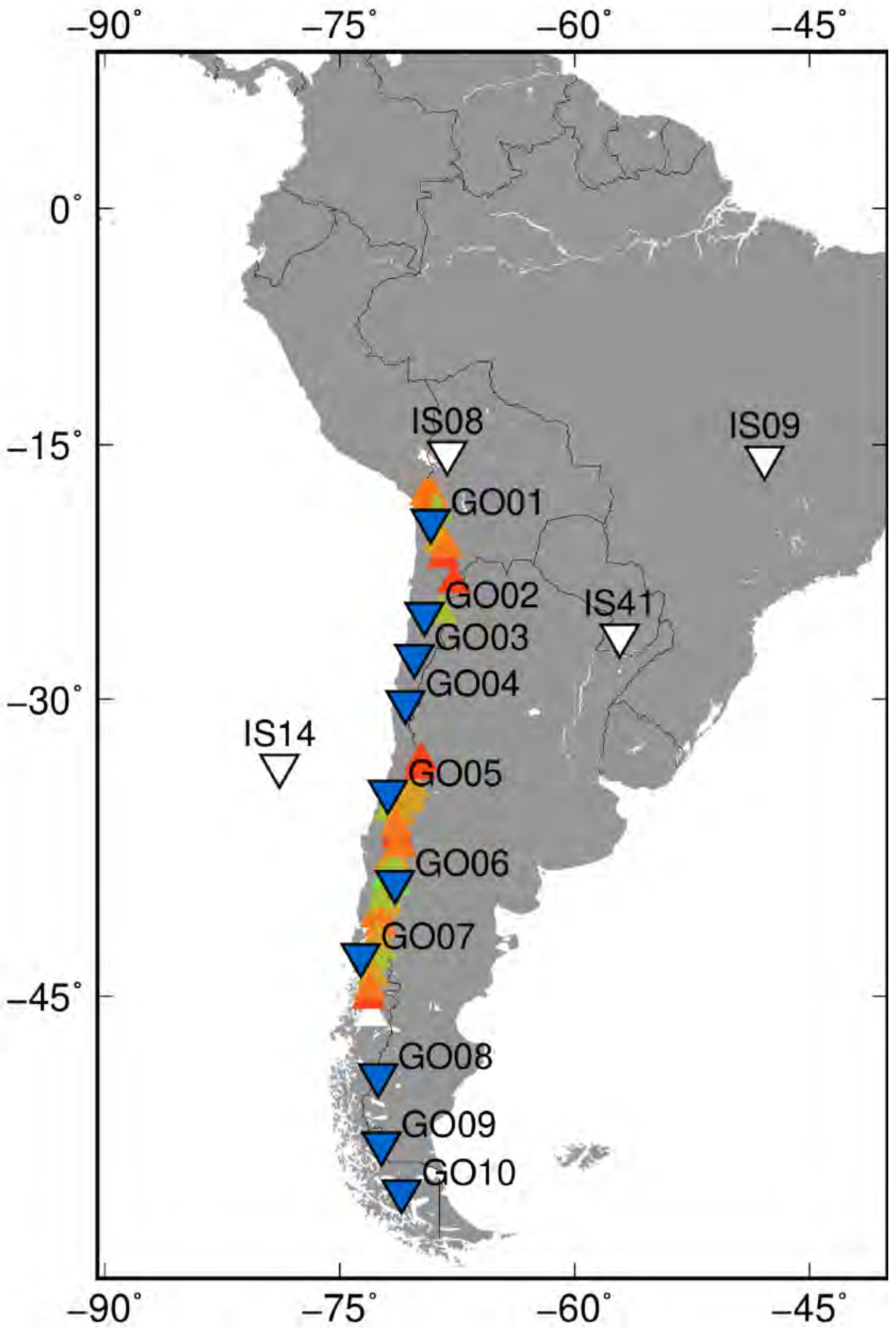

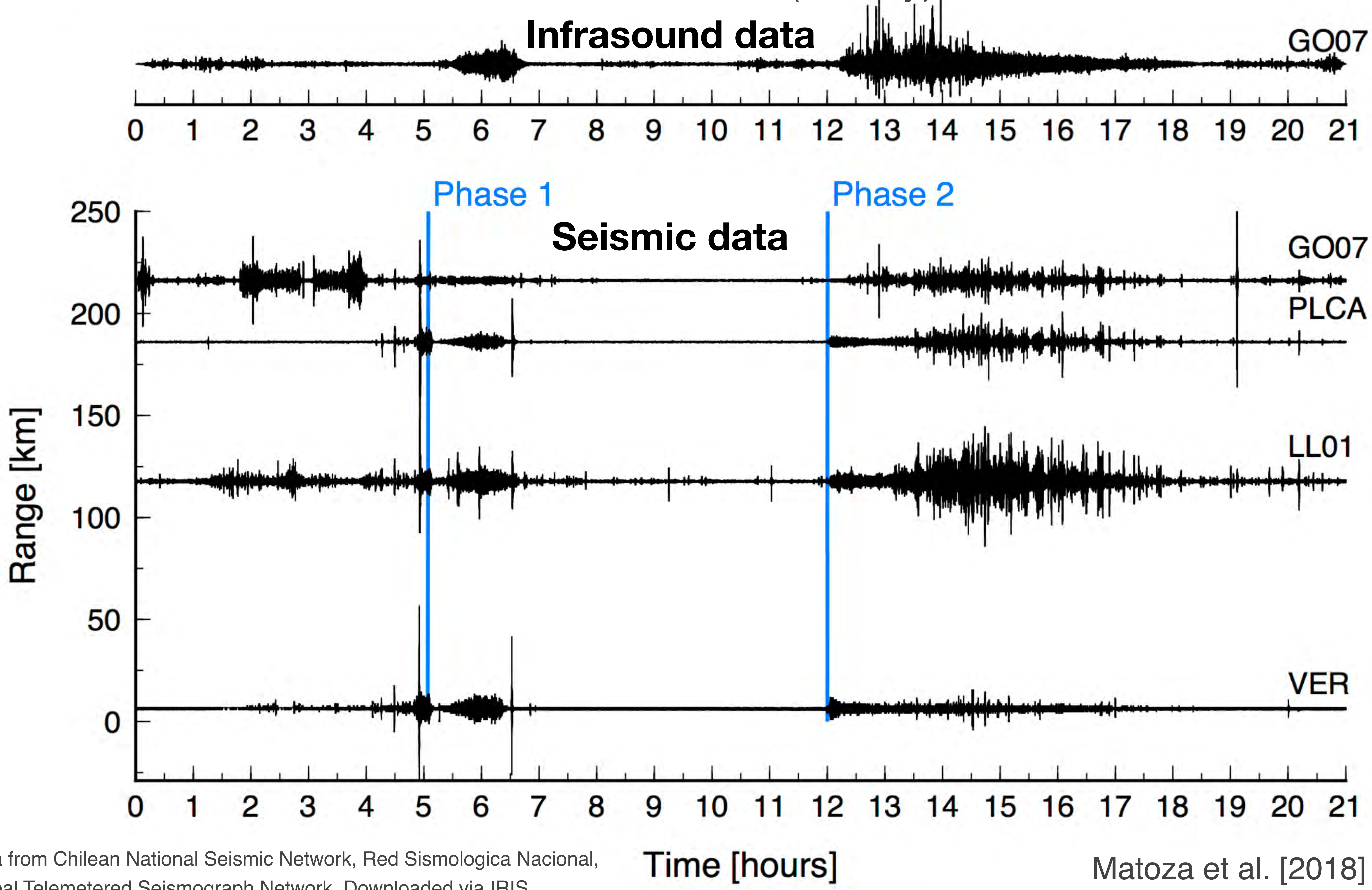

Data from Chilean National Seismic Network, Red Sismologica Nacional, Global Telemetered Seismograph Network. Downloaded via IRIS

Matoza et al. [2018]

Seismo-acoustic cross-correlation and coherence

Examine air-ground coupling using cross-correlation and coherence

Ichihara et al. [2012], Matoza and Fee. [2014]

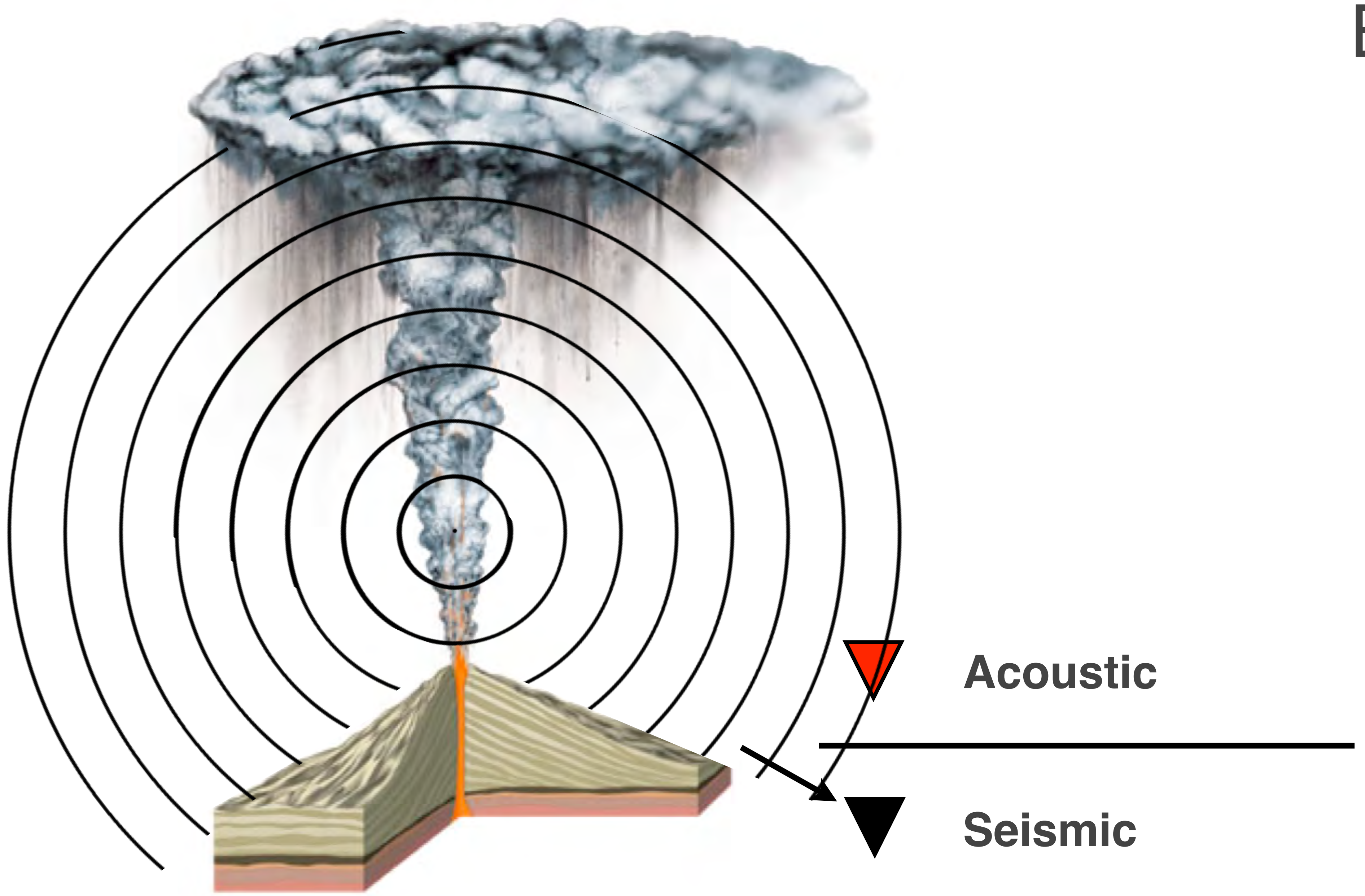

coherence $\gamma_{wp}^2(f) = \frac{|S_{wp}|^2}{S_{ww}S_{pp}}$

cross spectrum (numerator)

power spectra (denominator)

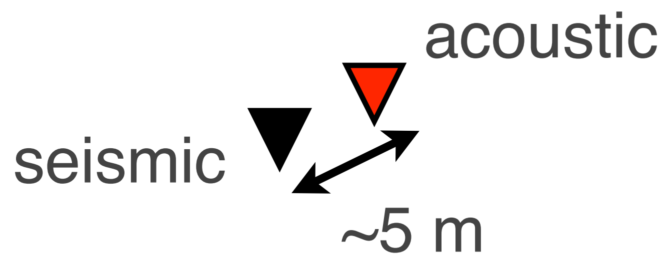

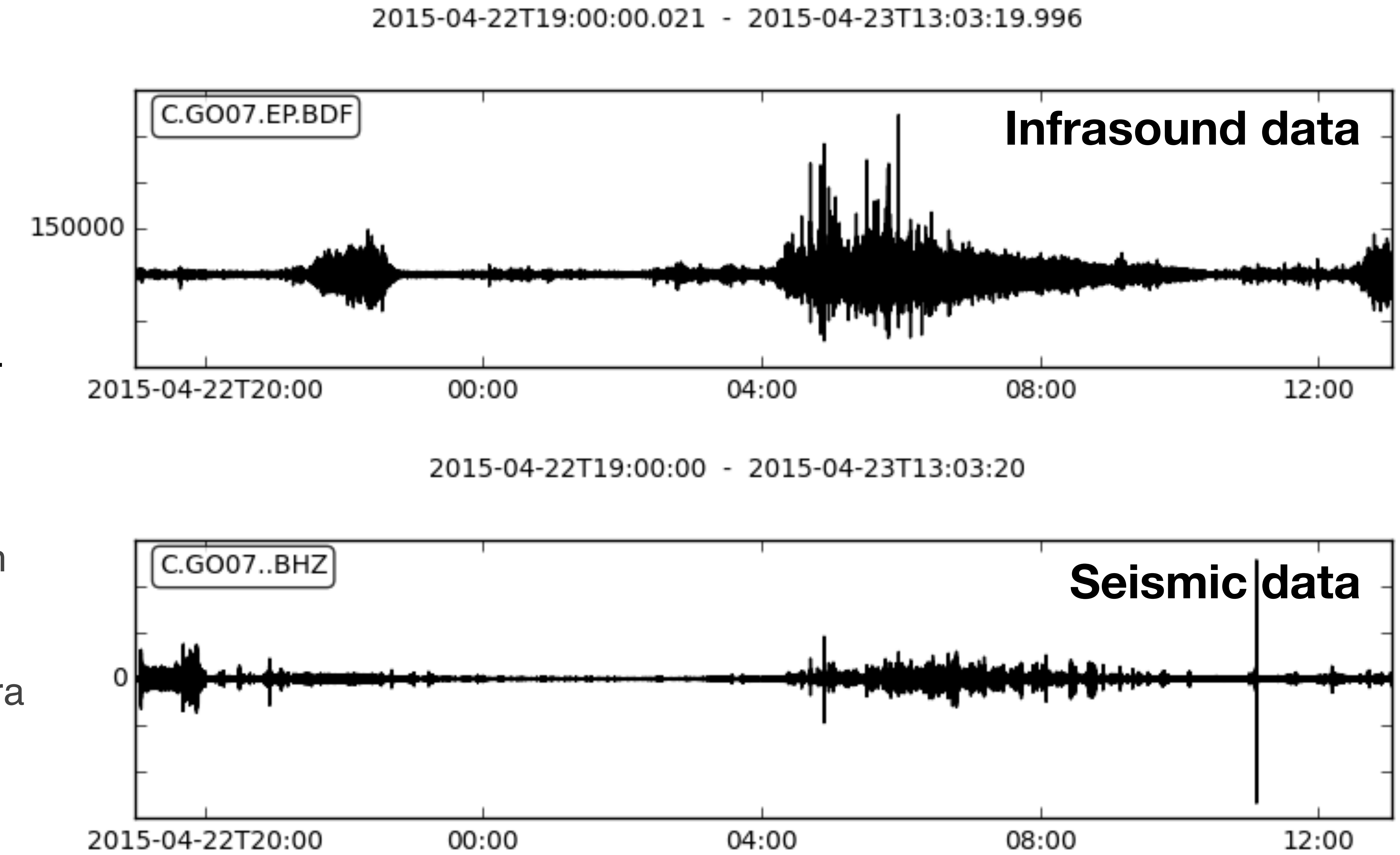

Station GO07 (216 km)

Seismo-acoustic cross-correlation and coherence

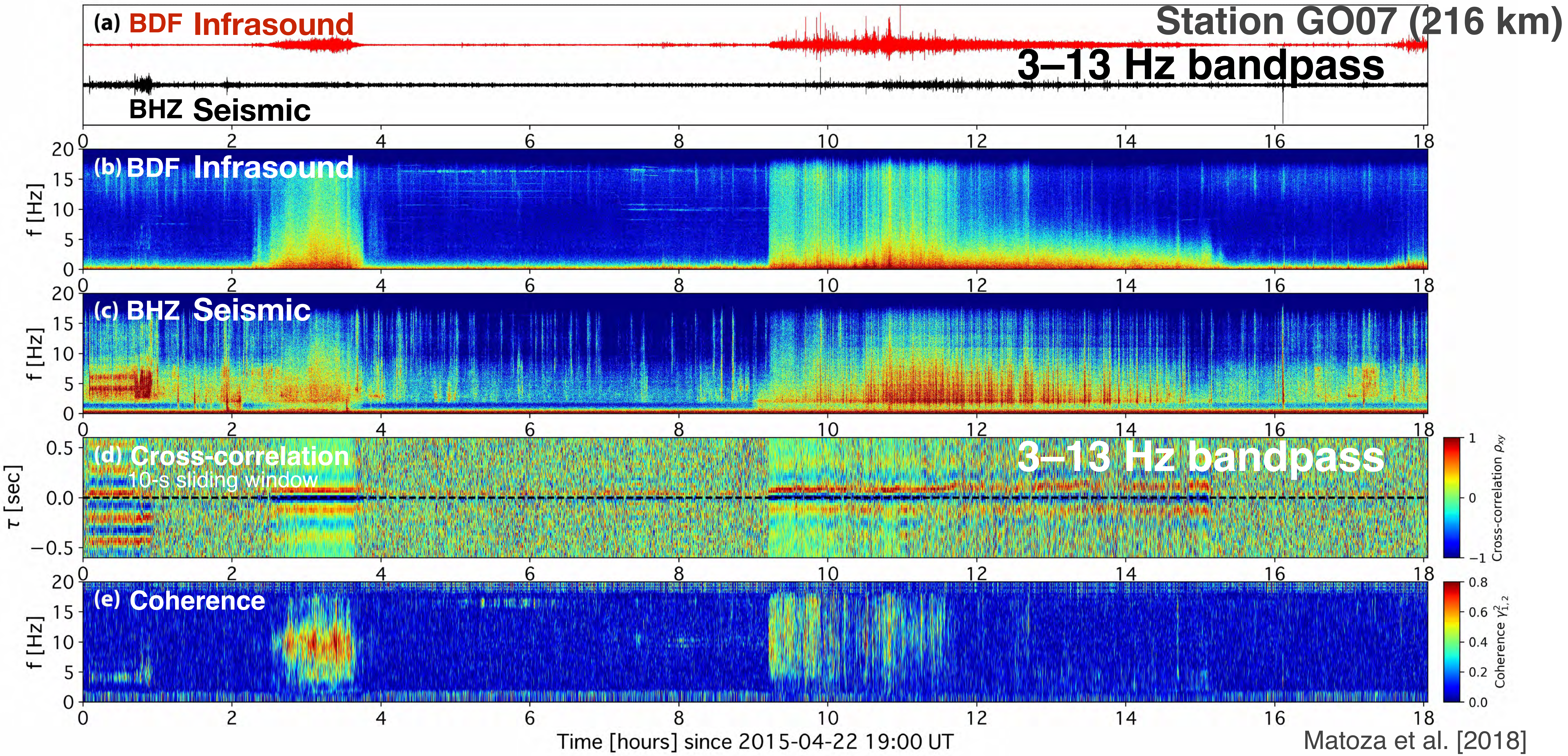

Matoza et al. [2018]

EarthScope TA Reverse-Time Migration (RTM)

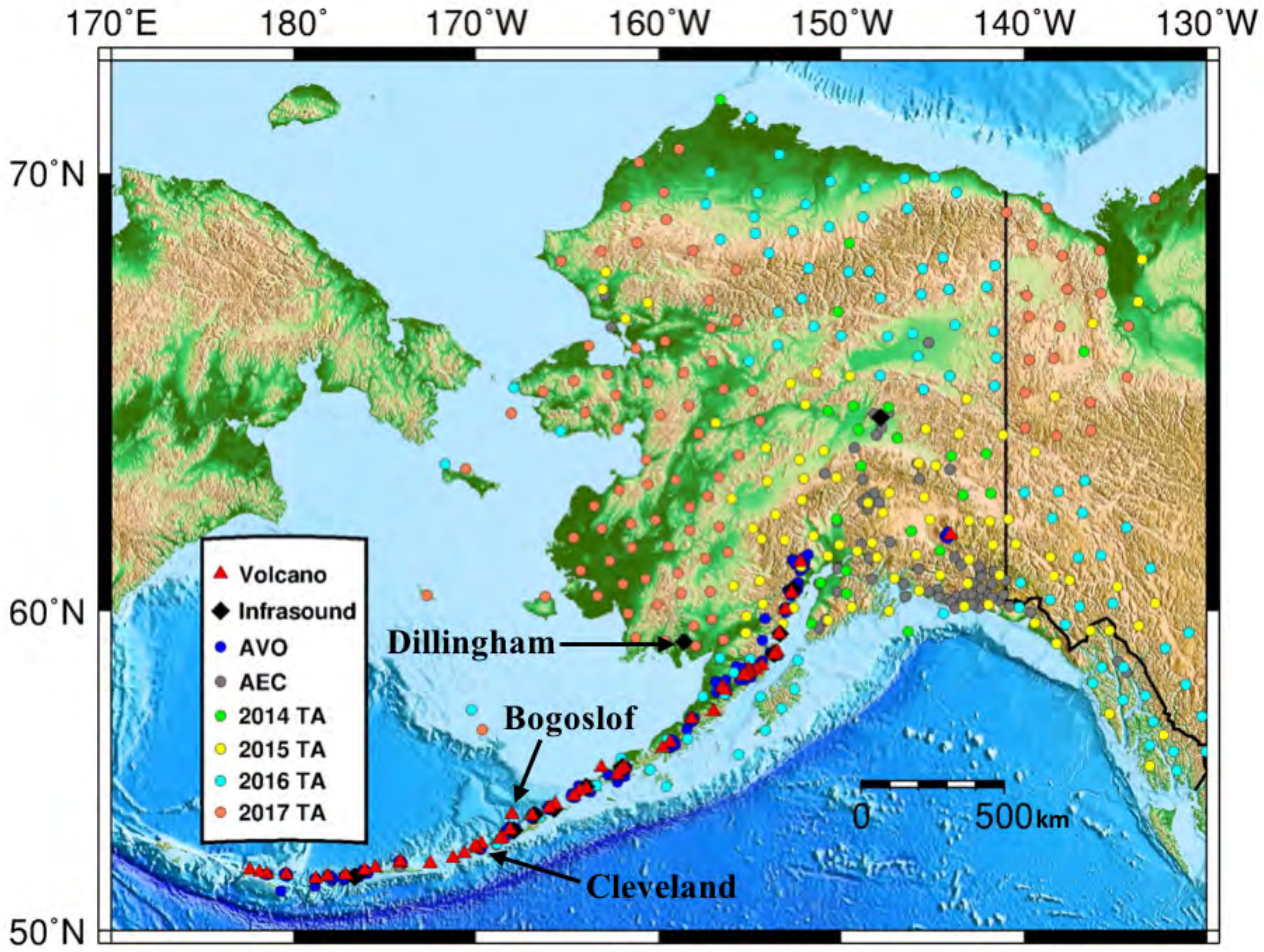

Figure: D. Fee, UAF

210 EarthScope Transportable Array (TA) colocated seismic and infrasound stations spread across Alaska, ~85 km spacing

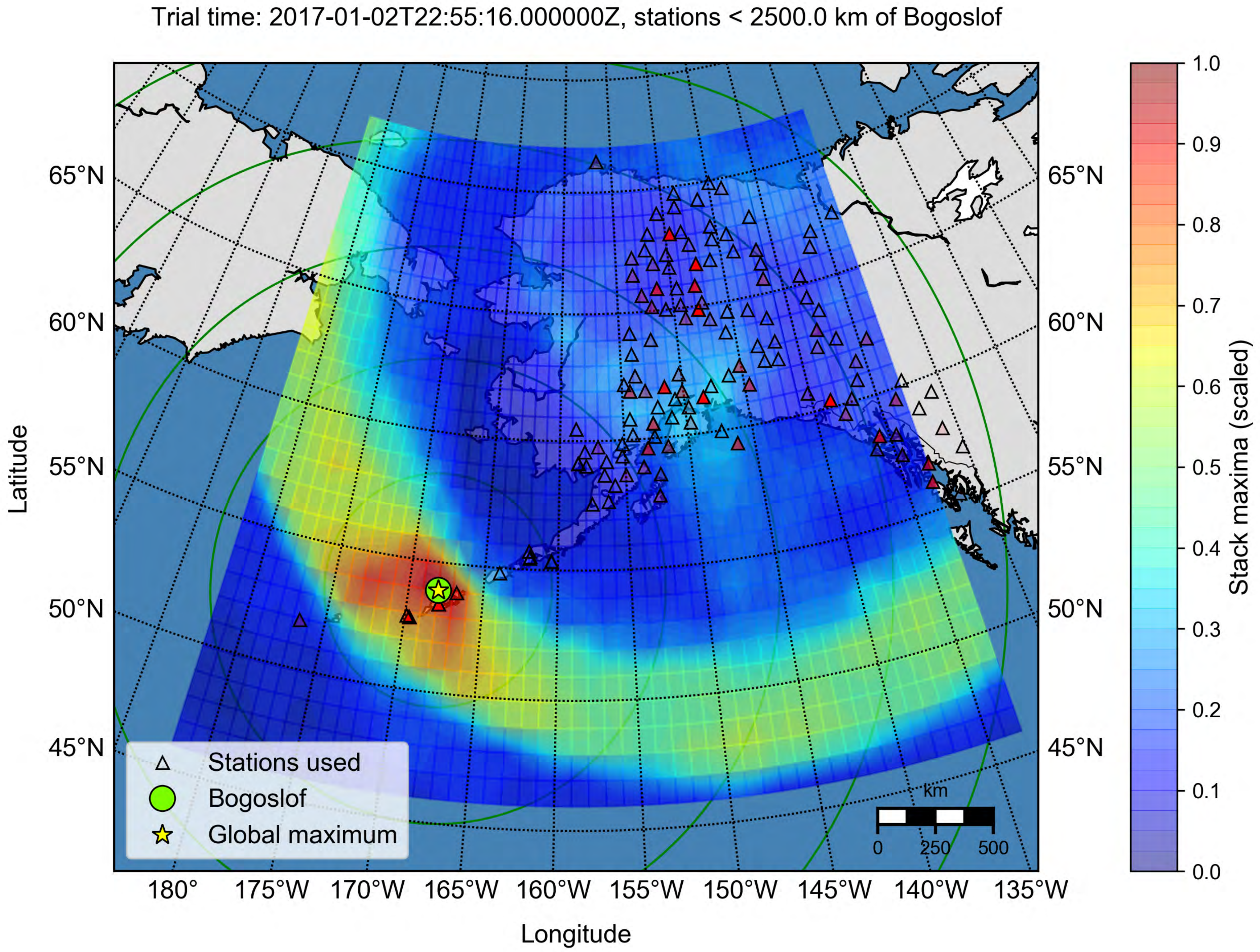

Bogoslof

- Bogoslof volcano; eruptions December 2016 to August 2017
- More than **60** eruptive events from Bogoslof provide a unique calibration dataset

Sanderson et al.; *Identifying and Mitigating Hazards in the 21st Century*

H2. Remote explosive volcanic eruption detection, location, and characterization using the EarthScope Transportable Array in Alaska

EarthScope TA Reverse-Time Migration (RTM)

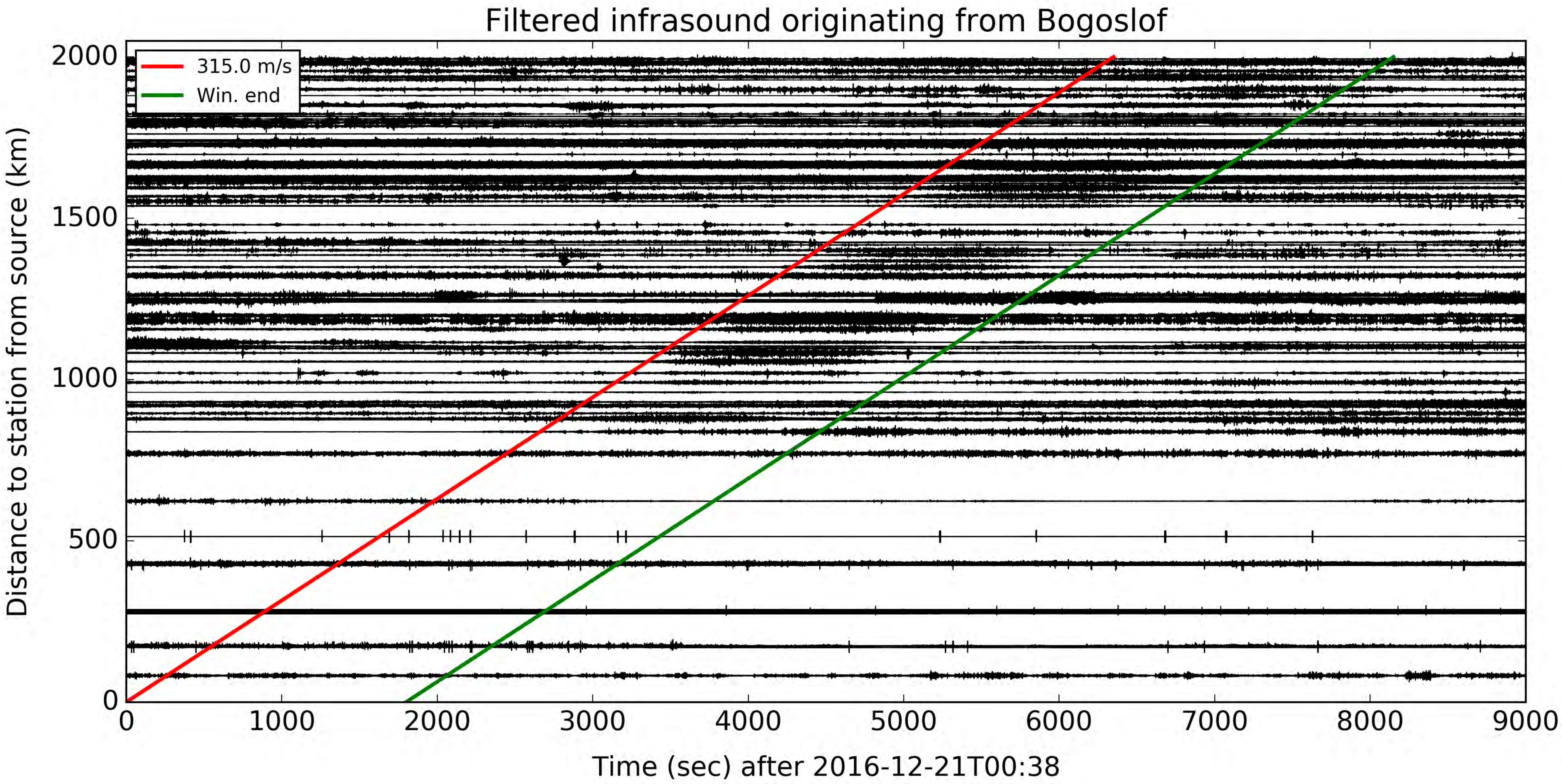

Sanderson et al.; *Identifying and Mitigating Hazards in the 21st Century*

H2. Remote explosive volcanic eruption detection, location, and characterization using the EarthScope Transportable Array in Alaska

EarthScope TA Reverse-Time Migration (RTM)

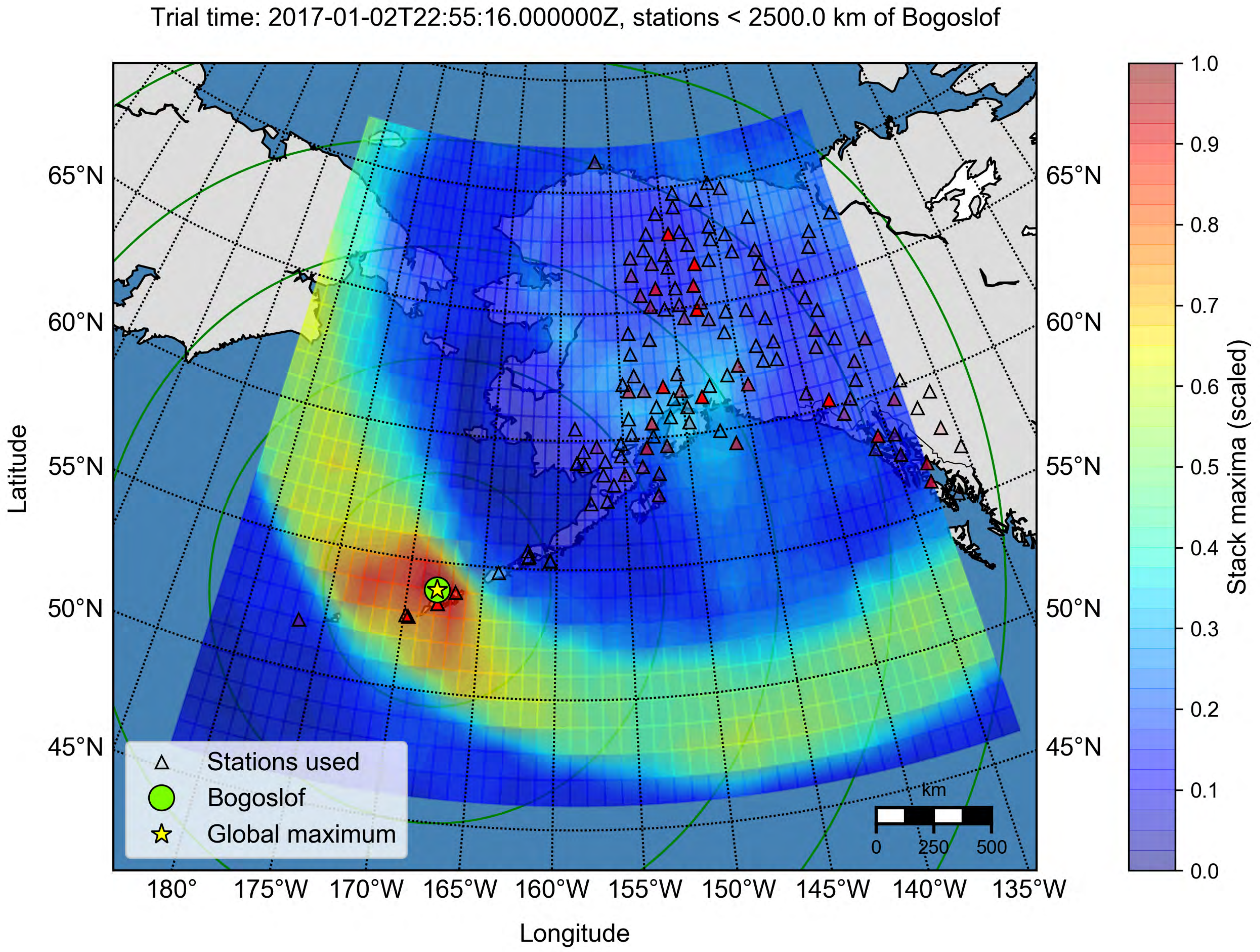

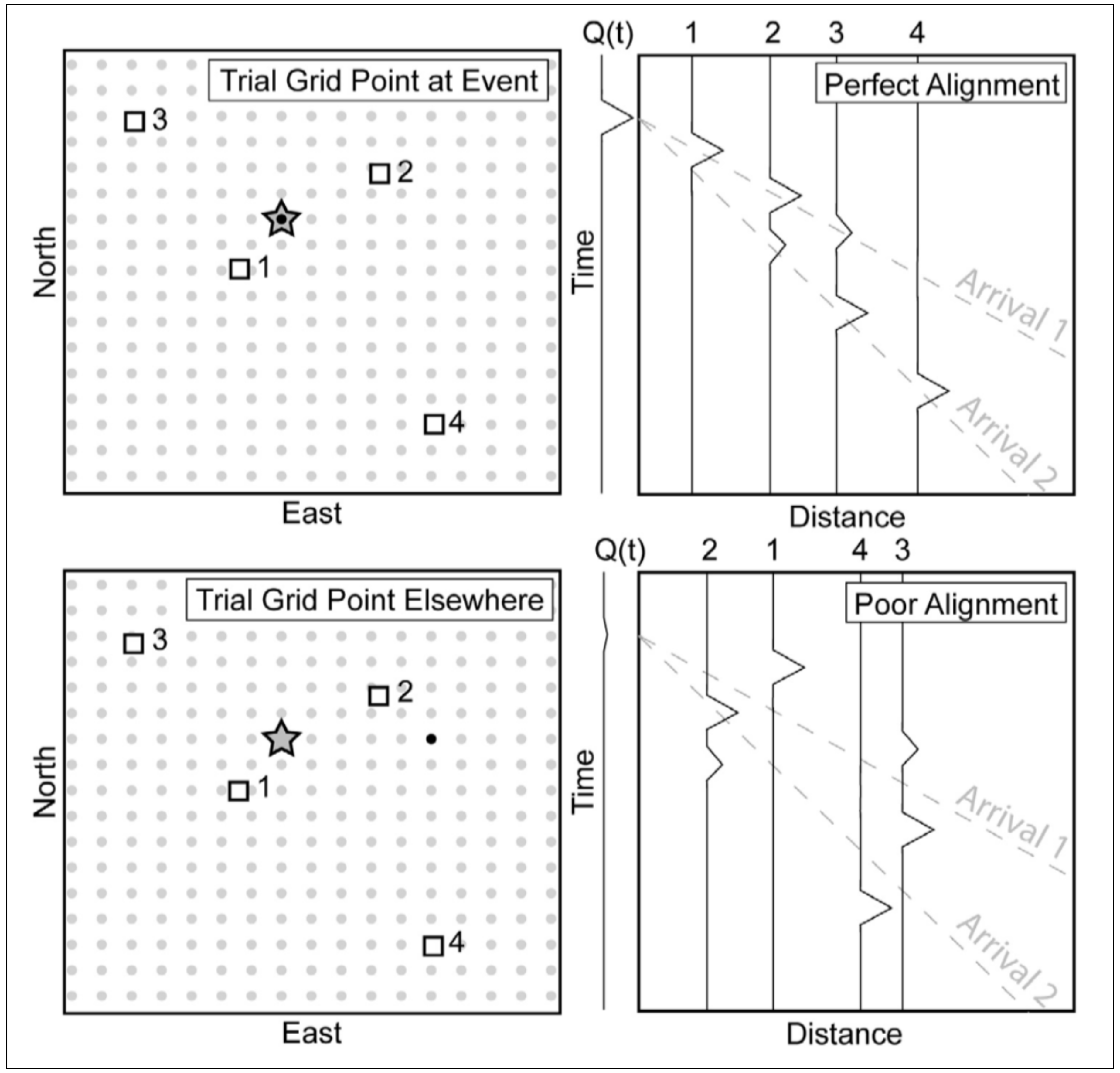

Walker et al. [2010]

Sanderson et al.; *Identifying and Mitigating Hazards in the 21st Century*

H2. Remote explosive volcanic eruption detection, location, and characterization using the EarthScope Transportable Array in Alaska

Conclusions

- Seismology and infrasound are complementary methods for understanding and monitoring volcanoes
- Source size varies: from tiny ~10 m^3 volumetric oscillations of fluid-filled cracks, observable only within crater, to explosive eruptions detectable globally with infrasound
- Rich multi-year seismo-acoustic datasets are becoming available from volcanoes worldwide
- Developing computational techniques to systematically investigate datasets, compare and contrast different volcanic systems, catalog and quantify Earth's volcanism, and test hypotheses about how volcanoes work

Recommendations

- Automated detection and cataloging of global explosive eruptions feasible with IMS
- Augmenting seismic networks with infrasound sensors in volcanic regions will dramatically enhance volcanic signal detection, reduce latency, and improve discrimination capability
- Adding single infrasound sensors to seismic stations helps significantly (~250–500 km spacing)
- Adding small arrays (e.g., 3–4 infrasound sensors, ~100 m aperture) would help even more

Acknowledgements

Lars Ceranna
Bernard Chouet
Phillip Dawson
David Fee
Rebecca Fitzgerald
Luis Franco
Milton Garces
David Green
Matthew Haney
Michael Hedlin
Alexandra Iezzi
Richard Johnson
Arthur Jolly
Megan Kelley
Ben Kennedy
Guoqing Lin
Alexis Le Pichon
John Lyons
Kathleen McKee
Pierrick Mialle
T. Dylan Mikesell
Seth C. Moran
Paul Okubo
Richard Sanderson
Peter Shearer
O. Alberto Valderrama
Julien Vergoz
Gregory Waite
Cecily Wolfe

image: A. Austin